

**NASA TECHNICAL
MEMORANDUM**

NASA TM X-72685

NASA TM X-72685

(NASA-TM-X-72685) THE EFFECT OF MEASUREMENT
ERRORS AND COMPUTATIONAL APPROXIMATIONS ON A
PERSPECTIVE ILM RADAR IMAGE (NASA) 151 p HC
\$6.25 CSCL 01E

N75-24764

Unclas
G3/09 25391

THE EFFECT OF MEASUREMENT ERRORS AND COMPUTATIONAL
APPROXIMATIONS ON A PERSPECTIVE ILM RADAR IMAGE

by

W. Thomas Bundick



This informal documentation medium is used to provide accelerated or special release of technical information to selected users. The contents may not meet NASA formal editing and publication standards, may be revised, or may be incorporated in another publication.

**NATIONAL AERONAUTICS AND SPACE ADMINISTRATION
LANGLEY RESEARCH CENTER, HAMPTON, VIRGINIA 23665**

1. Report No. NASA TM X-72685		2. Government Accession No.		3. Recipient's Catalog No.	
4. Title and Subtitle THE EFFECT OF MEASUREMENT ERRORS AND COMPUTATIONAL APPROXIMATIONS ON A PERSPECTIVE ILM RADAR IMAGE				5. Report Date	
				6. Performing Organization Code	
7. Author(s) W. Thomas Bundick				8. Performing Organization Report No.	
				10. Work Unit No. 513-52-01-13	
9. Performing Organization Name and Address NASA Langley Research Center Hampton, VA 23665				11. Contract or Grant No.	
				13. Type of Report and Period Covered Technical Memorandum	
12. Sponsoring Agency Name and Address National Aeronautics and Space Administration Washington, DC 20546				14. Sponsoring Agency Code	
15. Supplementary Notes Special technical information release, not planned for formal NASA publication					
16. Abstract This report examines the effect of aircraft position and attitude, of measurement errors, and of computational approximations on the size, shape, and position of a perspective radar image of an airport runway as might be displayed by an Independent Landing Monitor in transport aircraft. The effect on runway image geometry was examined for different aircraft attitudes and different aircraft positions relative to a standard three degree glide slope. Measurement errors investigated were errors in radar azimuth angle and range and errors in those aircraft parameters supplied to the radar for use in converting the radar image into a perspective format, namely pitch, roll, and altitude. Also investigated were the effects of using certain mathematical approximations, such as small angle, in the coordinate transformation which converts the image to a perspective format.					
17. Key Words (Suggested by Author(s)) (STAR category underlined) <u>Radar</u> Landing display Independent landing monitor			18. Distribution Statement Unclassified - Unlimited STAR Category 09		
19. Security Classif (of this report) Unclassified		20. Security Classif (of this page) Unclassified		21. No of Pages 149	
				22. Price* \$5.75	

* Available from { The National Technical Information Service, Springfield, Virginia 22151
STIF/NASA Scientific and Technical Information Facility, P O. Box 33, College Park, MD 20740

NATIONAL AERONAUTICS AND SPACE ADMINISTRATION

THE EFFECT OF
MEASUREMENT ERRORS AND COMPUTATIONAL APPROXIMATIONS
ON A PERSPECTIVE ILM RADAR IMAGE

By W. Thomas Bundick

SUMMARY

A forward looking imaging radar which displays the runway and its surroundings in a perspective format is one of the systems under consideration for use as an Independent Landing Monitor in transport aircraft. In this report computer drawn images are used to demonstrate how the size, shape, and relative position of radar perspective images of the runway and horizon are affected 1) by changes in aircraft attitude and position with respect to the runway, 2) by errors in the imaging radar measurements and in the measurements of aircraft attitude and altitude which are provided to the radar, and 3) by mathematical approximations in the computations which transform the radar data to a perspective format.

The computer generated images show that flight path errors equal in magnitude to the errors allowable in the Microwave Landing System can be detected on the perspective display when the correct runway outline is available for reference. However, it cannot be concluded that a real-world radar image without the reference runway is sufficient for an ILM. It is also shown that some errors in the radar range and angle measurements and in aircraft attitude measurements distort the radar image to look like changes in aircraft position or attitude. From the computer images it appears that the use of

small angle approximations in generating the perspective format might be acceptable.

INTRODUCTION

In recent years much has been said about the need for an Independent Landing Monitor, or ILM, to provide the pilot of transport aircraft with the capability to assess the progress of an automatic landing and the aircraft's situation with respect to the runway. While no agreement has been reached concerning the type of display to be used as part of an ILM, there are many, particularly pilots, who advocate some type of perspective image, either real or symbolic, of the runway and its surroundings, perhaps with the addition of aiding symbology. One type of potential sensor for producing a perspective ILM image is a forward looking imaging radar.

A perspective image is a natural output of such imaging sensors as television and infrared. However, a forward looking radar naturally images the target in range-angle coordinates, and a coordinate transformation to angle-angle coordinates must be accomplished in the radar electronics to generate a perspective image. In order to exactly accomplish this transformation, it is necessary that aircraft attitude and altitude be measured and provided to the radar.

The purpose of the research described in this report is to investigate how the size, shape, and relative position of radar generated perspective images of the runway and horizon are affected 1) by changes in aircraft attitude and position with respect to the runway, 2) by errors in the imaging radar measurements and in the measurements of aircraft attitude and altitude which are provided to the radar, and 3) by mathematical approximations in the

computations which transform the radar data to a perspective format.

It should be emphasized that this research was not a human factors experiment. The ability of a pilot to use the information presented by a perspective image was in no way measured.

DISCUSSION OF THE INVESTIGATION

The technique used in the investigation was to draw images of the runway and horizon which demonstrated one of the three effects being investigated. These images were then examined visually and compared with other images when appropriate to determine what conclusions could be reached.

A computer program was written to generate the outline of a perspective radar image of the runway and the horizon as a function of aircraft position and attitude, which were read into the computer as input data. The mathematics of the problem are discussed in detail in Appendices A, and C and the details of the computer program are described in Appendix D. The approximations that could be used by the radar in transforming from radar coordinates to a perspective image are described in Appendix B.

The radar horizon corresponds to the maximum range of the radar beyond which the ground image is obscured by radar receiver noise and cannot be distinguished from sky. The actual horizon is shown by a dashed line for comparison. It is recognized that the transition from ground image to noise occurs gradually and not abruptly as implied by the radar horizon line shown on the computer generated images. Thus, the computer generated radar horizon should be used as an indication of the area on the image where the terrain is becoming obscured by noise. The maximum radar range used in the investigation was 5 mi.

The computer drawn images were produced with a magnification ratio of one at a viewing distance of 20 in. The images in figures 3 through 35 have been reduced in size by approximately 60 percent and must be viewed at a distance of 12 in. for a unity magnification ratio. Most images were produced with a CRT screen size of 8.87 in. square, which corresponds to a field-of-view of $25^{\circ} \times 25^{\circ}$.

Images were normally produced for aircraft ranges to touchdown (measured along the extended runway centerline) of 2 mi., 1 mi., and 0.5 mi. and for aircraft altitudes of 100 ft. and 50 ft. Examples of the computer produced images are shown in figures 1 and 2. In figure 1 the aircraft is in level flight on a 3° glide slope. In figure 2 the aircraft is off the glide path and in a yaw right, pitch up, roll right attitude. The alpha-numeric code in the upper right corner of all images is for identification only.

Three versions of the computer program were produced. The first generates a perspective image from a set of input data (aircraft position and attitude) as in figures 1 and 2. Each of the other two versions produce two images superimposed on the same plot frame, where one of these superimposed images is a reference image. In one version of the program, the reference image is drawn for the aircraft on glide path in level flight, while the second, or comparison, image depicts the runway and radar horizon with the aircraft at some other position and/or attitude for purposes of image comparison. In the remaining version of the program, the reference image is drawn using the exact mathematical transformations with no measurement errors, while the comparison image is generated using an approximate transformation or using measured data which include measurement errors. Throughout this report the comparison image is denoted by arrows on the first page of each figure.

RESULTS

Aircraft Position

Since an Independent Landing Monitor may be used to monitor the progress of an automatic landing using the Microwave Landing System (MLS), radar images were produced to demonstrate the change in the runway perspective produced by aircraft displacements from a nominal 3° glide slope. These displacements were selected to equal the bias plus noise (2σ) accuracy requirements of the MLS as quoted in reference 1, page F-1, and shown below in Table I.

TABLE I.- ACCURACY SPECIFICATIONS FOR
K CONFIGURATION MLS (ref. 1)

Angle coordinate	Bias error (2σ)	Noise error (2σ)
Azimuth	0.072°	0.045°
Elevation	0.1°	0.070°

The resulting images for a localizer offset of 0.117° , for a glide slope offset of $+0.17^{\circ}$, and for a glide slope offset of -0.17° are shown in figures 3 through 5, respectively. In figures 6 and 7 are shown images with the aircraft positions being linear, rather than angular, offsets from the nominal glide path. In figure 6 the aircraft is 10 ft. to the left of the runway centerline, and in figure 7 the aircraft is 5 ft. above the 3° glideslope.

In all of the above images the changes in aircraft position are detectable on the computer generated radar image when the reference image is present. One cannot conclude that these position changes could be detected and determined with sufficient accuracy by the pilot without the reference image present.

or with a real world radar image even with the reference image superimposed.

Aircraft Attitude

An ILM may be used also to indicate aircraft attitude. Figures 8, 9, and 10 show images with the aircraft on a 3° glide slope with attitudes of 0.1° yaw right, 1.0° pitch up, and 1.0° roll right, respectively. The yaw angle of 0.1° was selected because one proposed function for the ILM is to determine heading (relative to the runway) within 0.1° . The value of 1.0° for roll and pitch was chosen rather arbitrarily.

Examination of figures 8 through 10 reveal that these changes in attitude are detectable on the computer produced images. Once again these changes may not be detectable on a realistic radar display without the reference image. Changes in pitch are detected more easily than changes in roll.

Effect of Measurement Errors

Figures 11 through 25 contain the images generated with errors in the measured data. The aircraft is either in level flight on a 3° glide slope or is displaced 0.5° to the left of a 3° glide slope at an attitude of 10° yaw right, 5° pitch up, and 10° roll right.

Radar errors.— Figure 11 shows an image produced with an error of 5 ft + 1% in the radar range measurement, and figure 12 shows an image with a range error of 25 ft. + 5%.

Comparison of figure 12 with figures 4 and 5 reveals that the 25 ft. + 5% error in range produces a change in the image that is roughly comparable to the 0.17° change in glide slope which the ILM is trying to detect. Therefore, it is concluded that greater radar range accuracy is required.

Comparison of figure 11 with figures 4 and 5 reveals that the 5 ft. + 1% range error changes the image considerably less than does the 0.17° change in

glide slope. Comparison of figure 11 with figures 7 and 8 show that this range error distorts the image less than the image change produced by ± 5 ft. altitude bias relative to the glide slope.

Figures 13 and 14 are images produced with errors in the measured radar scan angle of 1 percent and of $1^\circ + 5$ percent, respectively.

From figure 13 it is evident that a 1 percent error produces almost no detectable change in the display. However, the error of $1^\circ + 5$ percent, as in figure 14, distorts the image much like a heading (yaw) change of 1° .

Figures 15 through 18 show comparable results with the aircraft off glide path and in an attitude of 10° yaw, 5° pitch, and 10° roll. The results are similar to those of the previous four figures, except that the 1 percent scan angle error is now detectable (figure 17).

Altitude error.— Figures 19 and 20 are images generated with the aircraft on glide path in level flight with errors of 2 ft + 2 percent and 5 ft + 5 percent, respectively, in the measured altitude. Figures 21 and 22 are similar, but the aircraft is off glide path in a non-level attitude.

Comparison of figures 20 and 22 with figures 4 and 5 reveal that the altitude error of 5 ft + 5 percent distorts the image similarly to a glide slope change of 0.17° , and this error is probably unacceptable. The 2 ft + 2 percent error in figures 19 and 21 produces a similar distortion of lesser magnitude.

Attitude errors.— Figures 23 and 25 illustrate the resulting images when the pitch attitude measurement has an error of $0.212^\circ + 0.5$ percent, and figures 24 and 26 illustrate the results with roll attitude errors of $0.707^\circ + 0.5$ percent. These error values were taken from reference 2 as being typical values for gyro errors.

The pitch error produces a distortion in the image which is similar to the change in the image produced by the glide slope change that the ILM is trying to detect, as can be seen by comparing figure 23 to figures 4 and 5. The runway image distortion caused by the roll error is almost undetectable in level flight on glide path (figure 24). There is some distortion, however, in the radar horizon and in the runway in non-level flight (figure 26). This distortion is similar to a change in roll attitude, as may be expected.

Effect of Mathematical Approximations

Small angle approximations.- Images generated using the small angle approximations as described in Appendix B are shown in figures 27 through 30. In figure 27 the aircraft is flying level on a 3° glide slope but displaced 0.117° left of the runway centerline. In figure 28 the aircraft is again in level flight but 0.17° above the 3° glide slope. The difference between the exact and approximate images is undetectable in these cases.

In figures 29 the aircraft is on glide path (3° glide slope), but the aircraft is in a 10° yaw, 5° pitch, 10° roll attitude. In this case there is a difference, though not large, in the exact and approximate images.

Figure 30 shows the displayed image when the aircraft is 25 ft to the left and 10 ft below the 3° glide path and in a 5° yaw, 3° pitch, 5° roll attitude. In this case the distortion caused by the approximation is very small.

Comparison of figures 28, 29, and 30 show that the distortion is not large for attitude angles up to 10° and that the approximate image improves as the attitude approaches $Y = P = R = 0$ and the aircraft nears the glide path.

Unstabilized display.- The unstabilized displays generated without using knowledge of the aircraft's attitude are shown in figures 31 through 35.

In figure 31 the aircraft is in level flight on a 3° glide slope, and there is almost no difference in the exact and approximate images. This result was expected, since the unstabilized display assumes an aircraft attitude of $Y = P = R = 0$, which was the actual attitude in this case. The very slight difference in the exact and approximate radar horizon images is caused by the small angle approximation for the radar scan angle, not by the approximations for aircraft attitude.

The aircraft situation in figure 32 is the same as in figure 31 except for a 10° yaw right. It can be seen from figure 32 that the unstabilized image is a good approximation to the exact image in this case.

In figure 33 the aircraft situation is the same as in figure 31 except for a pitch up to 5°. Similarly in figure 34 the aircraft is in a 10° roll right. It is obvious from these two figures that the unstabilized display cannot be used for determining aircraft attitude.

In figure 35 the aircraft is 25 ft left of and 10 ft below the glide path in a 5° yaw, 3° pitch, 5° roll attitude. The shape and position of the runway correctly indicate that the aircraft is left of centerline and yawed right. However, the usefulness of the unstabilized display for determining position relative to the glide slope cannot be determined from this investigation.

SUMMARY OF RESULTS

1. Aircraft displacements from a 3° glide path equal to the bias + noise (2σ) requirements for the Microwave Landing System Configuration K¹ are

¹Configuration K is one of the most sophisticated and accurate configurations defined for the MLS and is designed to provide guidance signals suitable for landing in Category III weather conditions. (See ref. 1, Part Three, p. IIA-3, for accuracy requirements.)

detectable on the computer generated outline of a perspective radar image with the reference image present. The reference image is the image obtained when the aircraft is on glide path.

2. Aircraft heading changes of 0.1° and roll and pitch changes of 1° are detectable on the computer generated images when the reference image ($Y = P = R = 0$) is present.

3. A radar range error of 25 ft + 5% distorts the image to look like a glide slope change. This distortion is sufficient to make the error intolerable. A radar range error of 5 ft + 1% produces similar distortion, but of a magnitude that might be acceptable.

4. The distortion produced by a 1% scan angle error is probably acceptable. A bias error in scan angle looks like a heading (yaw) change on the image.

5. Altitude measurement errors affect the image in a manner similar to glide slope changes. An altitude measurement error of 5 ft + 5% produces an image distortion roughly comparable to a change in glide slope of 0.17° .

6. Pitch attitude measurement errors distort the image somewhat like glide slope changes with the image changes due to a pitch error of 0.212° + 0.5% and the changes due to a 0.17° glide slope error being roughly comparable.

7. The effects of an error in roll attitude measurement are most noticeable in the radar horizon image, where they appear like roll attitude changes. This effect would be less noticeable in a noisy real-world radar image, since the horizon would not be as distinct as in the computer-generated image.

ORIGINAL PAGE IS
OF POOR QUALITY

8. The effects of using small angle approximations in the radar coordinate - image coordinate transformation are almost undetectable with the aircraft on glide path and with $Y = P = R = 0^\circ$.

9. Some distortion is produced by the small angle approximations with the aircraft in a non-zero attitude. However, since the distortion is small and the approximate image converges toward the exact image as attitude and position displacement go to zero, the small angle approximation might be acceptable.

10. The unstabilized display cannot be used to determine pitch and roll attitude.. Aircraft heading can be approximately determined using the unstabilized display, but with unknown accuracy.

CONCLUDING REMARKS

The changes in the size, shape, and position of a perspective radar image of the runway that are produced by changes in aircraft position with respect to the glide path and by changes in aircraft attitude have been demonstrated. Whether or not these changes in the image can be used by the pilot to monitor aircraft position and landing progress with sufficient accuracy must yet be proven through piloted simulations and flight tests.

The distortion in a perspective radar image produced by errors in the radar measurement of range and scan angle and by errors in the measurement of aircraft attitude and altitude has been demonstrated. In some cases this distortion appears similar to a change in aircraft position or attitude. In these cases the measurement accuracy must be sufficient to keep image distortion less than the image changes caused by the aircraft position or attitude deviations which must be detected.

The effects of using small angle approximations in the radar coordinate transformation also have been demonstrated. These effects are small for small Y , P , and R , and the small angle approximations will probably be satisfactory for an imaging radar ILM.

ORIGINAL PAGE IS
OF POOR QUALITY

13

1

4-1-A



(a) Distance to TD = 2 mi.

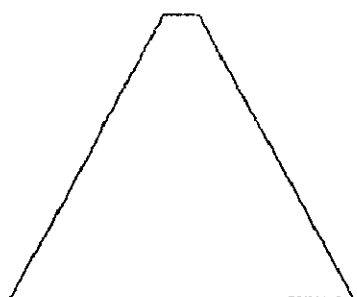
Figure 1.- Basic display with aircraft on 3° glide slope, $Y = P = R = 0^{\circ}$.



(b) Distance to TD = 1 mi.

Figure 1 - Continued.

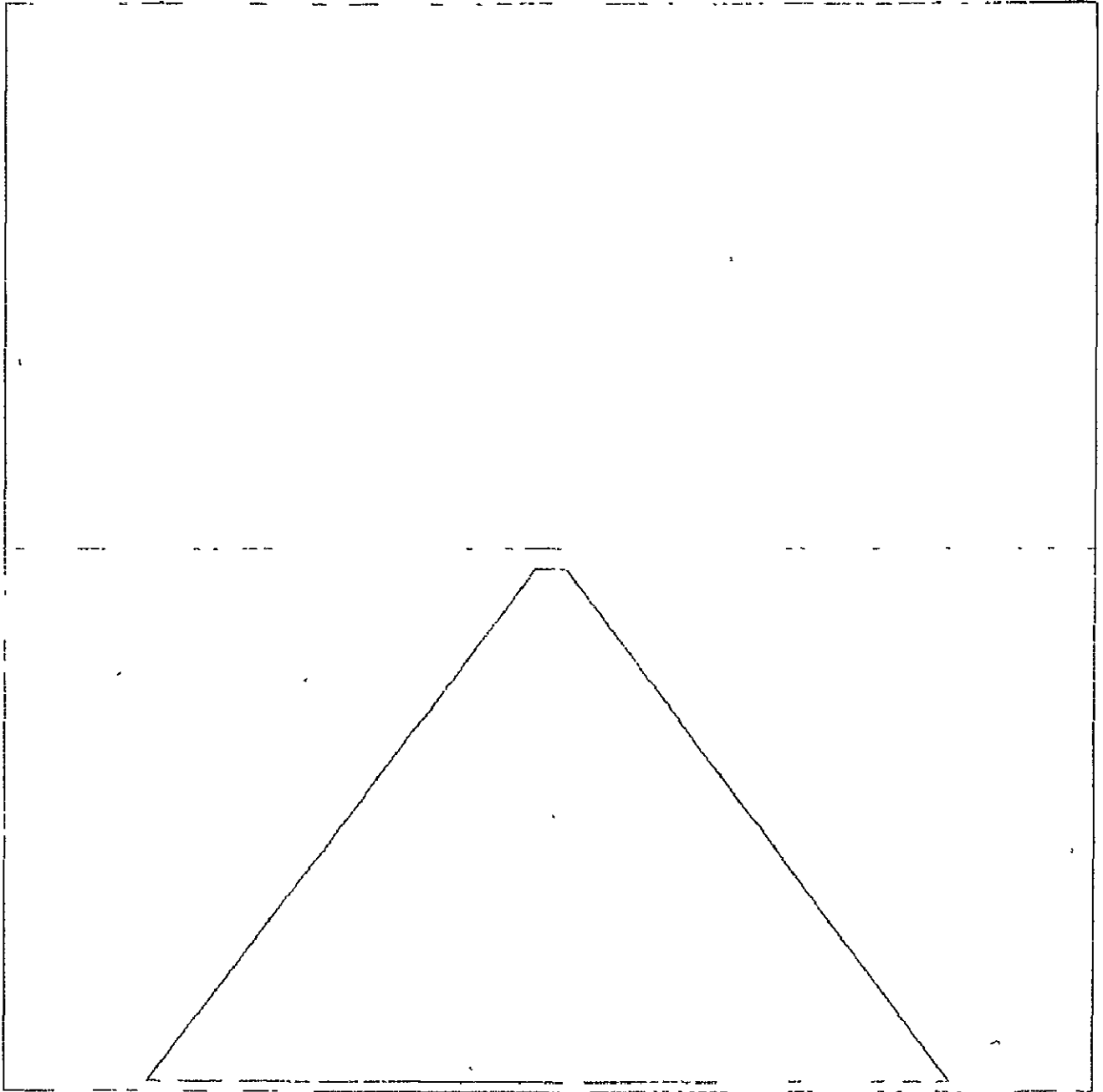
ORIGINAL PAGE IS
OF POOR QUALITY



(c) Distance to TD = 1/2 mi.

Figure 1 - Continued

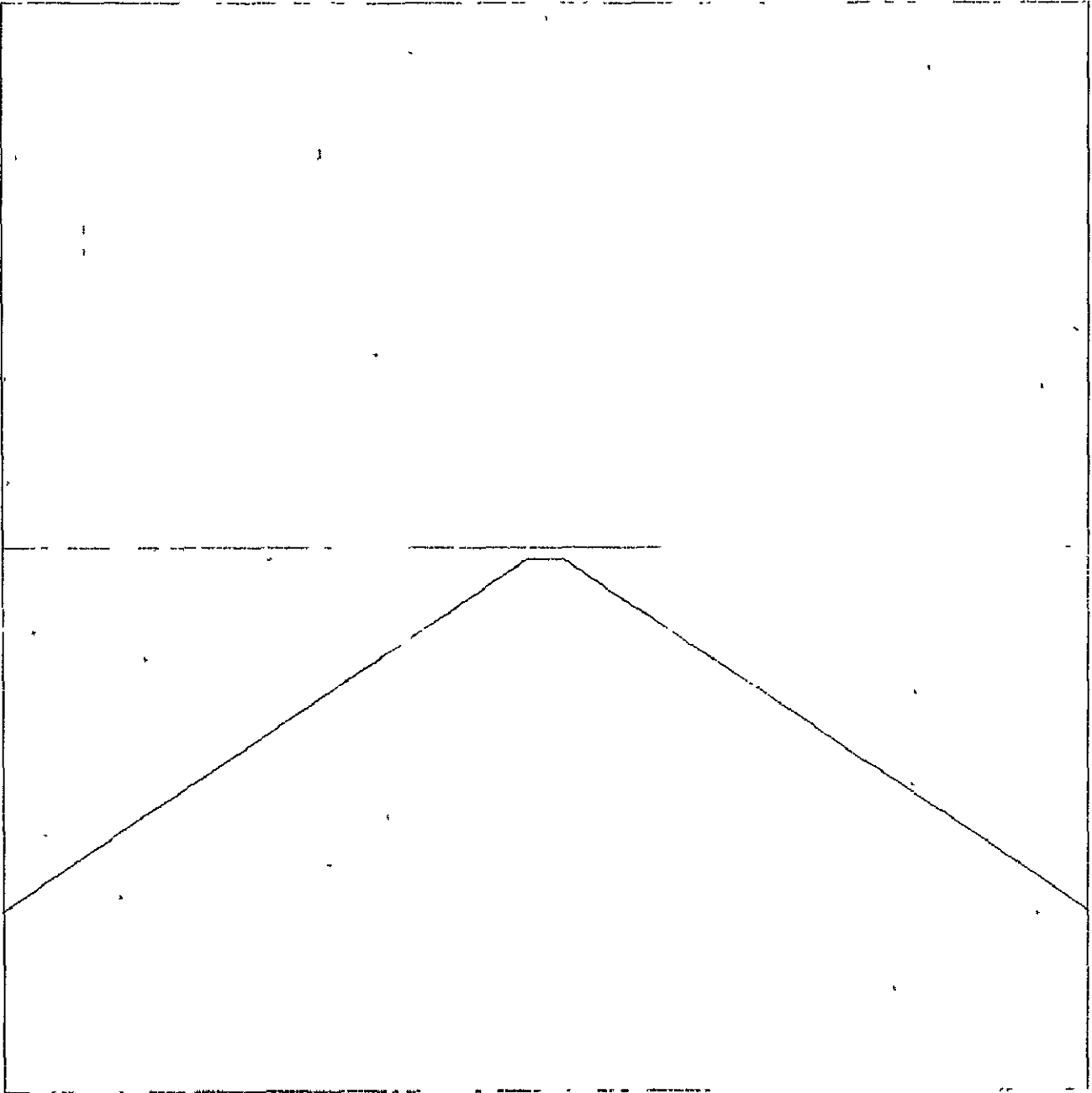
ORIGINAL PAGE IS
OF POOR QUALITY



(d) Altitude = 100 ft.,

Figure 1.- Continued.

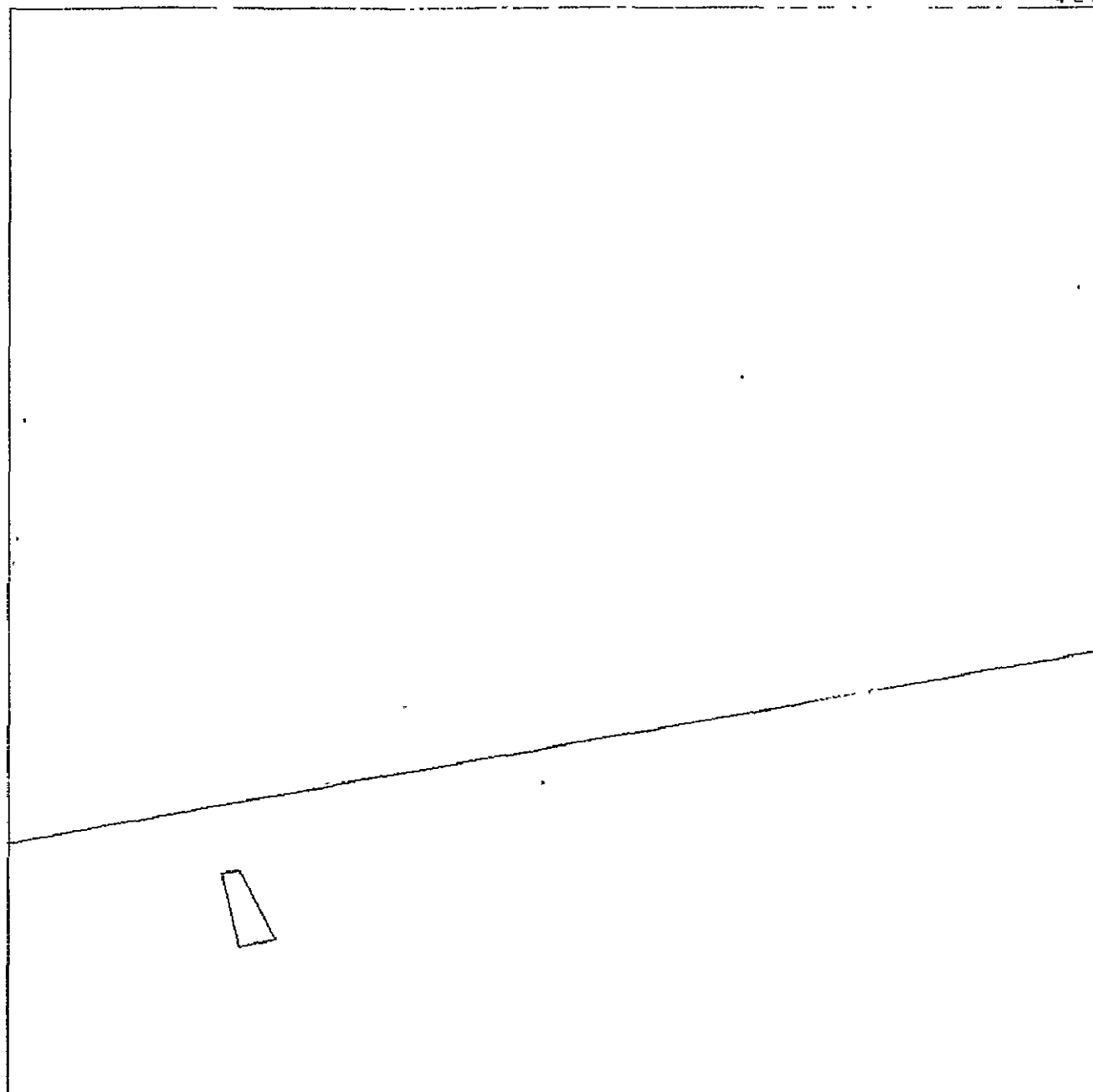
ORIGINAL PAGE IS
OF POOR QUALITY



(e) Altitude = 50 ft.

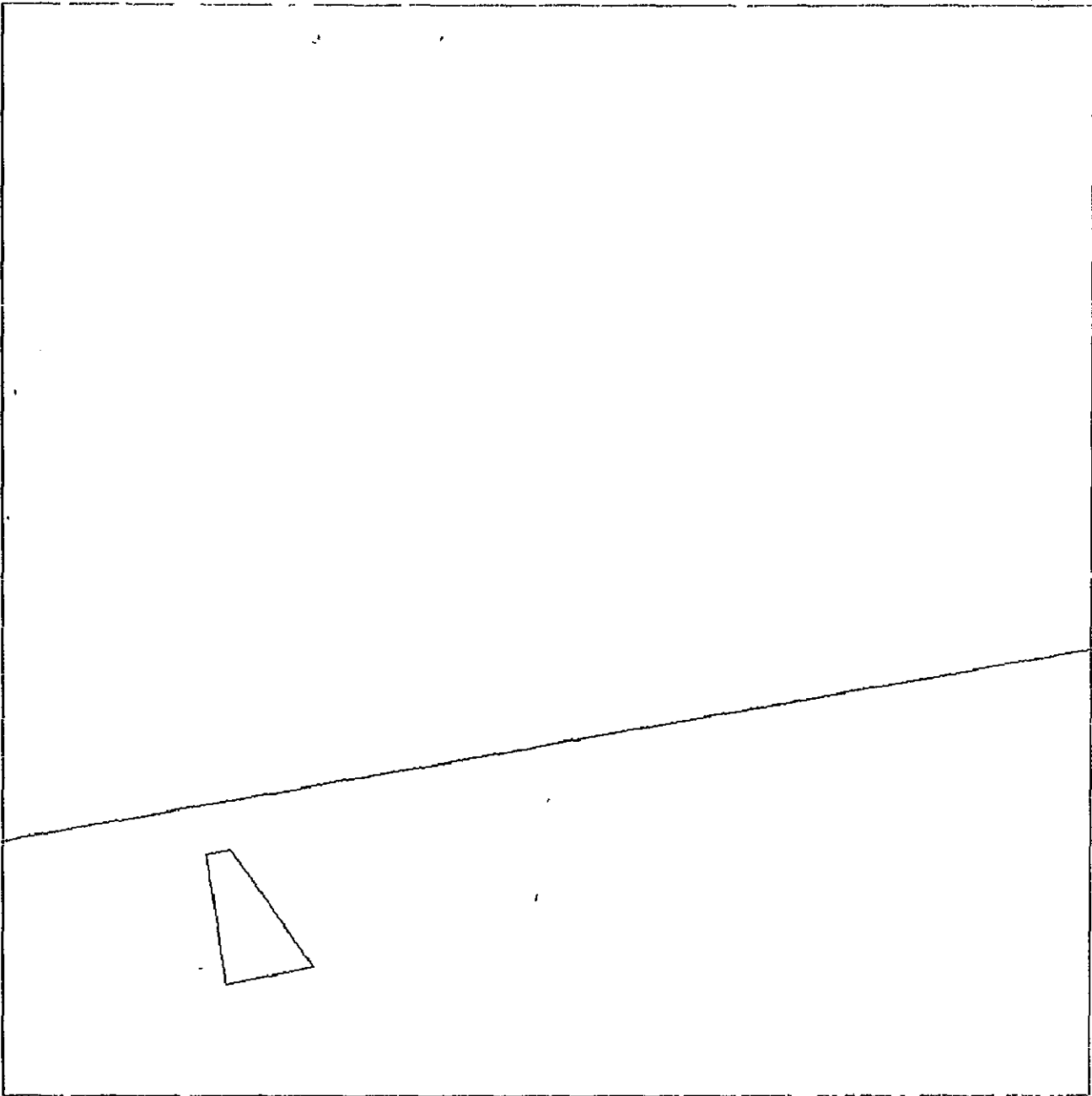
Figure.1 - Concluded

ORIGINAL PAGE IS
OF POOR QUALITY



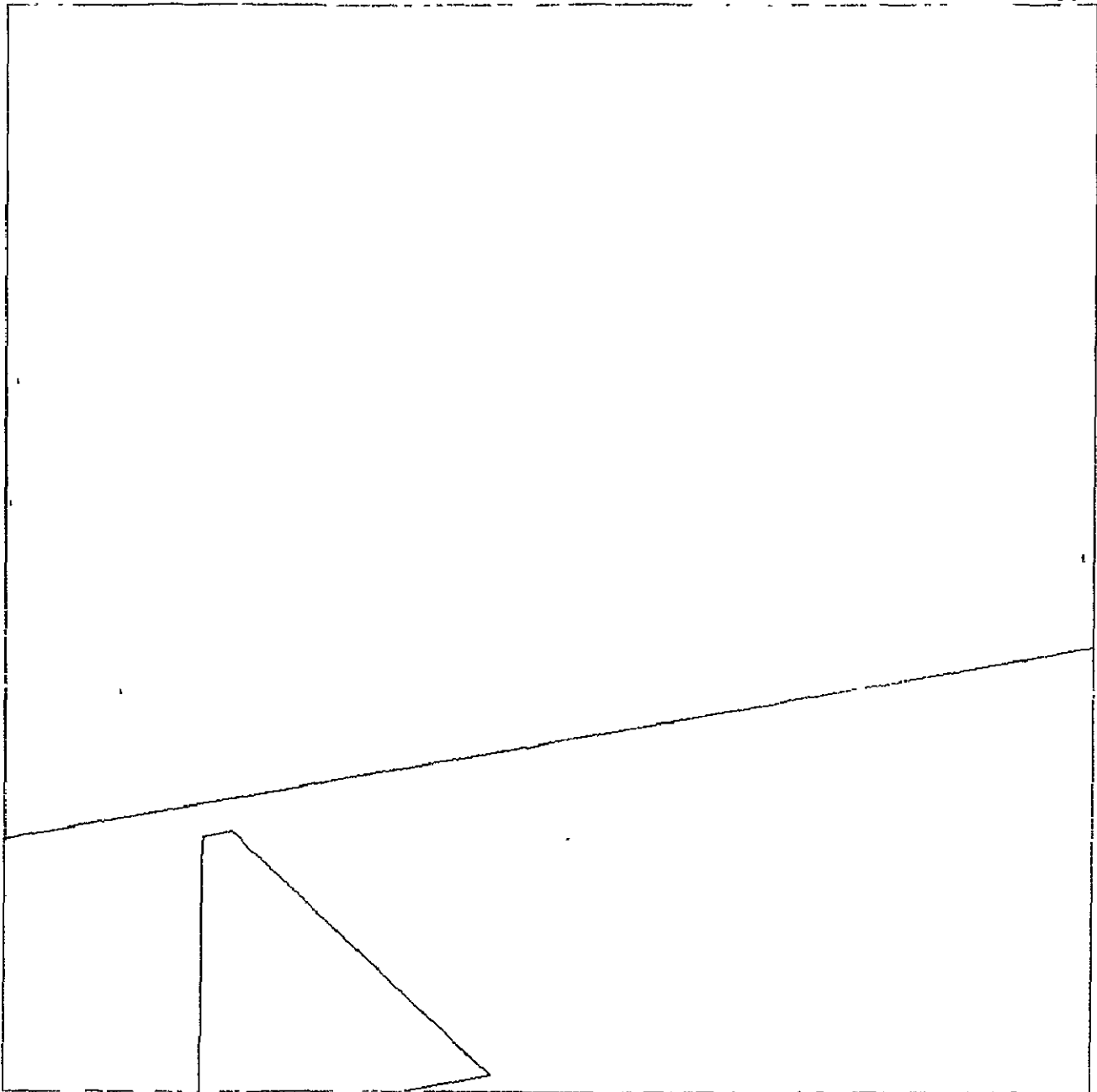
(a) Distance to TD = 2 mi.

Figure 2 - Basic display with aircraft displaced $0.5^\circ + 25$ ft to left of localizer, 25 ft. above glide slope, $Y = R = 10^\circ$, $P = 5^\circ$.



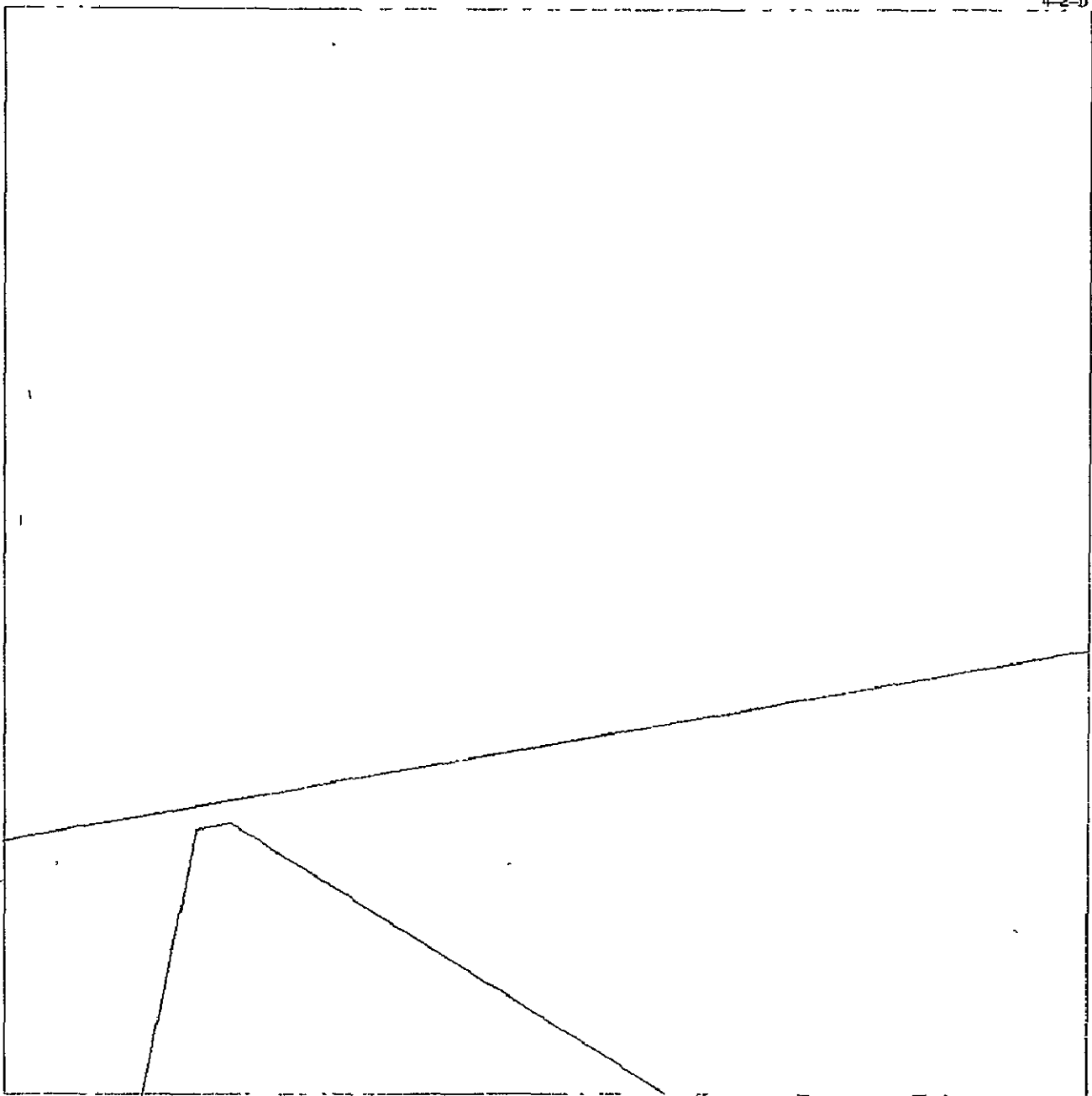
(b) Distance to TD = 1 mi

Figure 2.- Continued



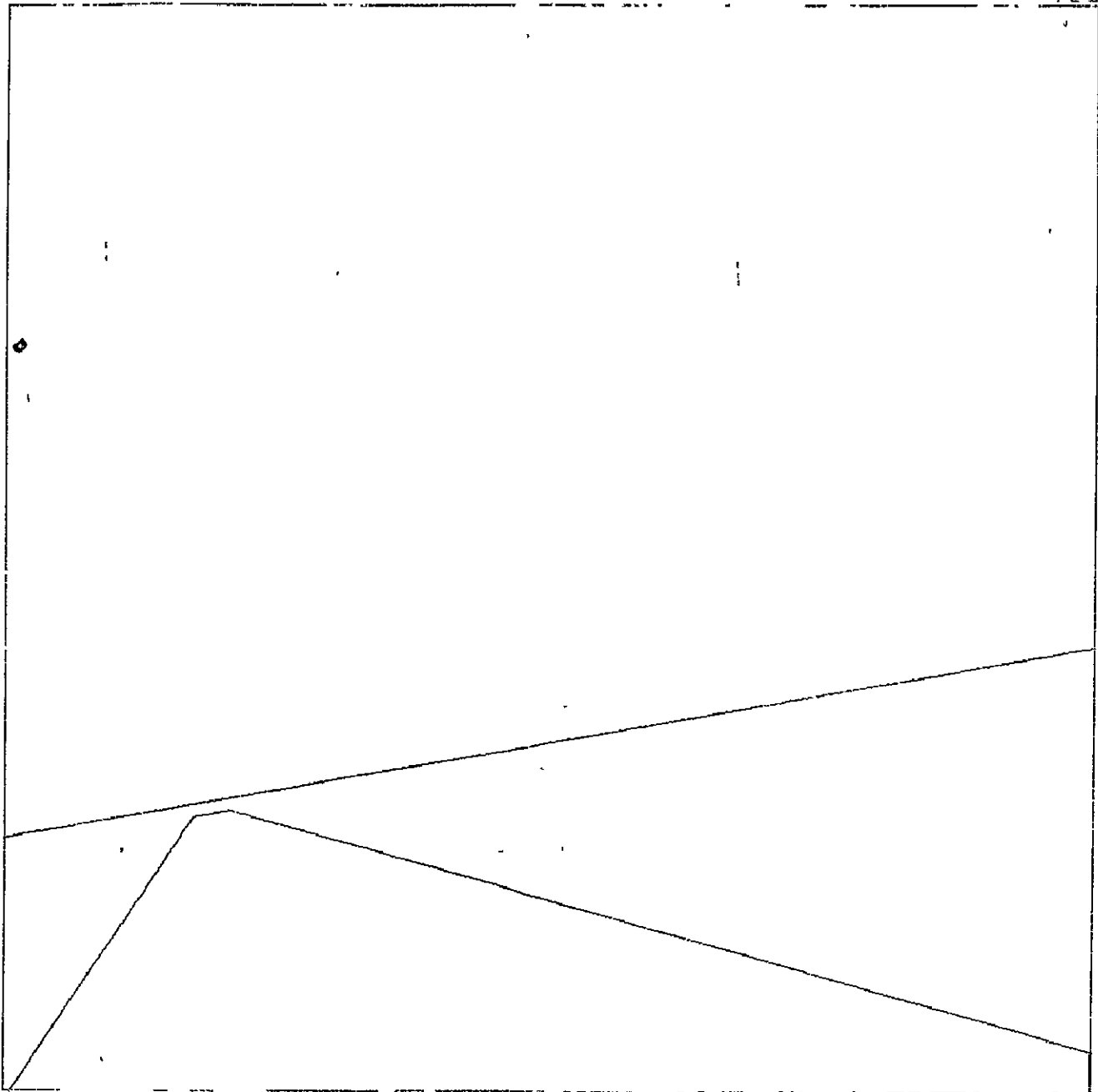
(c) Distance to TD = 1/2 mi.

Figure 2.- Continued



(d) Altitude = 100 ft

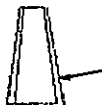
Figure 2.- Continued.



(e) Altitude = 50 ft.

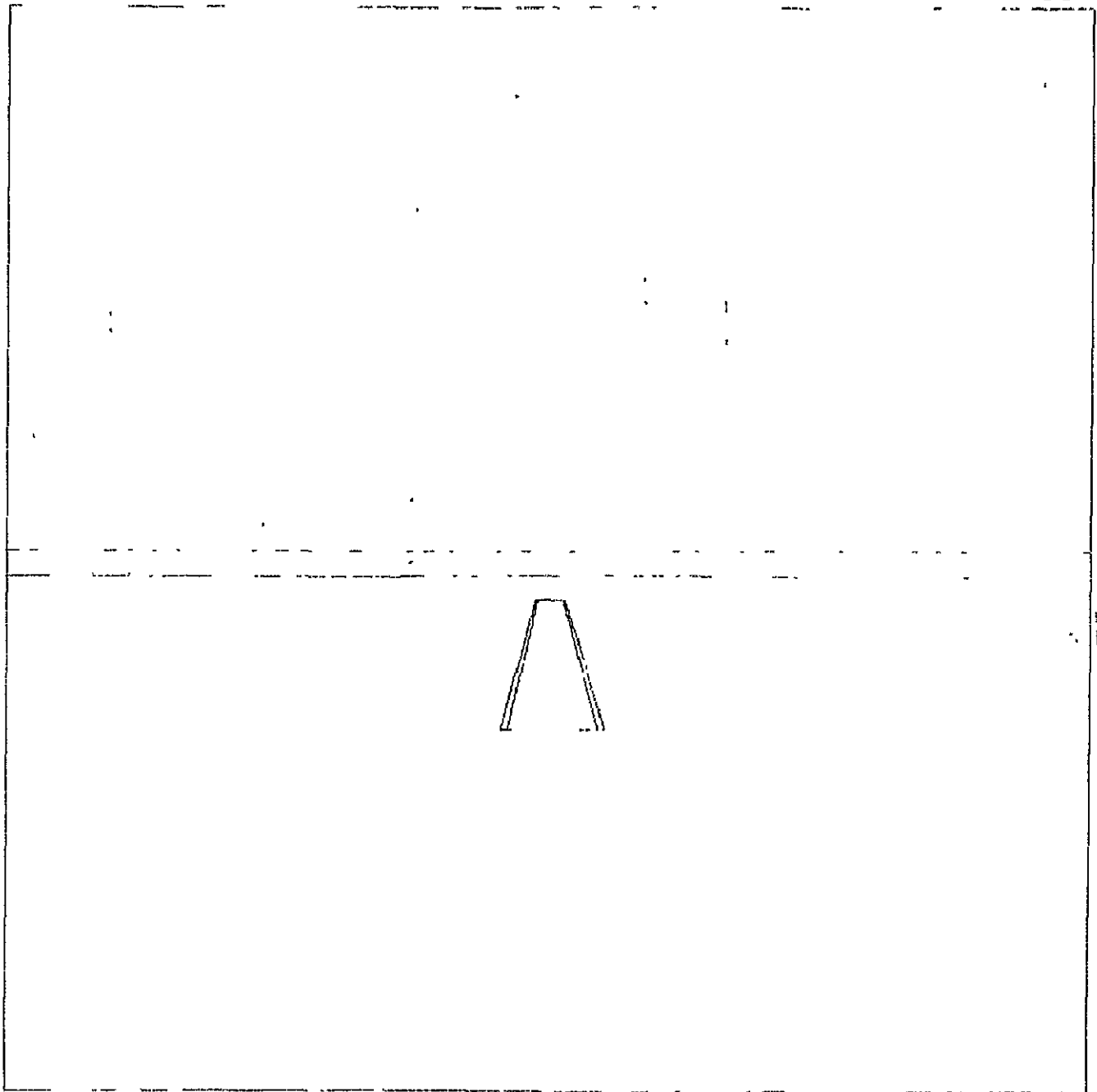
Figure 2.- Concluded

ORIGINAL PAGE IS
OF POOR QUALITY



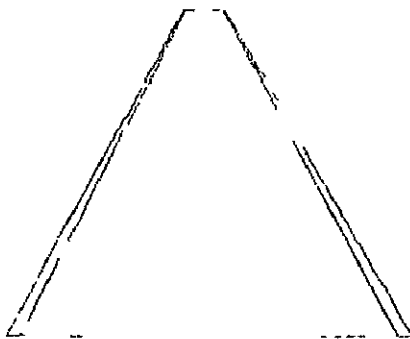
(a) Distance to TD = 2 ml.

Figure 3.- Aircraft 0.117° to left of localizer.



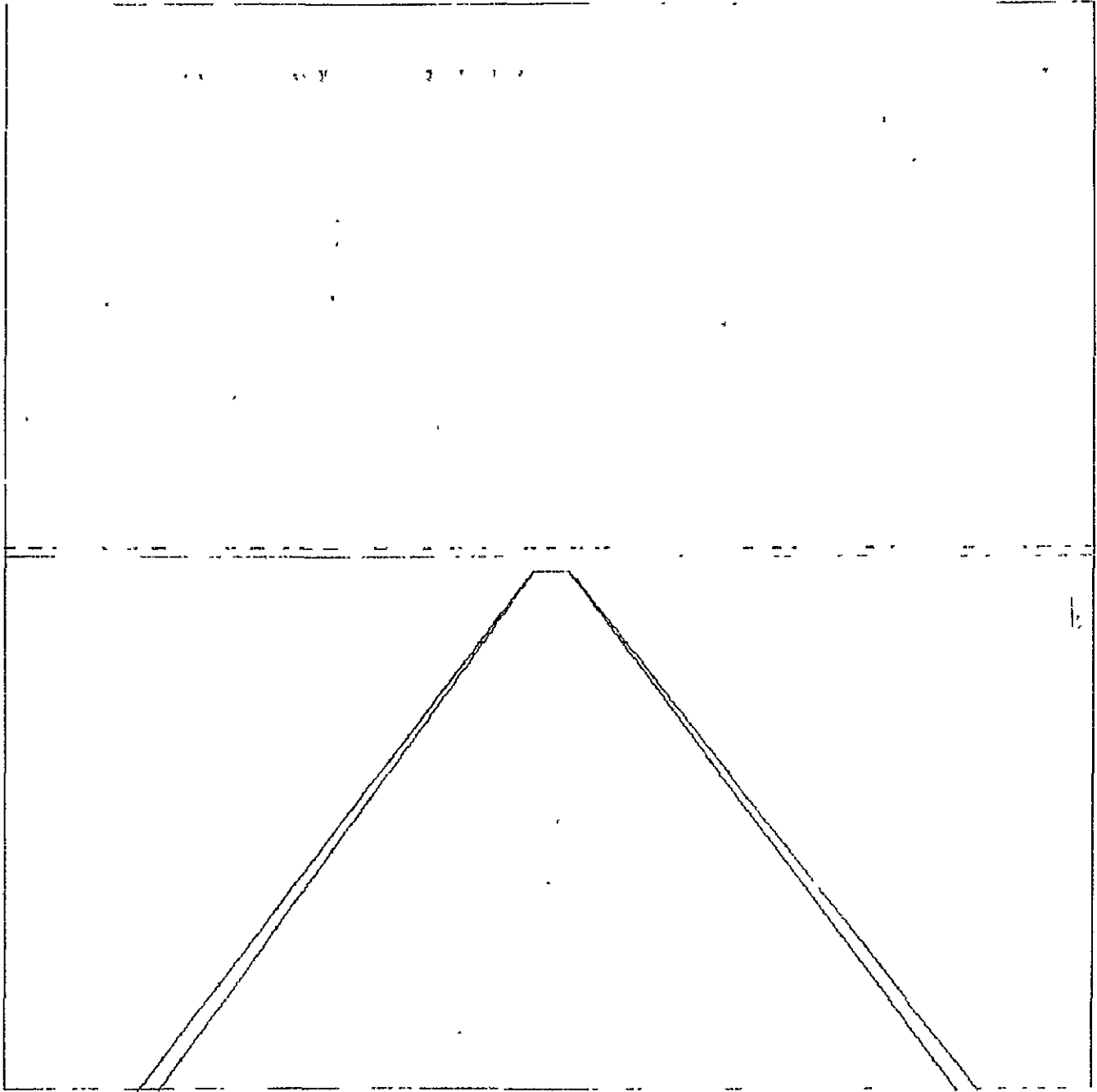
(b) Distance to TD = 1 mi.

Figure 3.- Continued.



(c) Distance to TD = 1/2 mi.

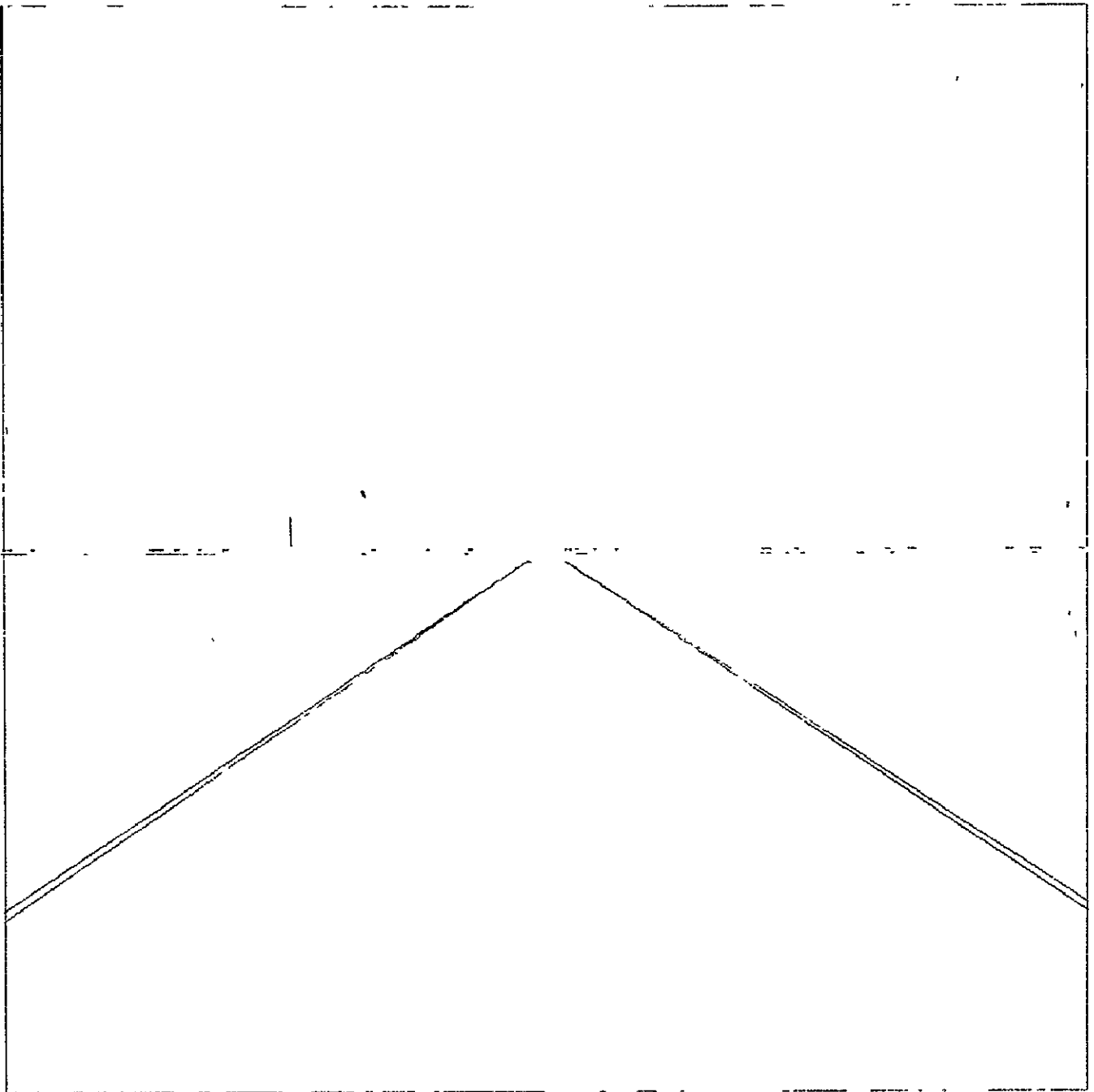
Figure 3.- Continued.



(d) Altitude = 100 ft.

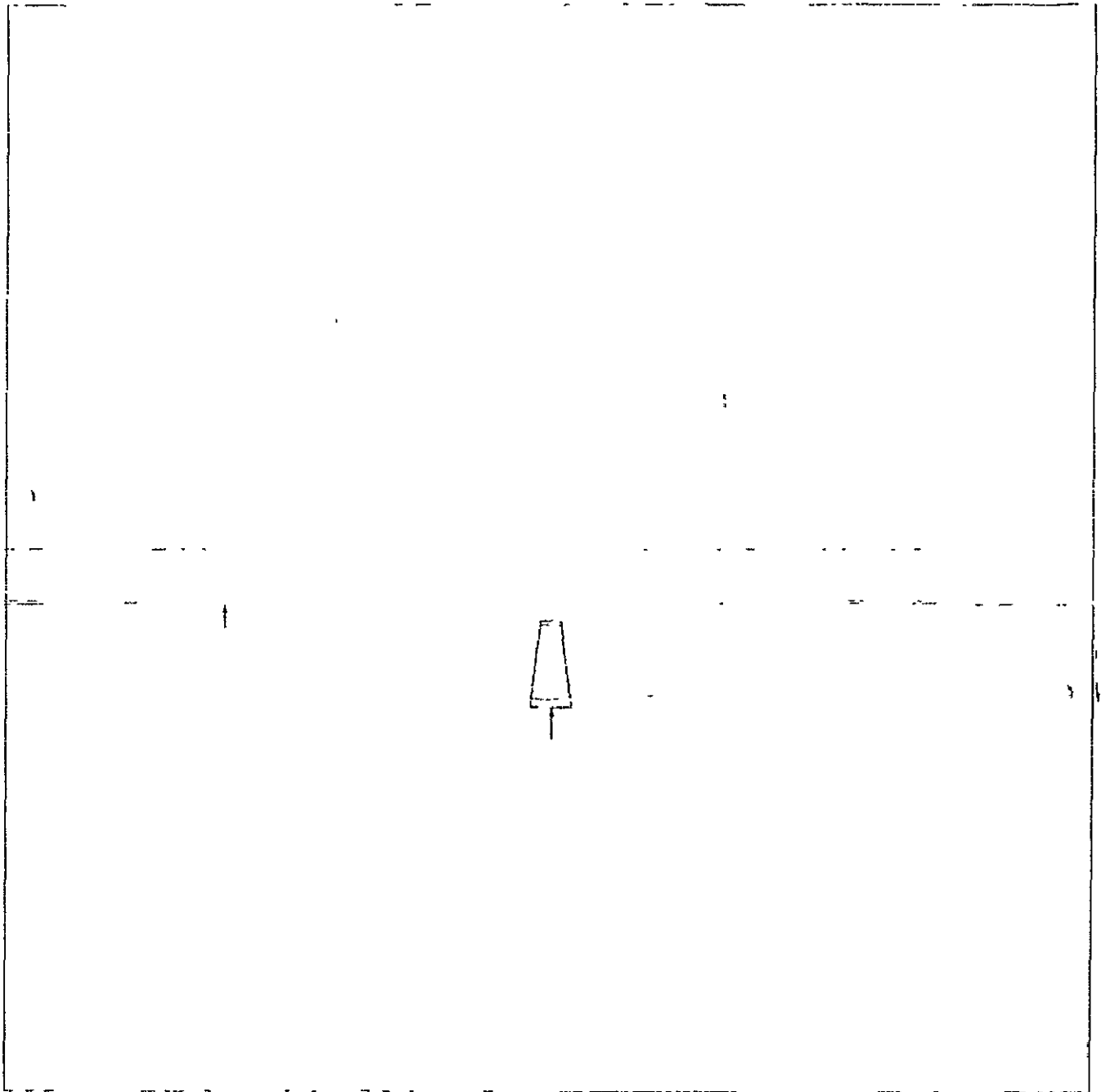
Figure 3.- Continued.

ORIGINAL PAGE IS
OF POOR QUALITY



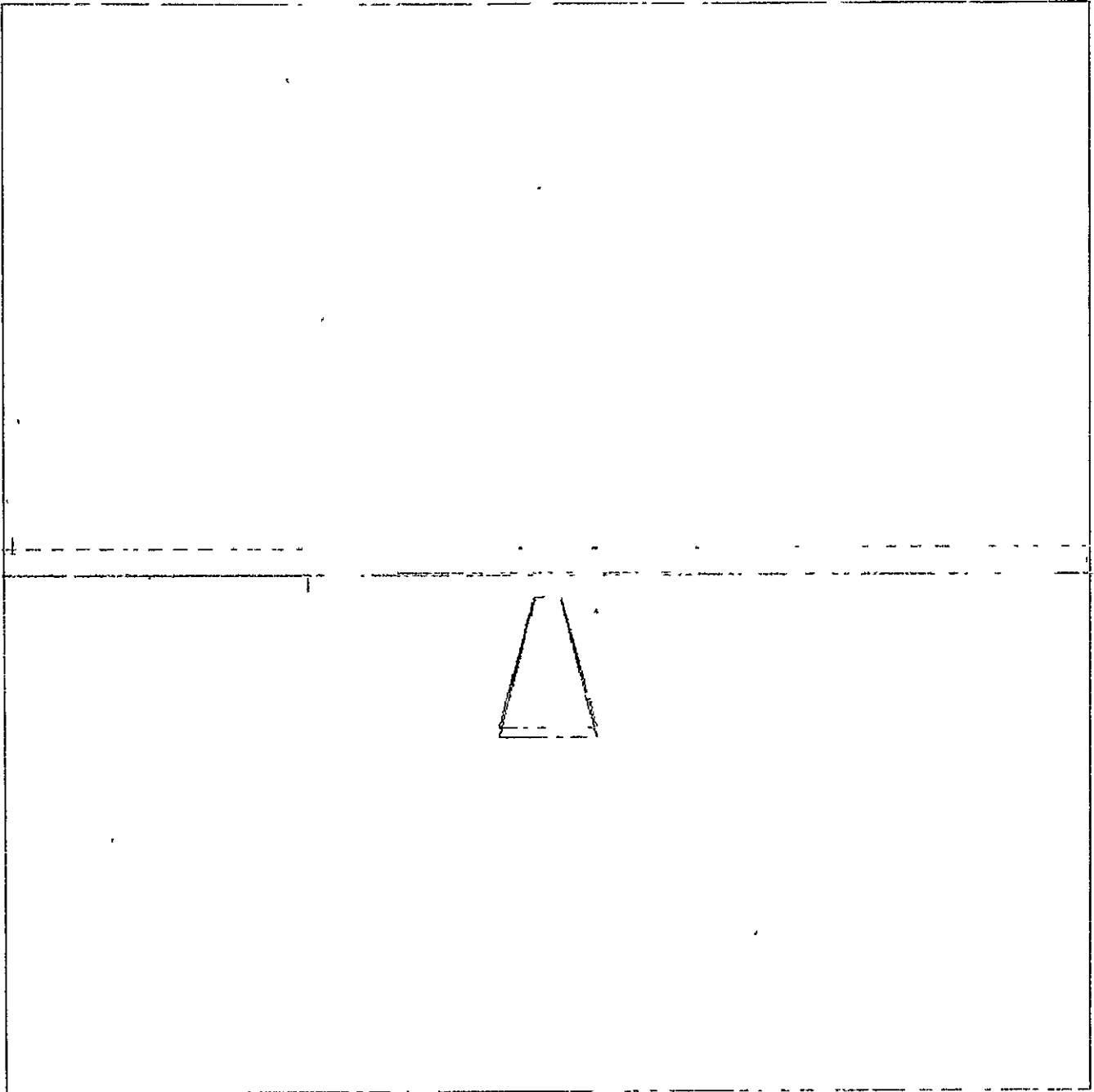
(e) Altitude = 50 ft.

Figure 3.- Concluded.



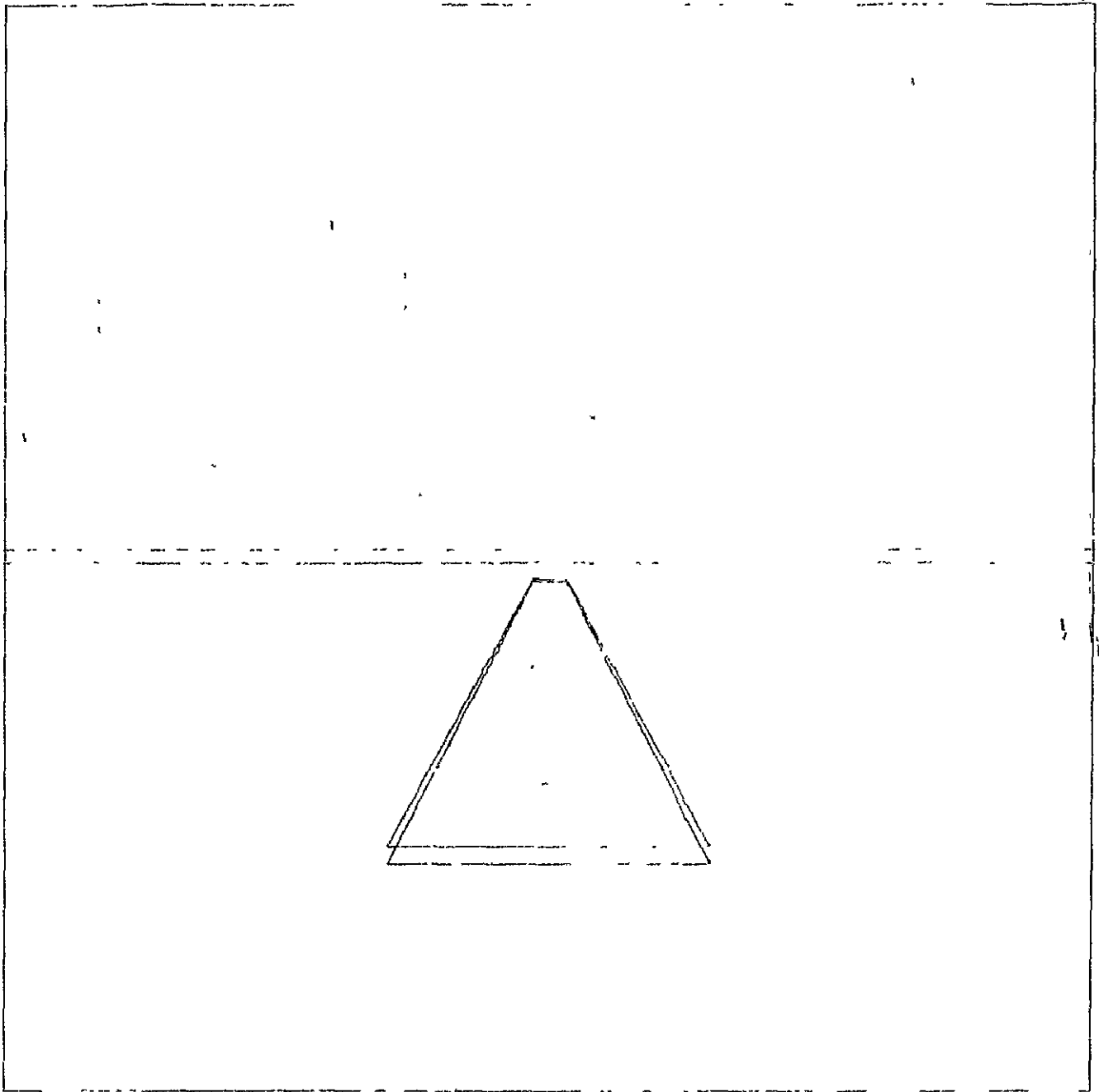
(a) Distance to TD = 2 mi.

Figure 4.- Aircraft on glide slope of 3.17° .



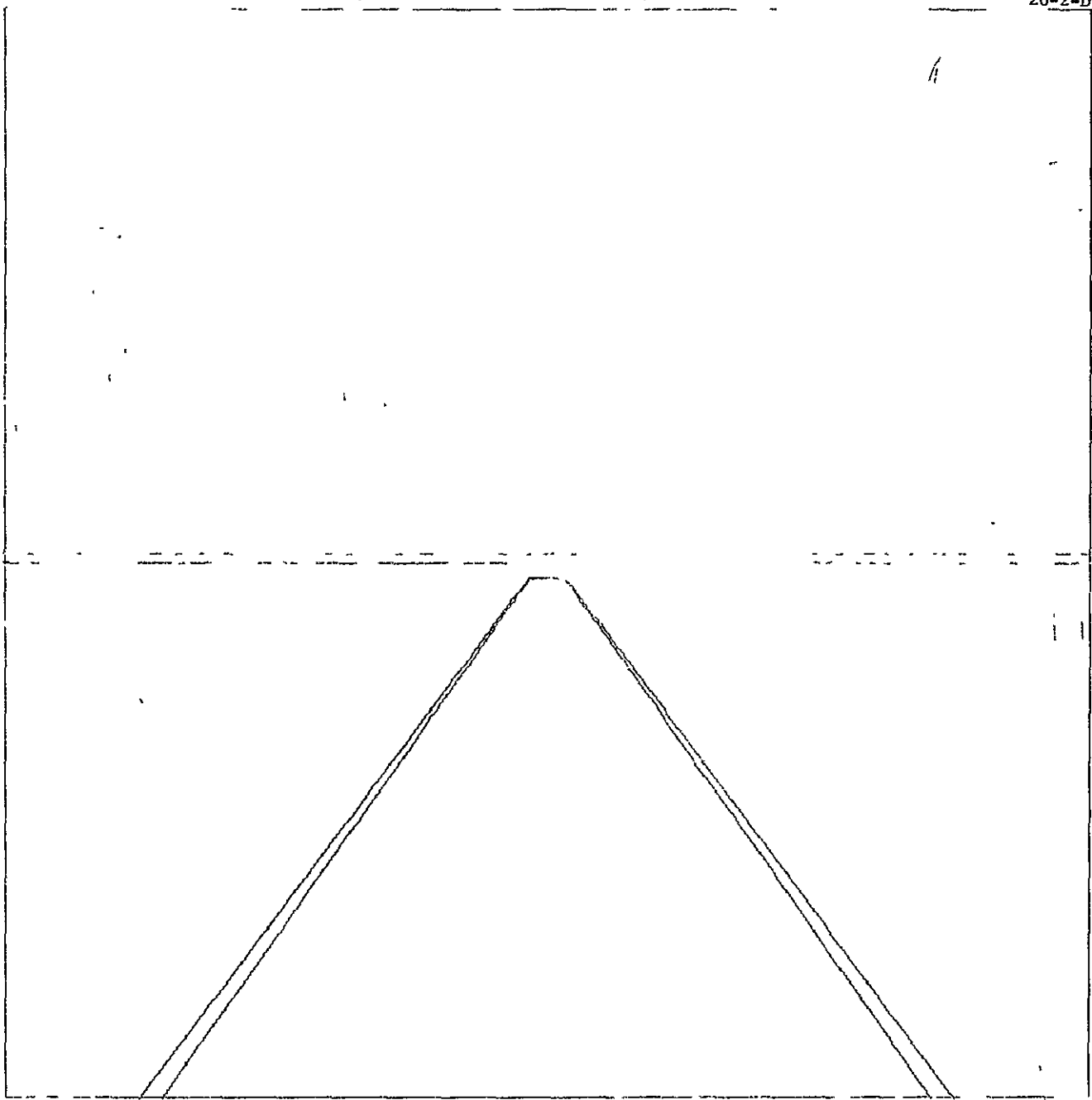
(b) Distance to TD = 1 mi.

Figure 4.- Continued.



(c) Distance to TD = 1/2 mi.

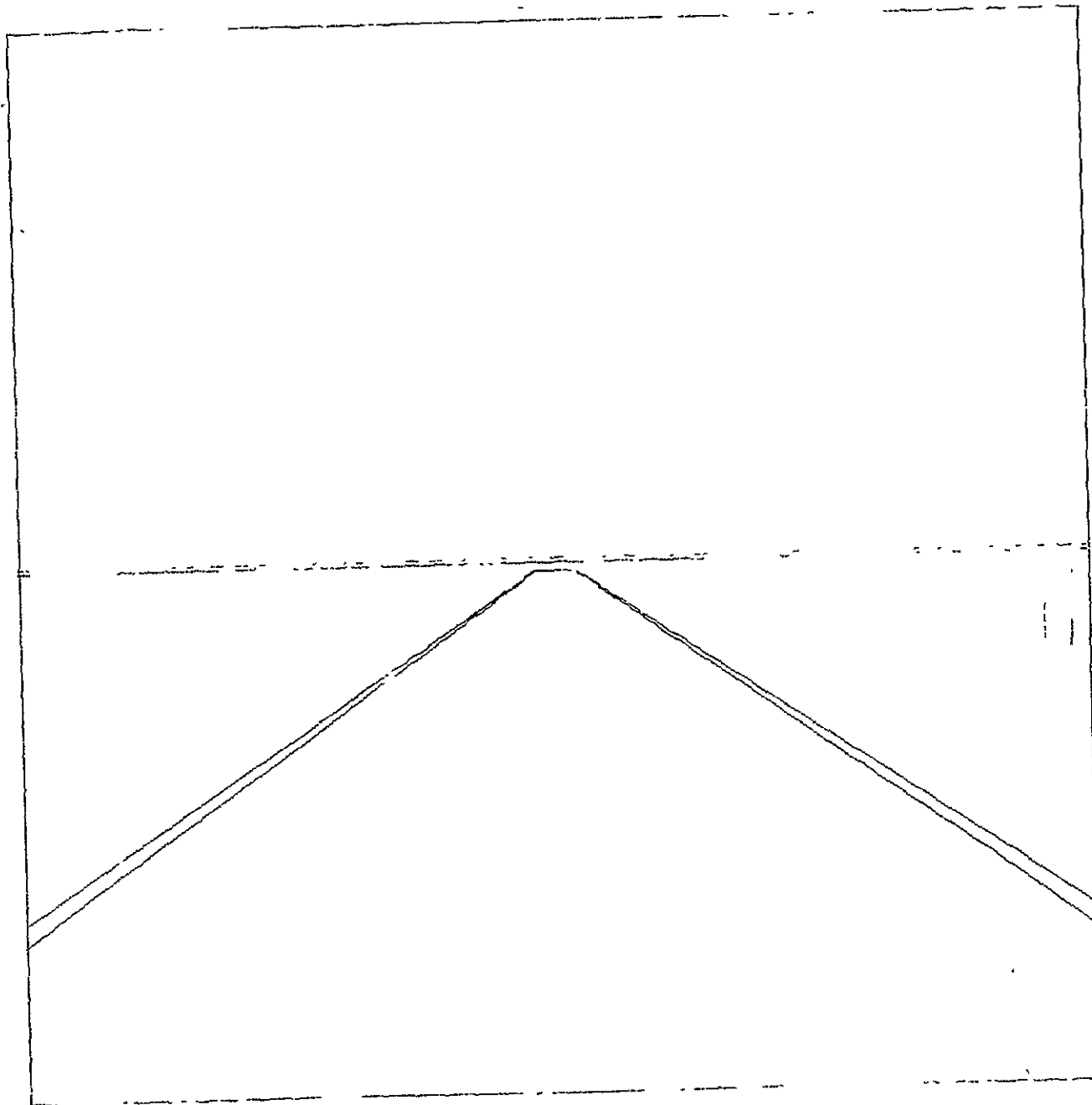
Figure 4.- Continued.



(d) Altitude = 100 ft.

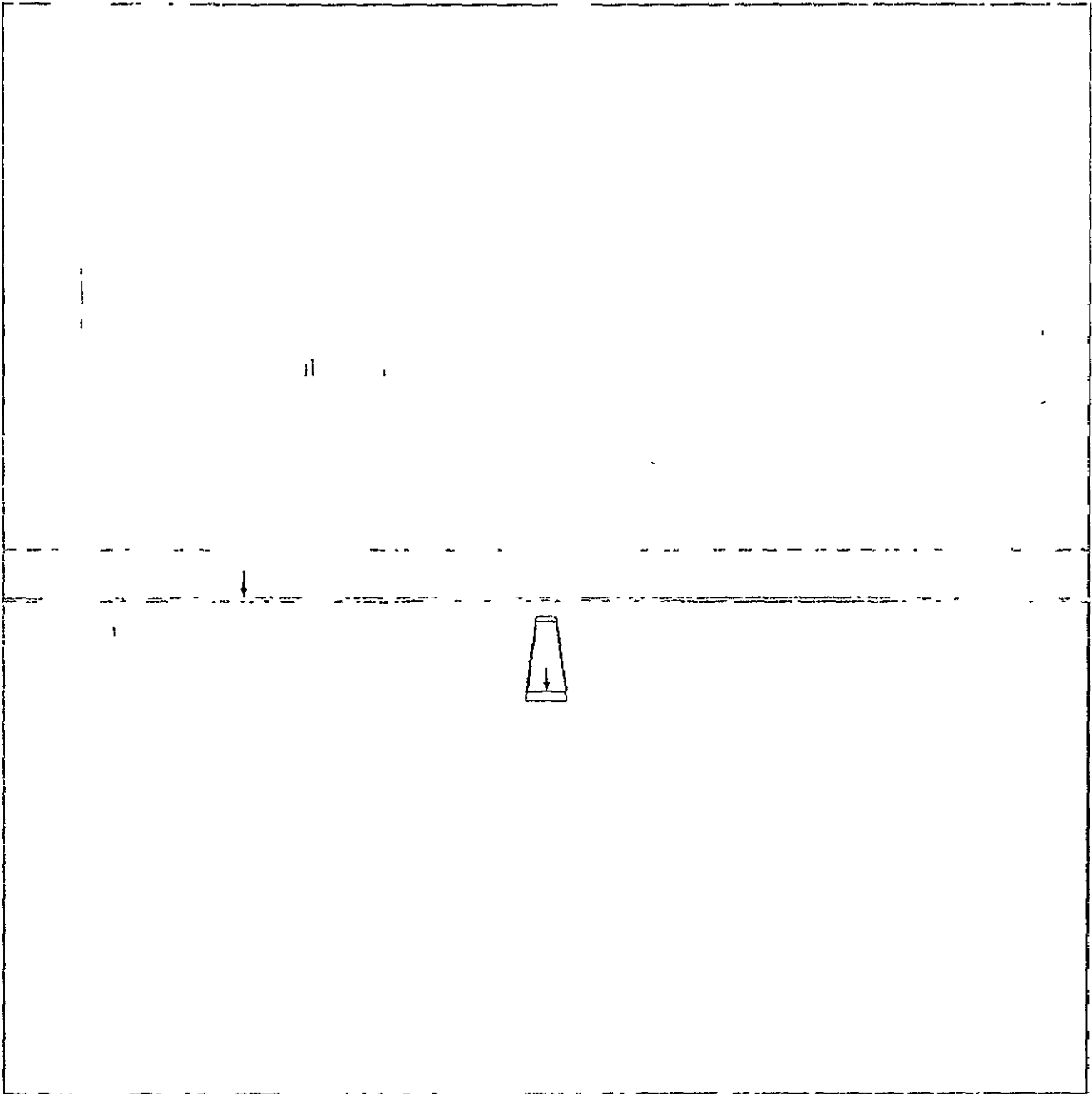
Figure 4.- Continued.

ORIGINAL PAGE IS
OF POOR QUALITY



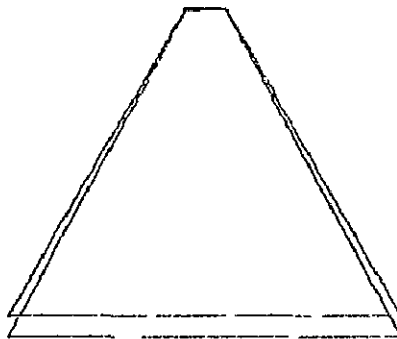
(e). Altitude = 50 ft.

Figure 4.- Concluded.



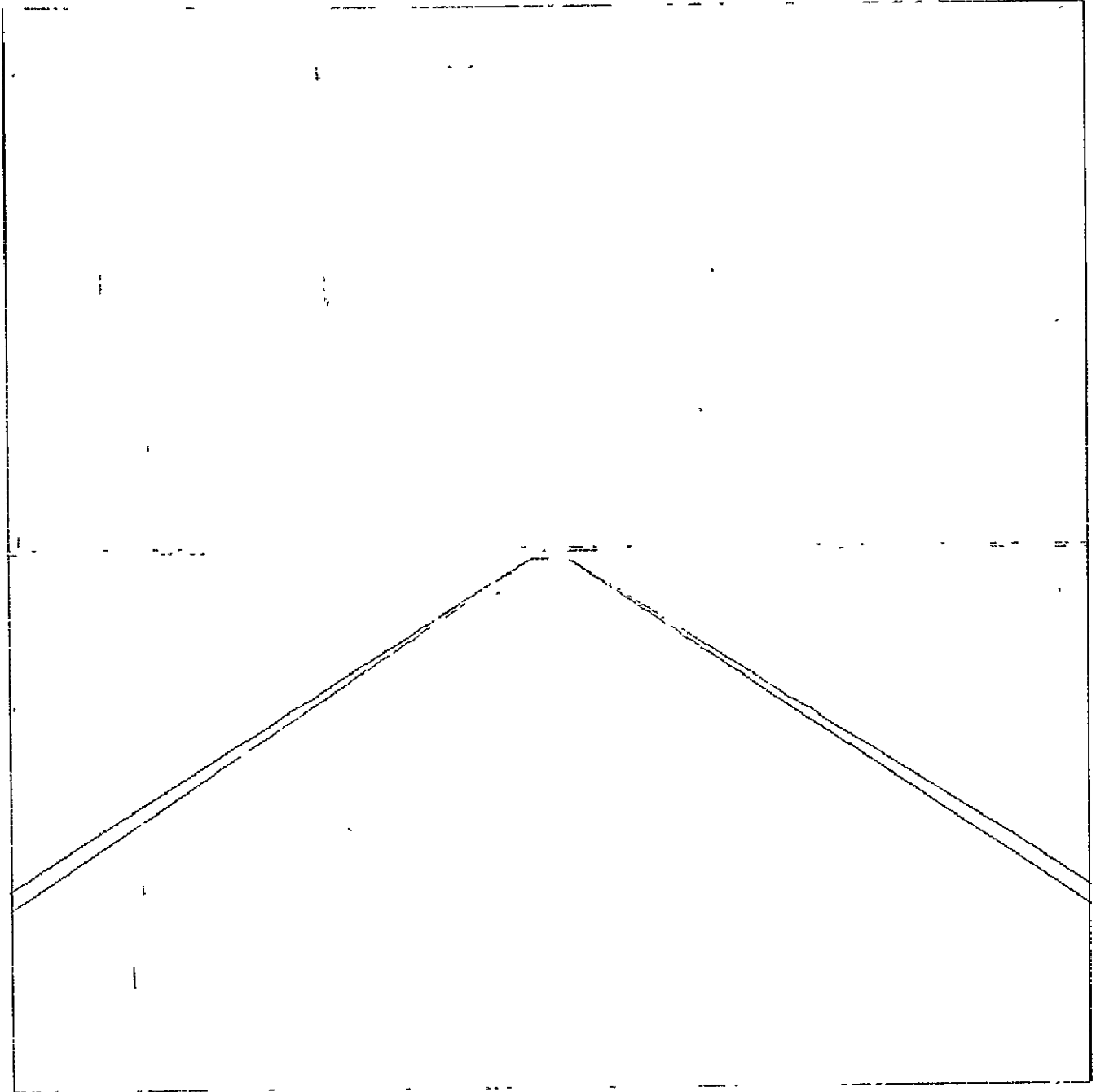
(a) Distance to TD = 2 mi.

Figure 5.- Aircraft on 2.83° glide slope.



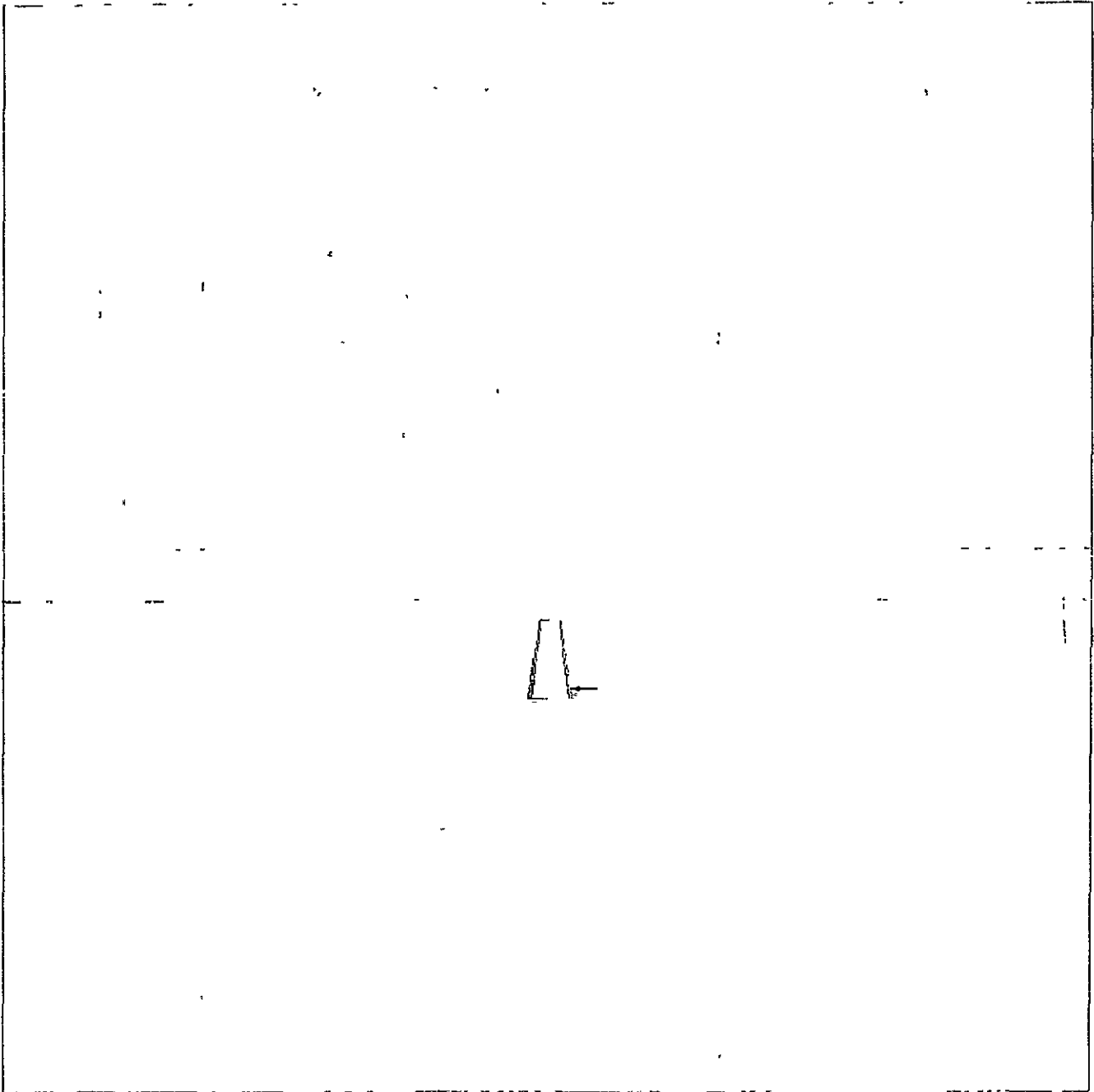
(b) Distance to TD = $1/2$ ml.

Figure 5.- Continued.



(c) Altitude = 50 ft.

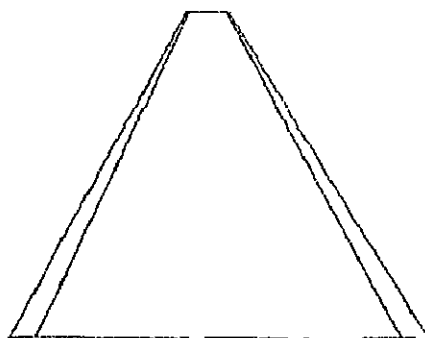
Figure 5.- Concluded.



(a) Distance to TD = 2 mi.

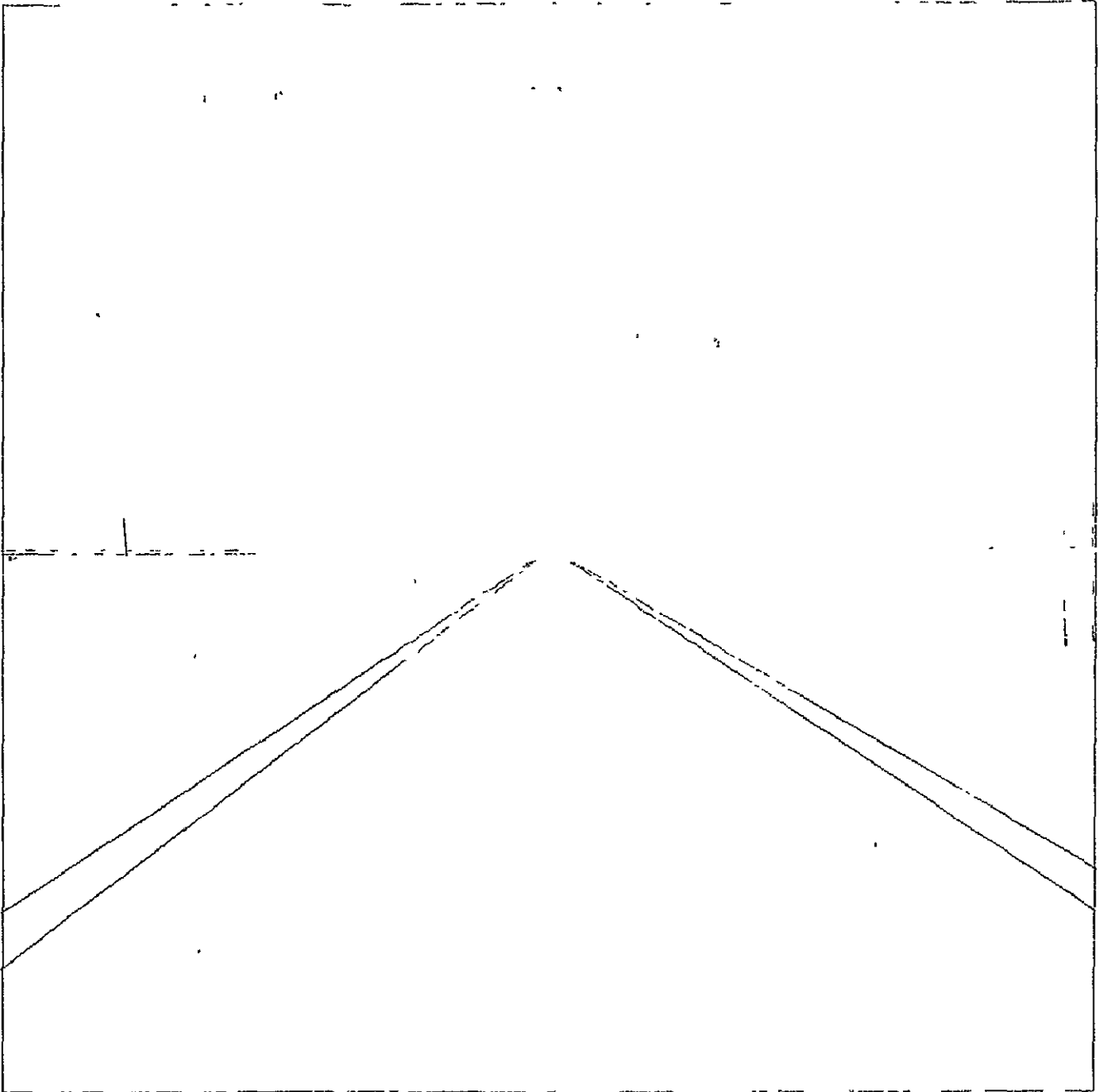
Figure 6.- Aircraft 10 ft. to left of centerline.

ORIGINAL PAGE IS
OF POOR QUALITY



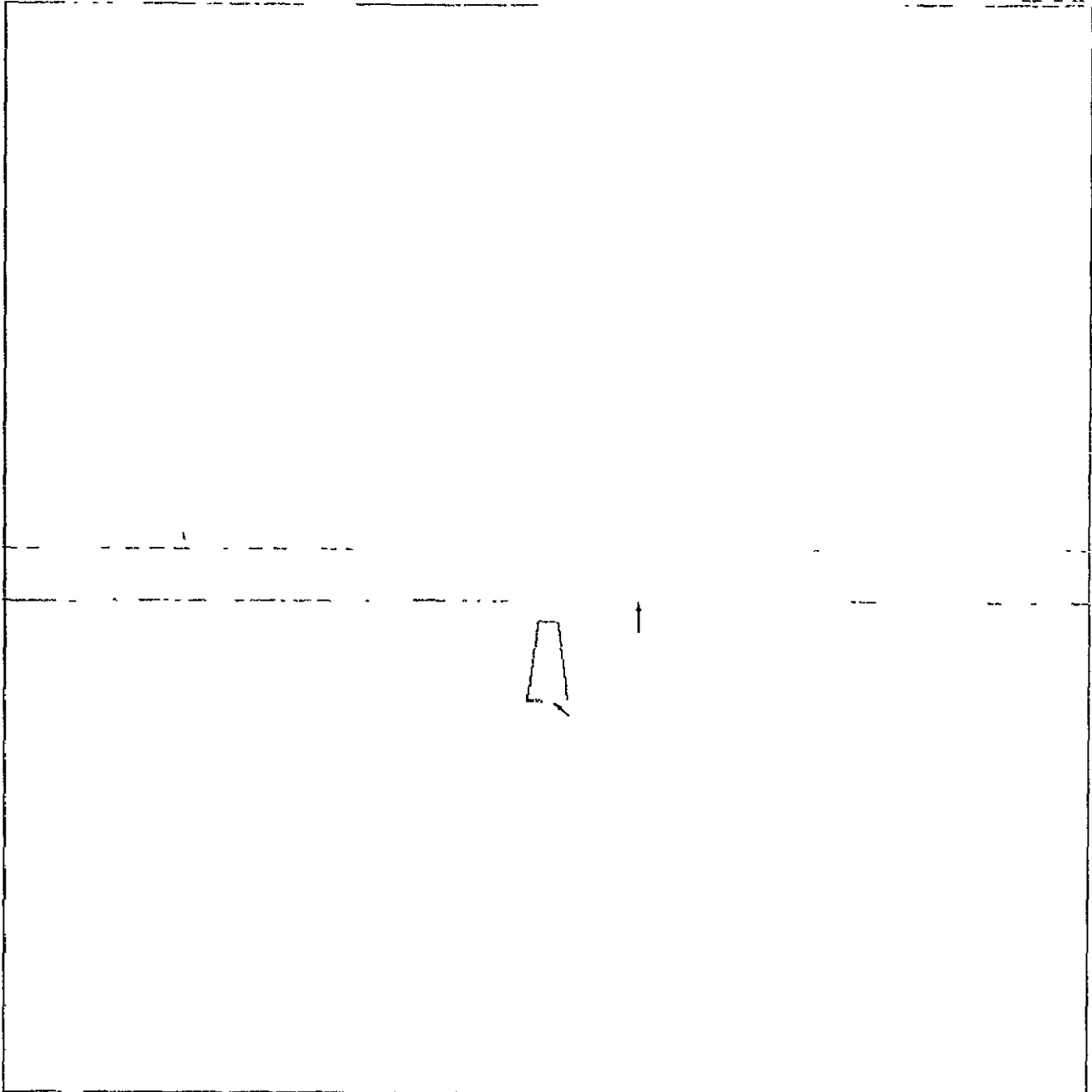
(b) Distance to TD = $1/2$ mi.

Figure 6.- Continued.



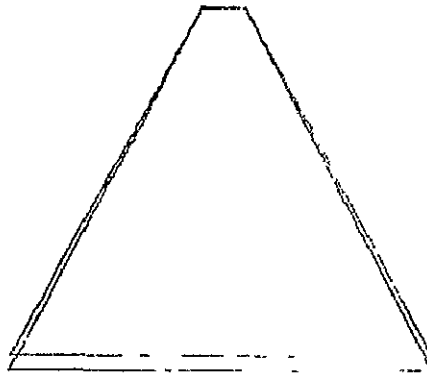
(c) Altitude = 50 ft.

Figure 6.- Concluded.



(a) Distance to TD = 2 mi.

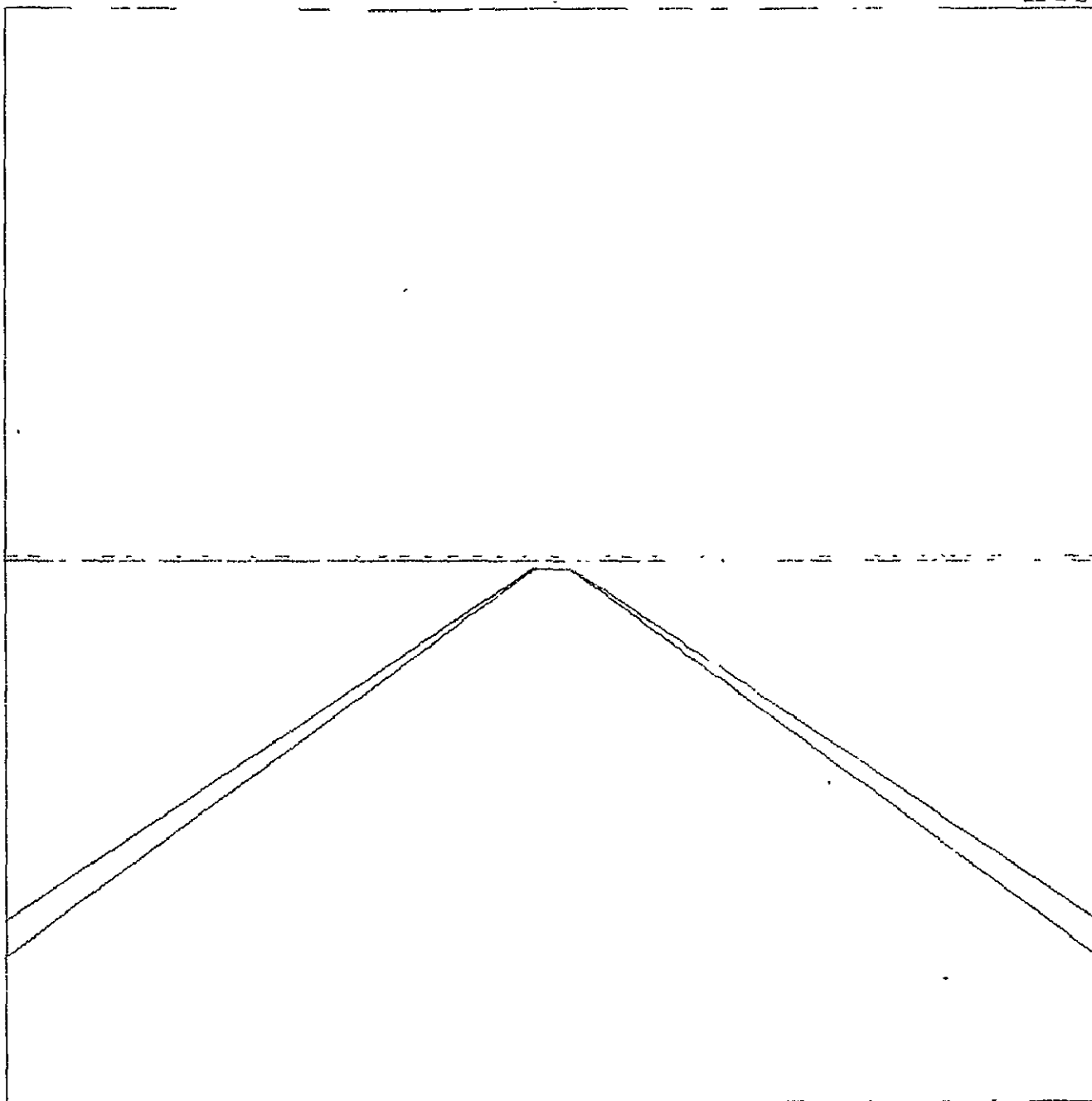
Figure 7.- Aircraft 5 ft. above 3° glide slope.



(b) Distance to TD = $1/2$ mi.

Figure 7.- Continued.

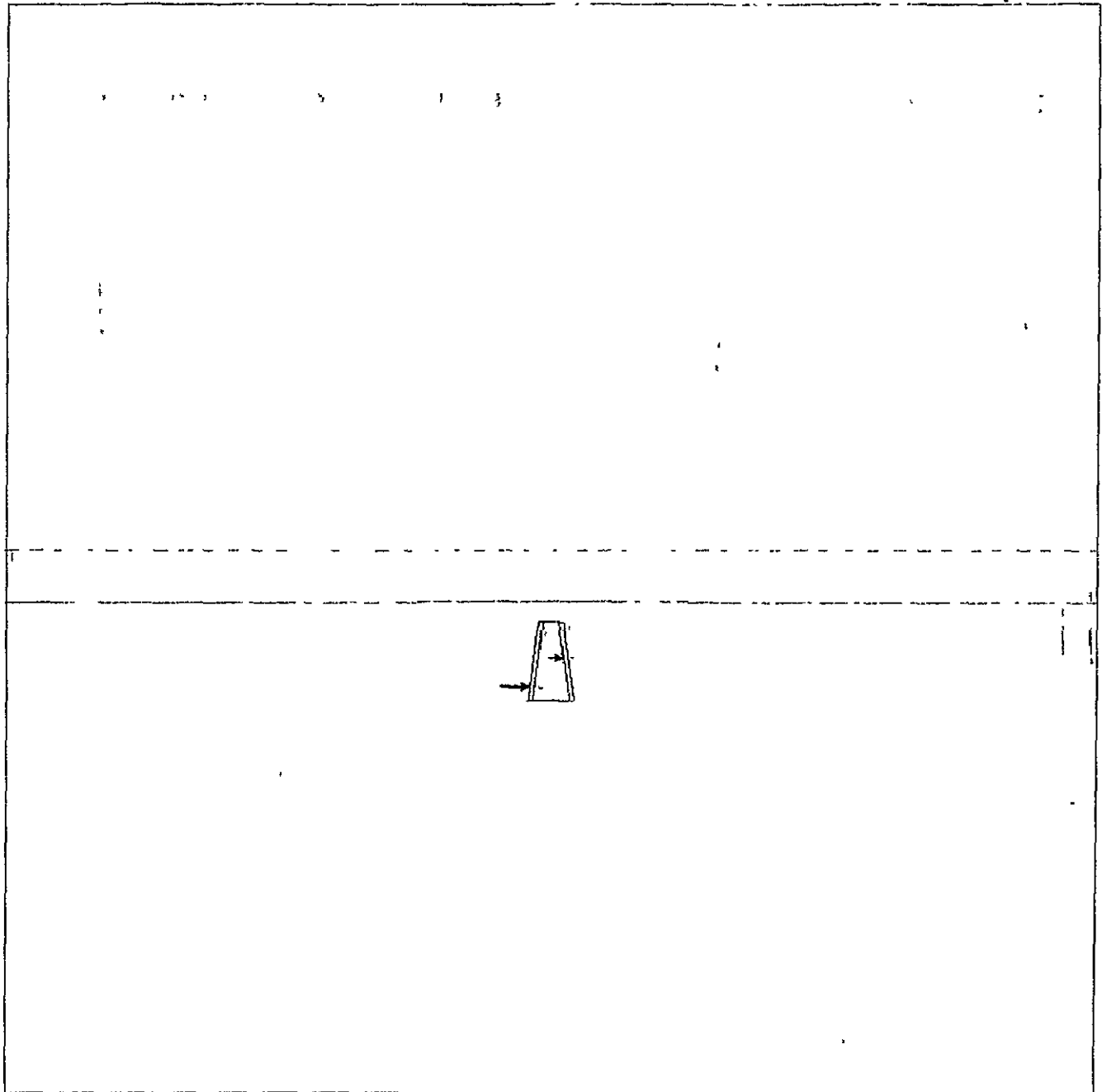
ORIGINAL PAGE IS
OF POOR QUALITY



(c) Altitude = 50 ft.

Figure 7.- Concluded.

ORIGINAL PAGE IS
OF POOR QUALITY



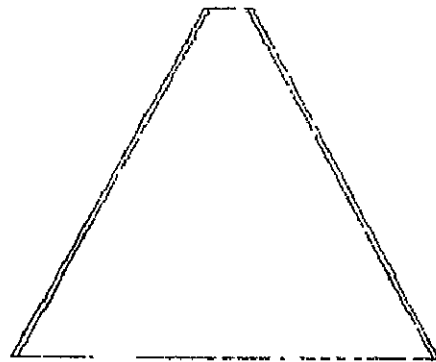
(a) Distance to TD = 2 mi.

Figure 8.- Aircraft on glide path, $Y = 0.1^\circ$, $P = R = 0^\circ$.



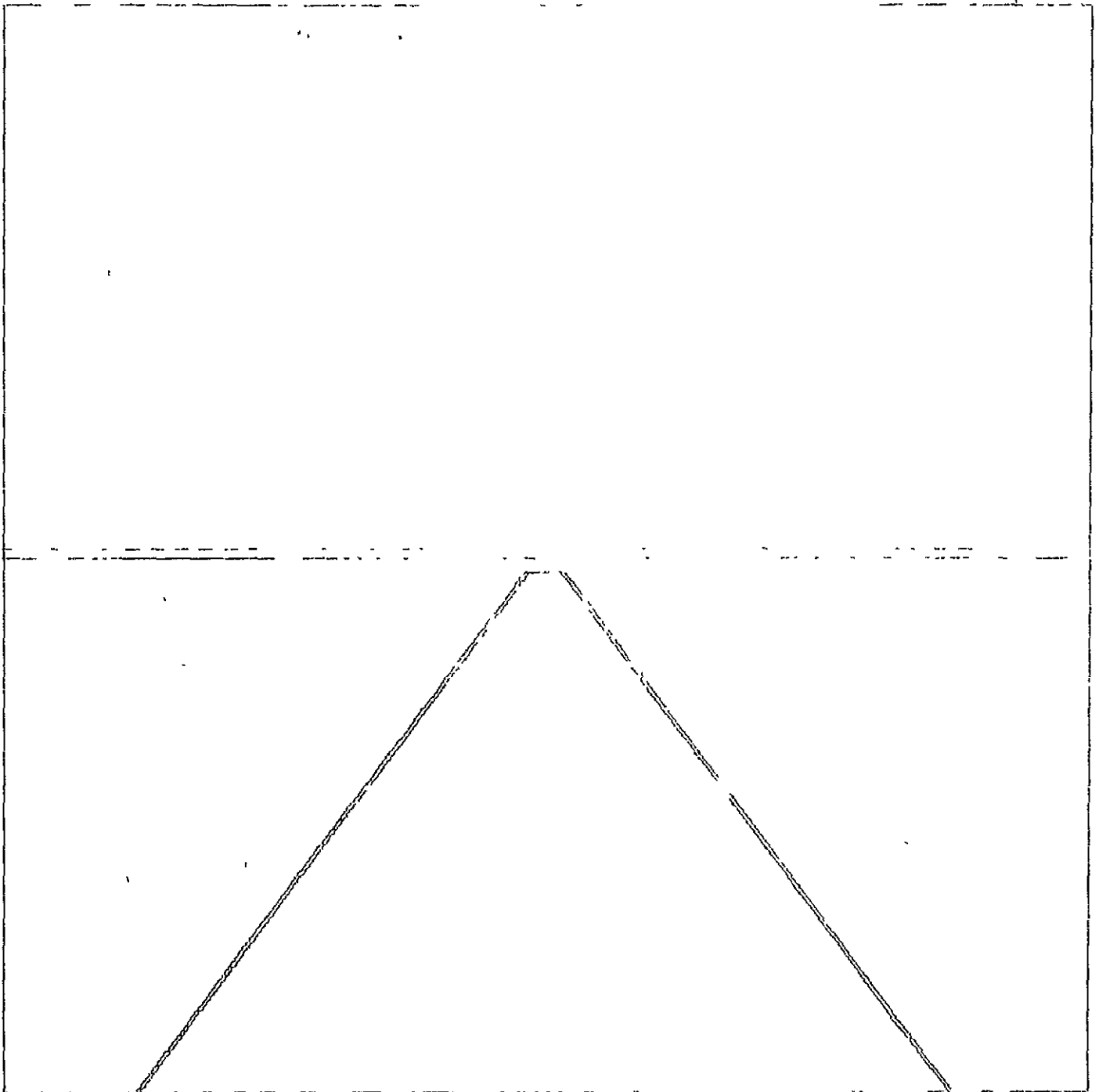
(b) Distance to TD = 1 mi.

Figure 8.- Continued.



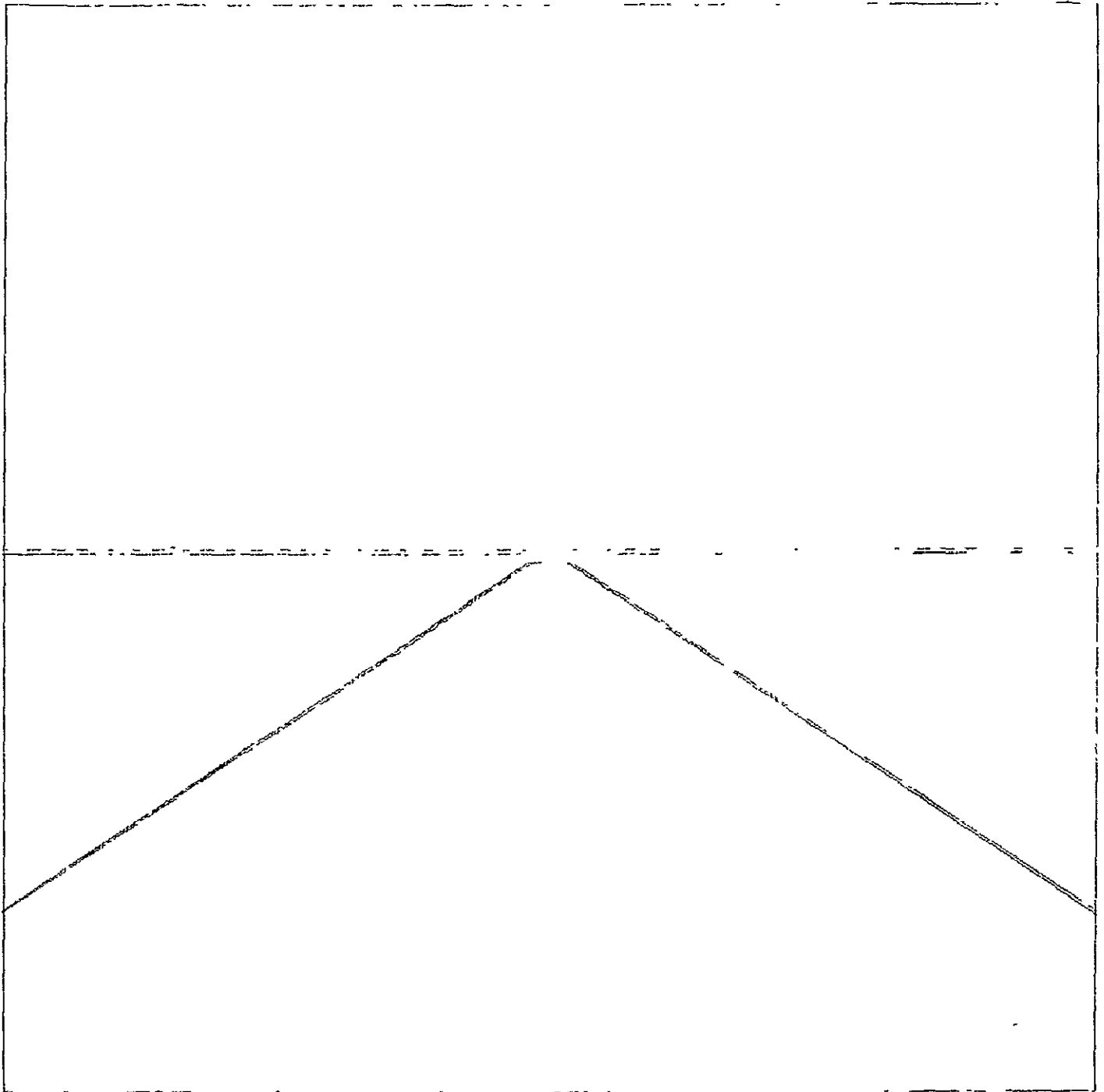
(c) Distance to TD = $1/2$ mi.

Figure 8.- Continued.



(d) Altitude = 100 ft.

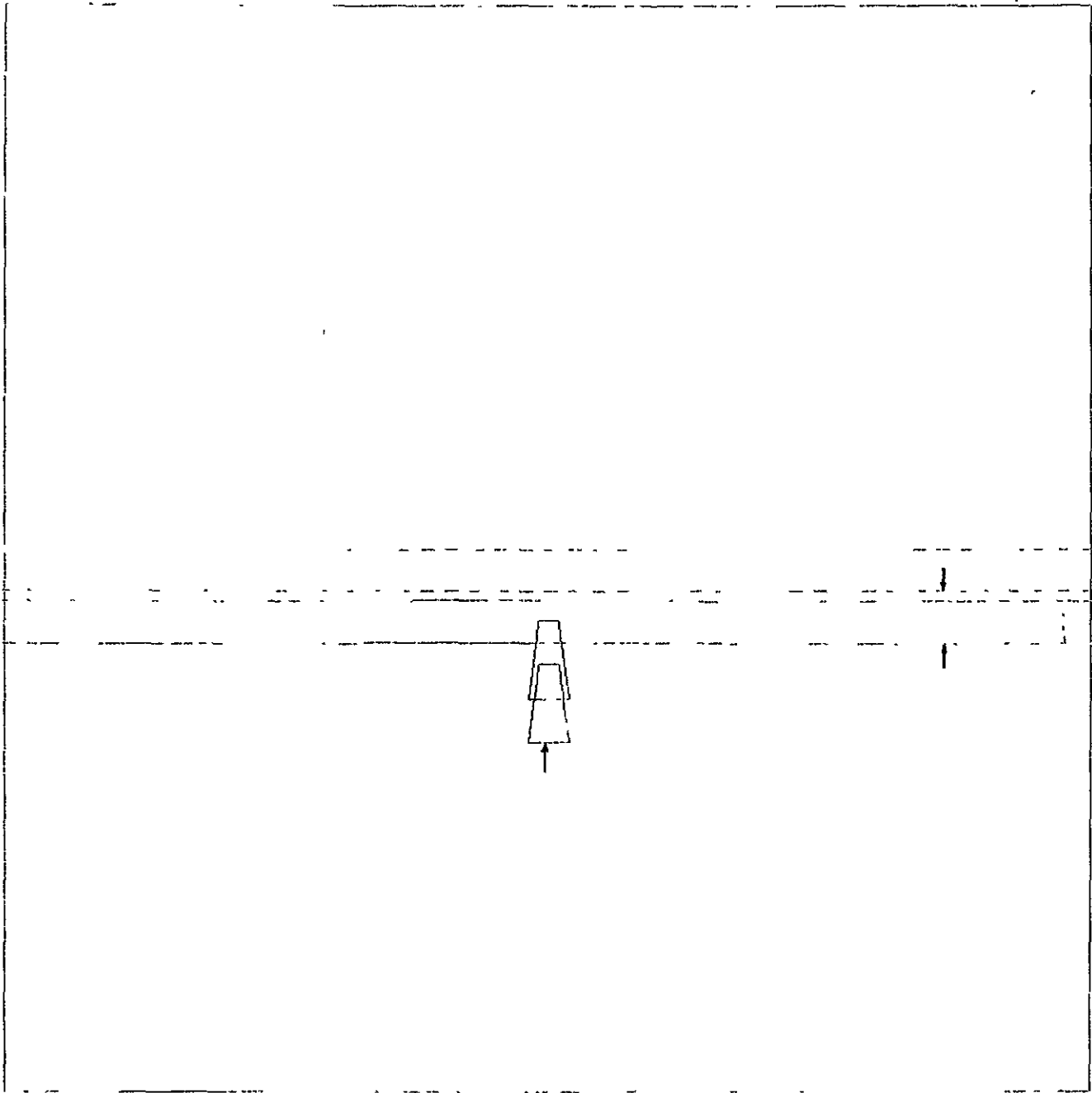
Figure 8.- Continued.



(e) Altitude = 50 ft.

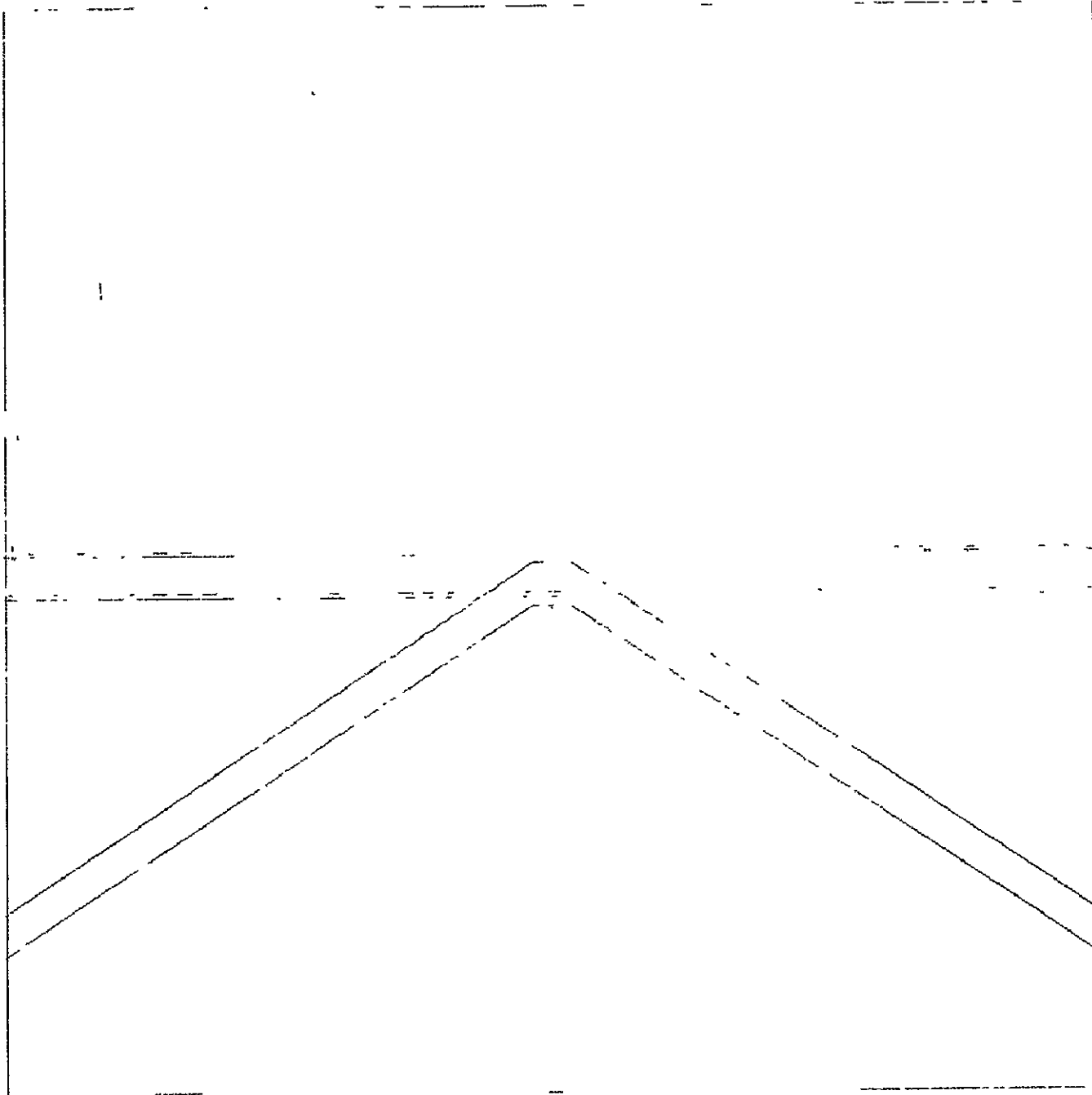
Figure 8.- Concluded.

ORIGINAL PAGE IS
OF POOR QUALITY



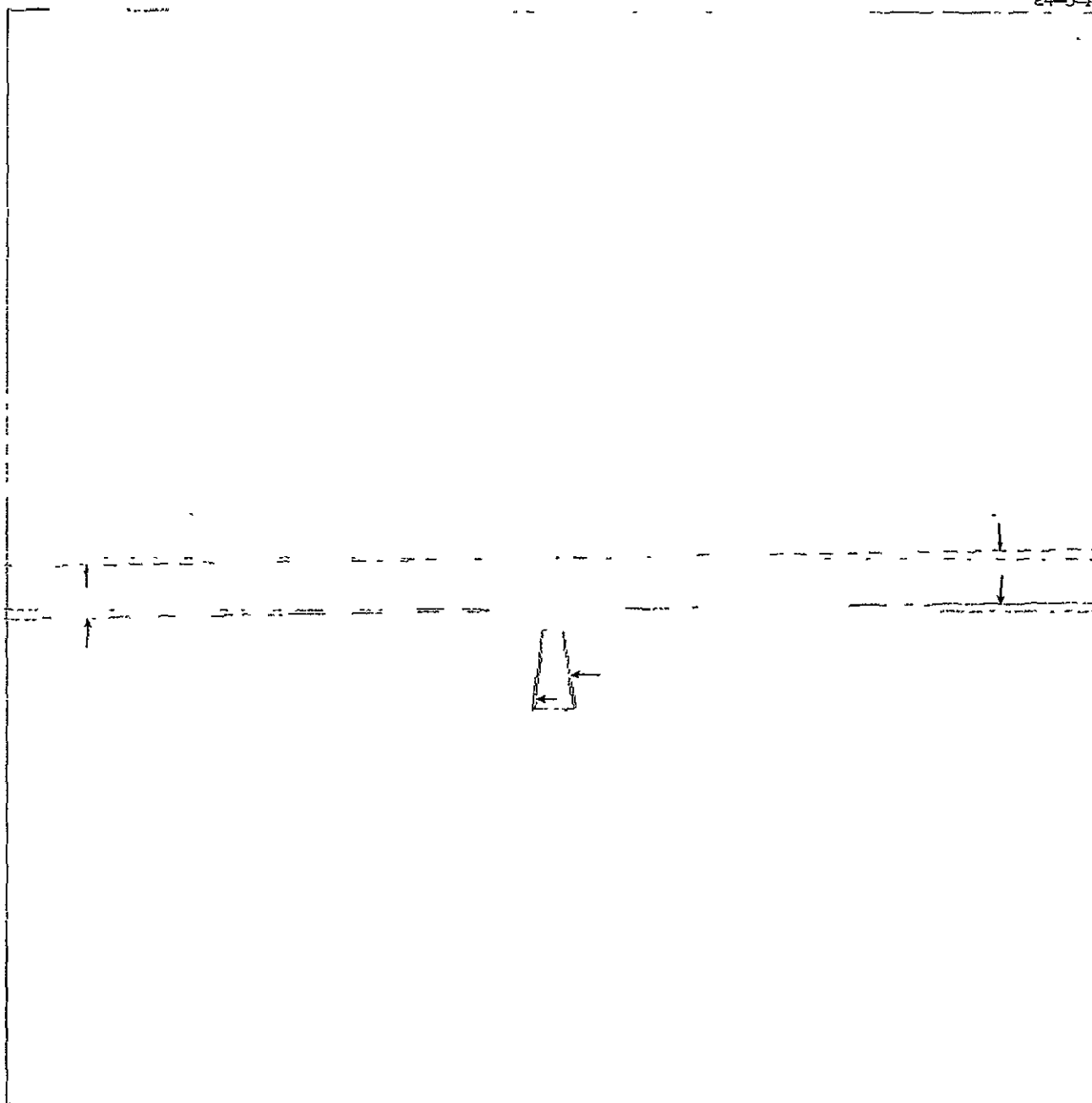
(a) Distance to TD = 2 mi

Figure 9 - Aircraft on glide path, $P = 1^\circ$, $Y = R = 0^\circ$.



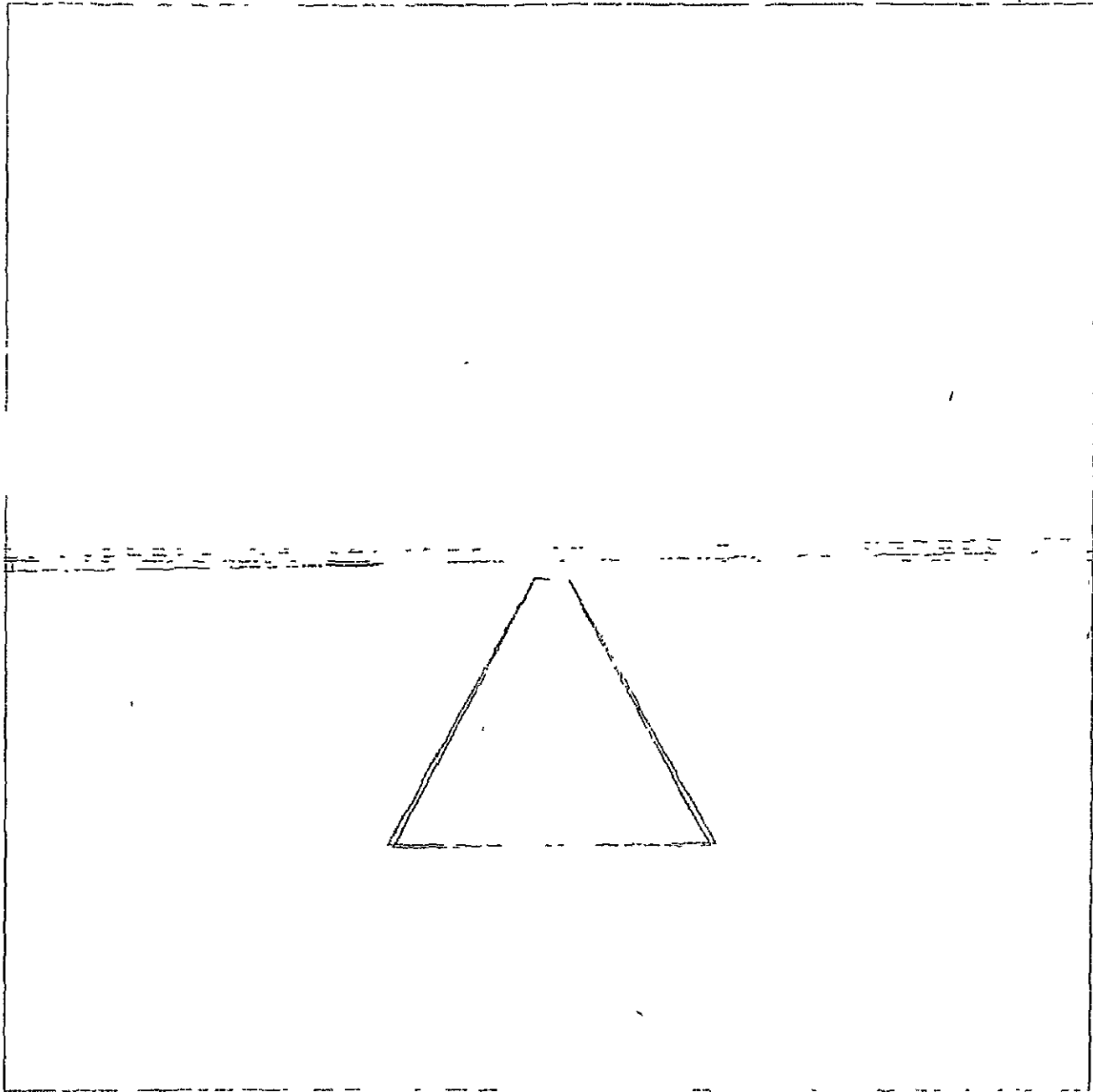
(b) Altitude = 50 ft.

Figure 9.- Concluded.



(a) Distance to TD = 2 mi.

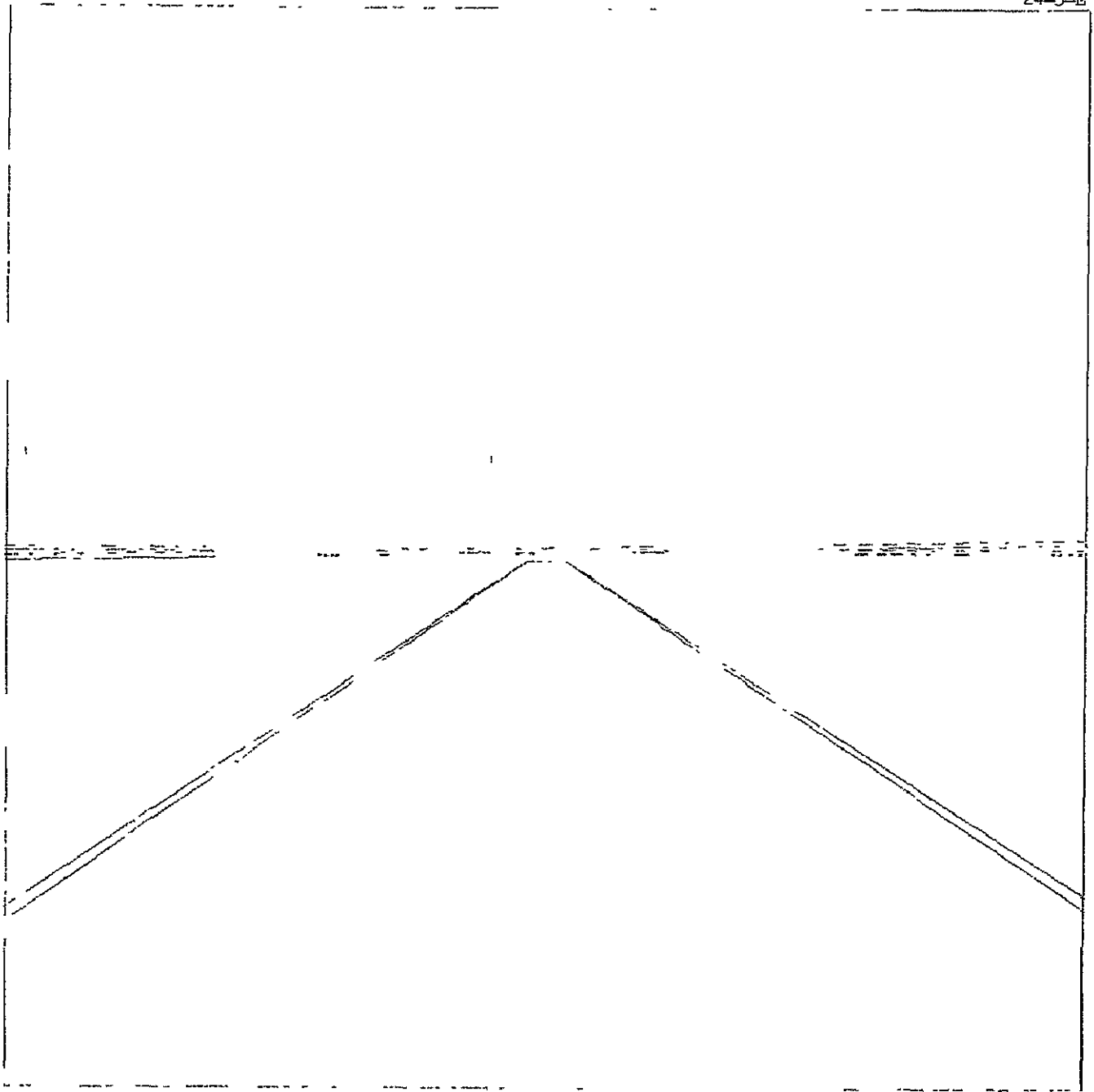
Figure 10.- Aircraft on glide path, $R = 1^\circ$, $Y = P = 0^\circ$.



(b) Distance to TD = $1/2$ mi.

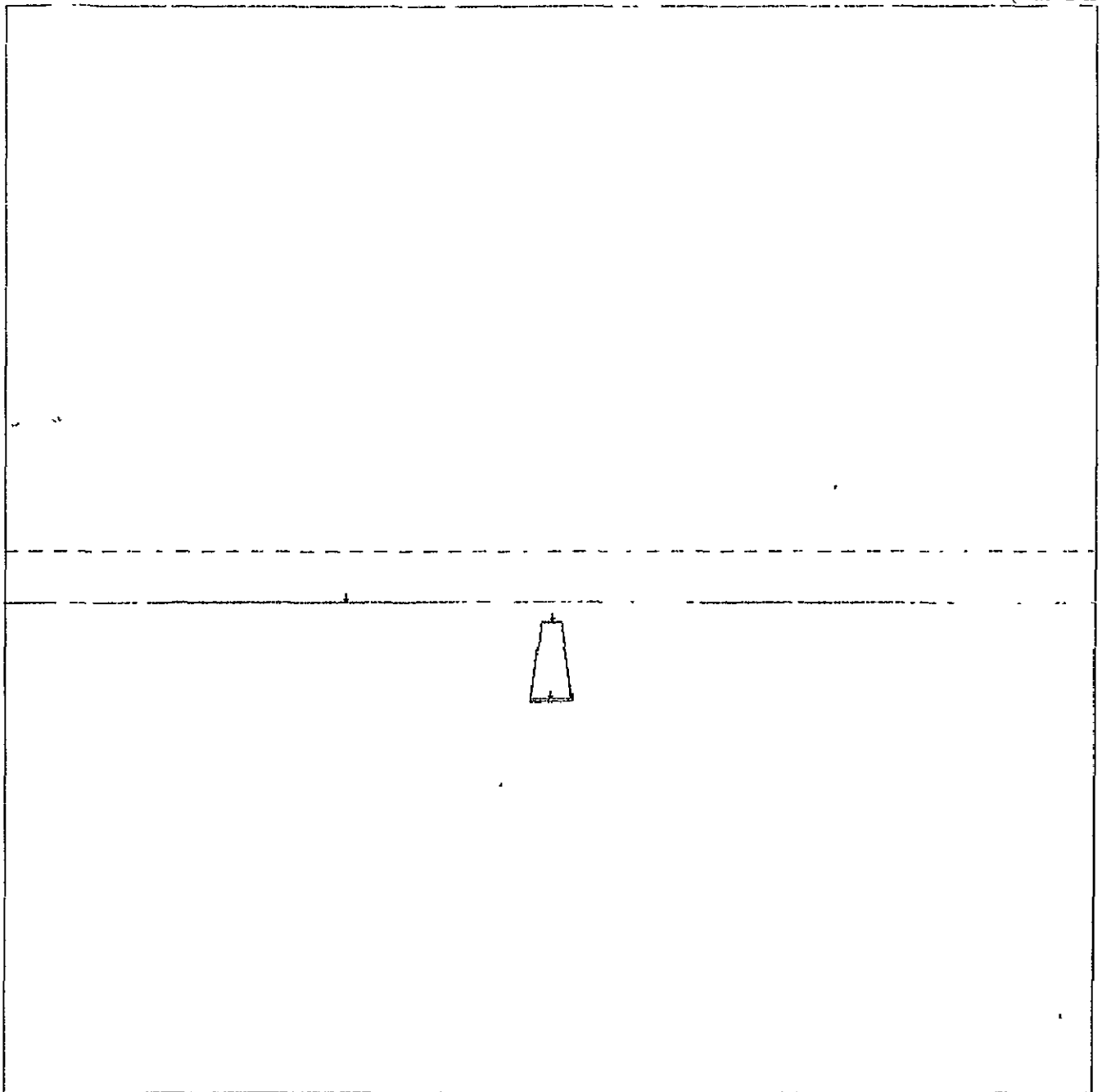
Figure 10.- Continued.

ORIGINAL PAGE IS
OF POOR QUALITY



(c) Altitude \approx 50 ft.

Figure 10.- Concluded.



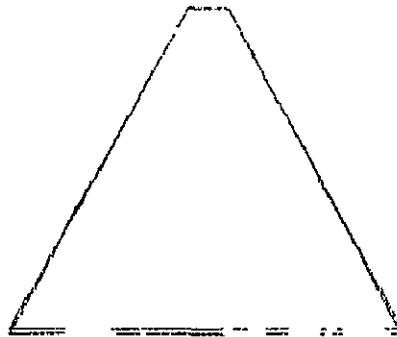
(a) Distance to TD = 2 mi.

Figure 11.- Range error of 5 ft + 1%, aircraft on glide path.



(b) Distance to TD = 1 mi.

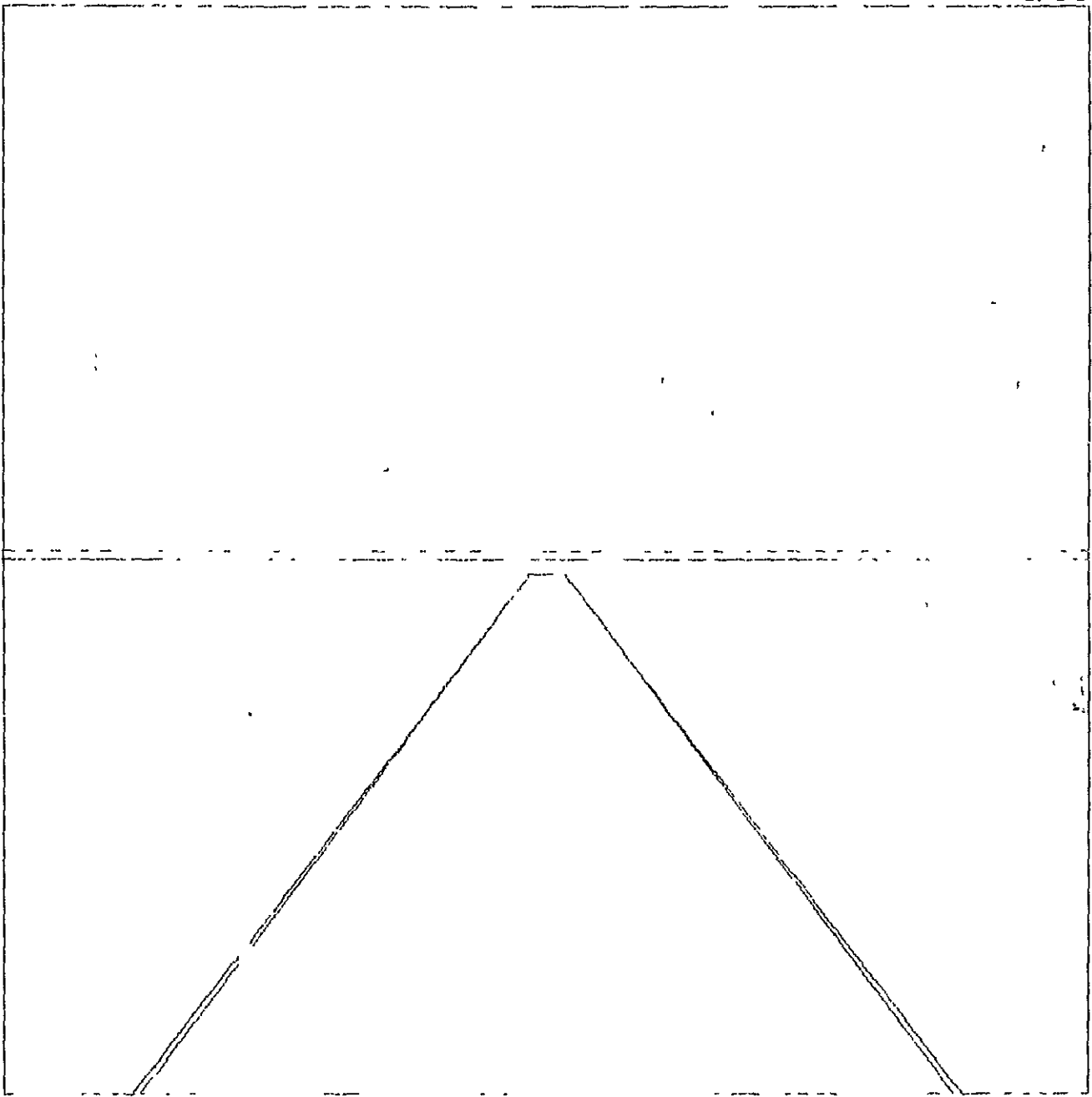
Figure 11.- Continued.



(c) Distance to touchdown = $1/2$ ml.

Figure 11.- Continued.

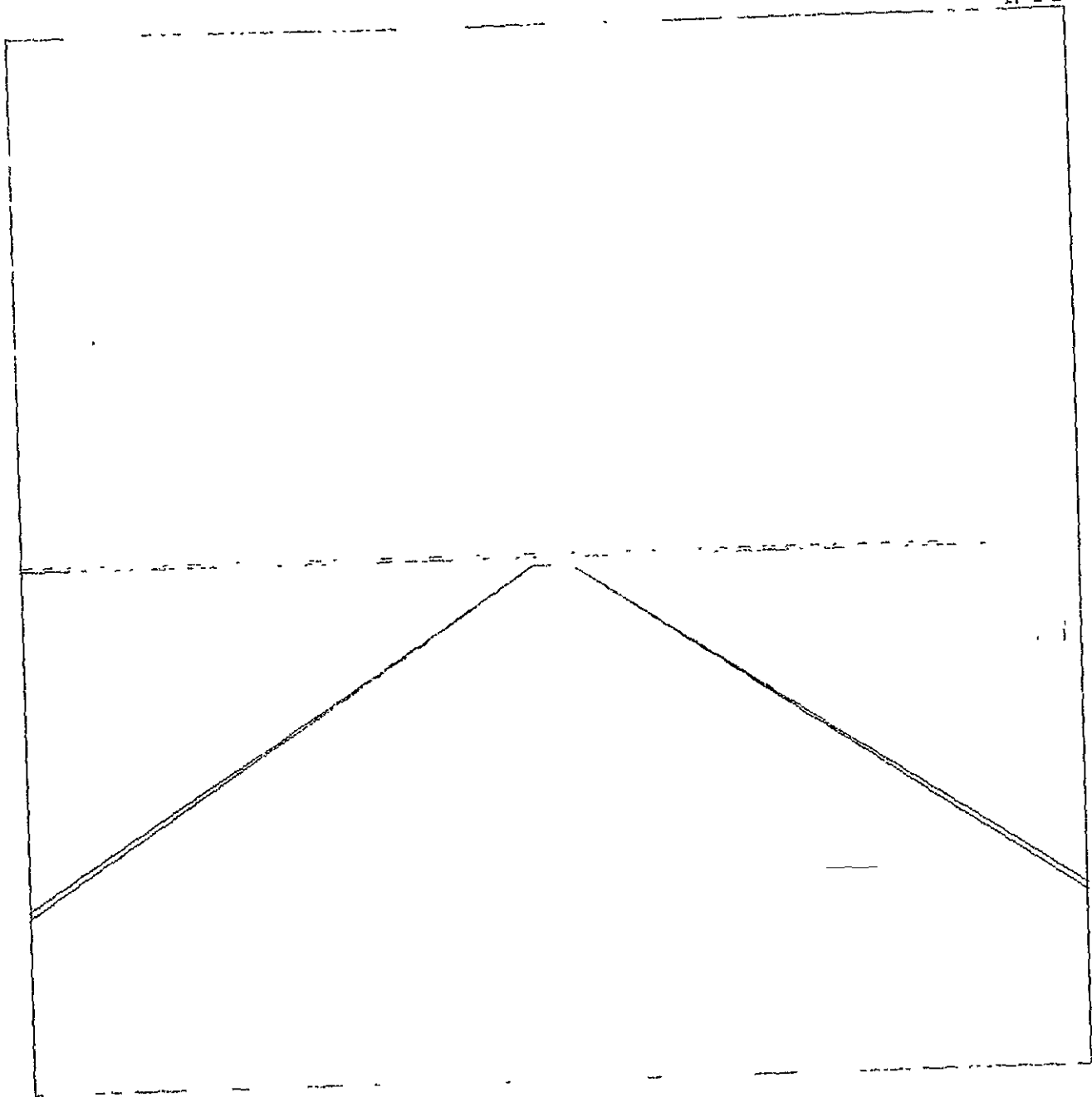
ORIGINAL PAGE IS
OF POOR QUALITY



(d) Altitude \approx 100 ft.

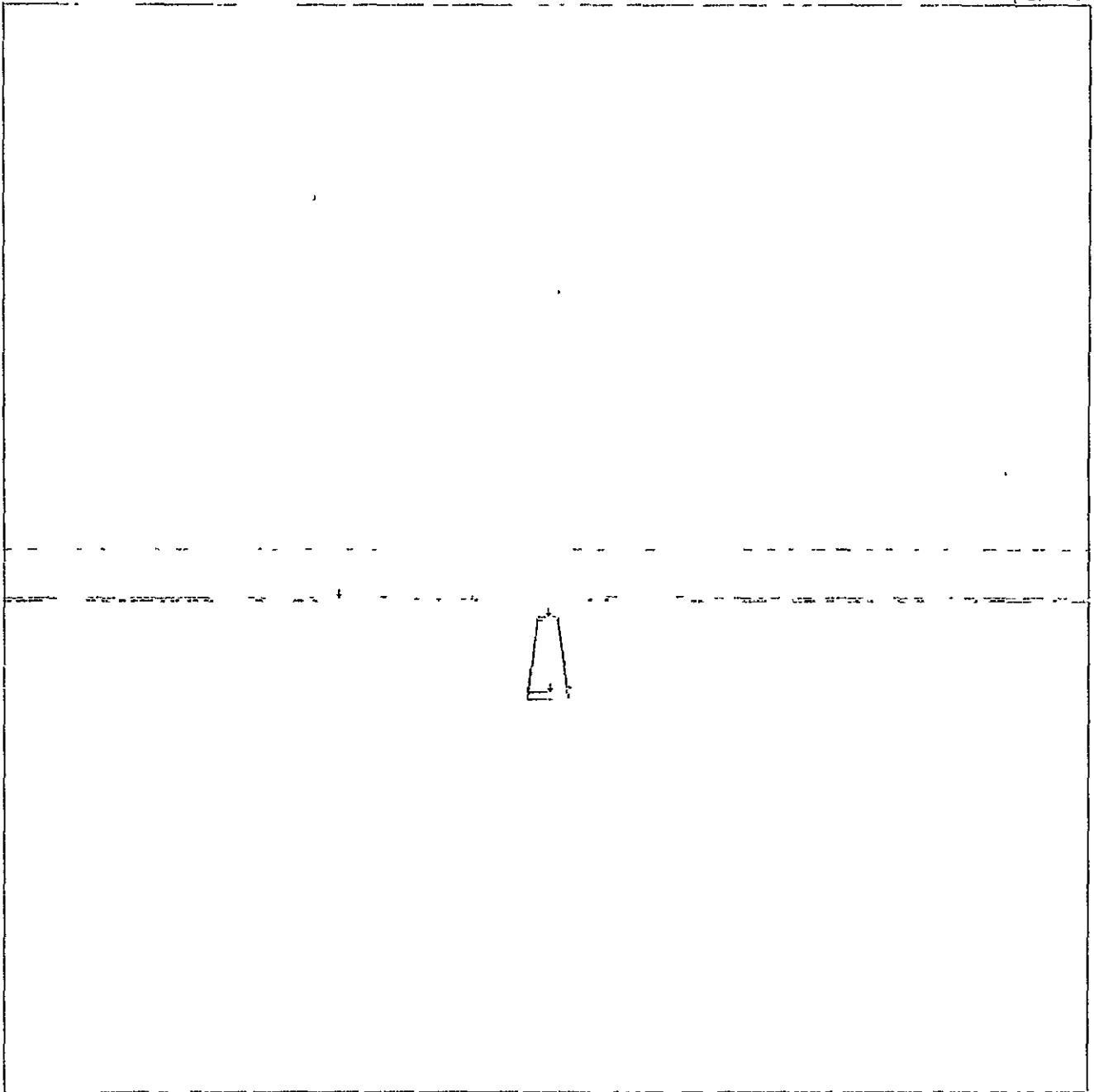
Figure 11.- Continued.

ORIGINAL PAGE IS
OF POOR QUALITY



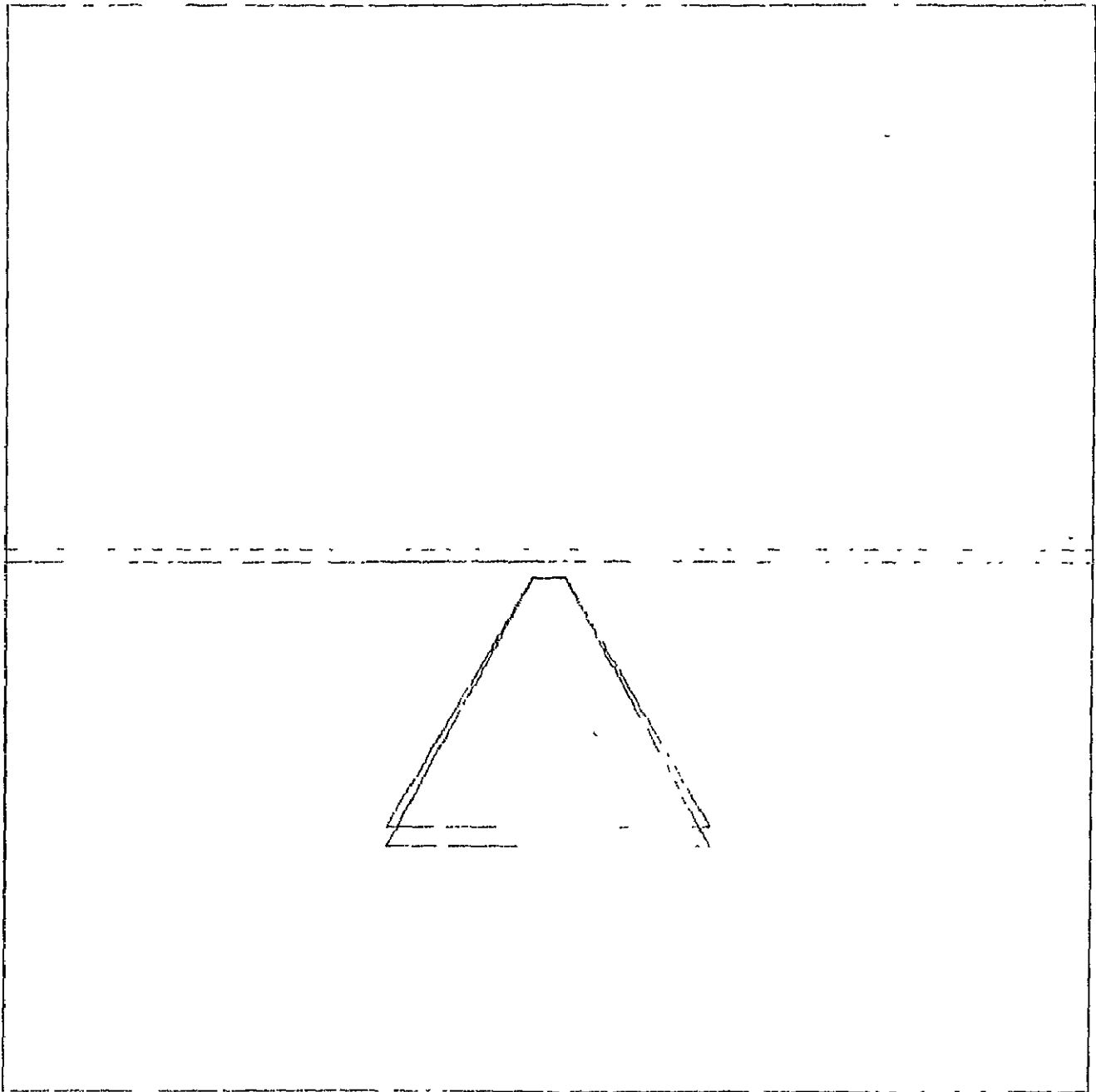
(e) Altitude = 50 ft

Figure 11.- Concluded.



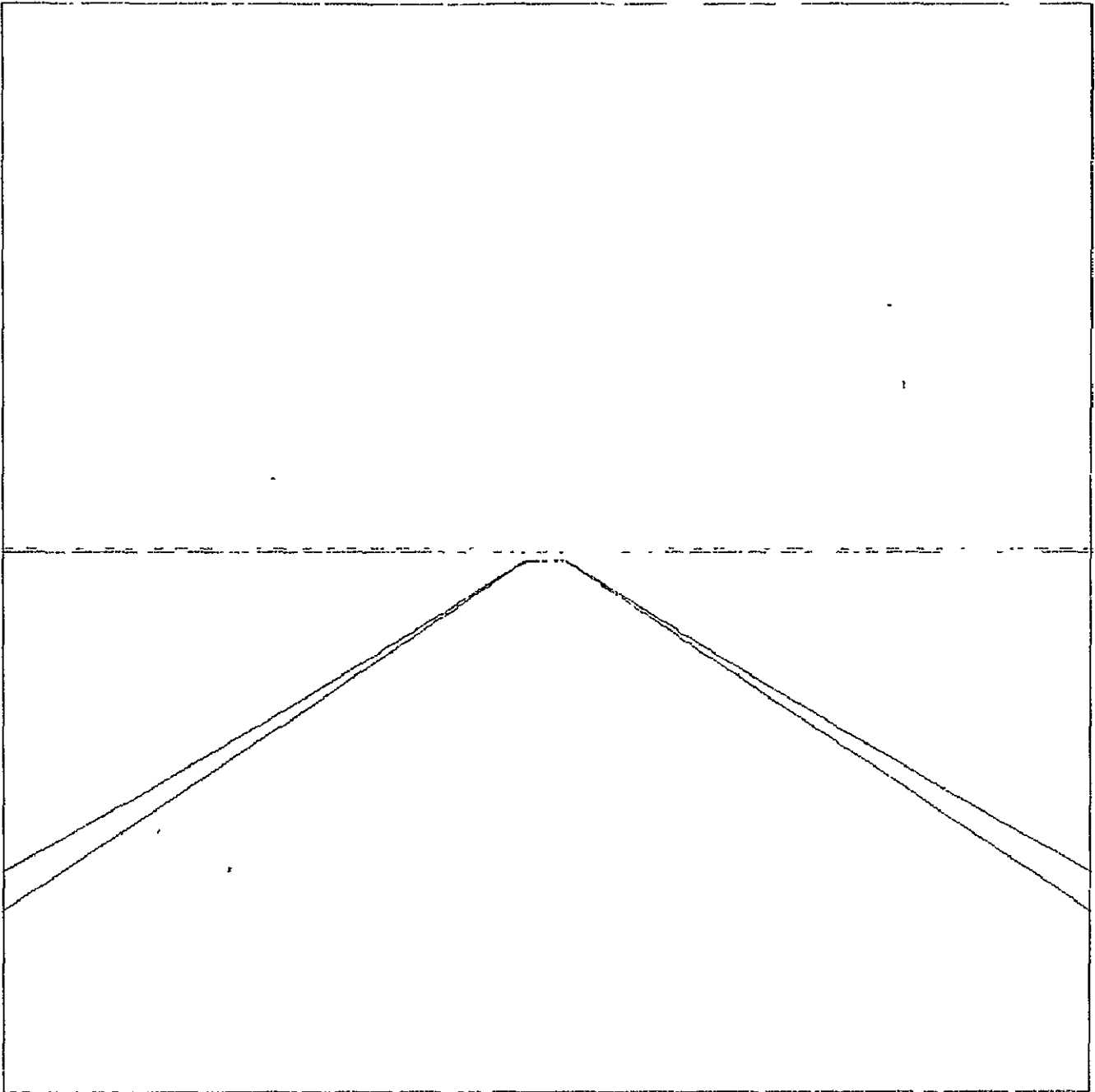
(a) Distance to TD = 2 mi.

Figure 12.- Range error of 25 ft. + 5%, aircraft on glide path.



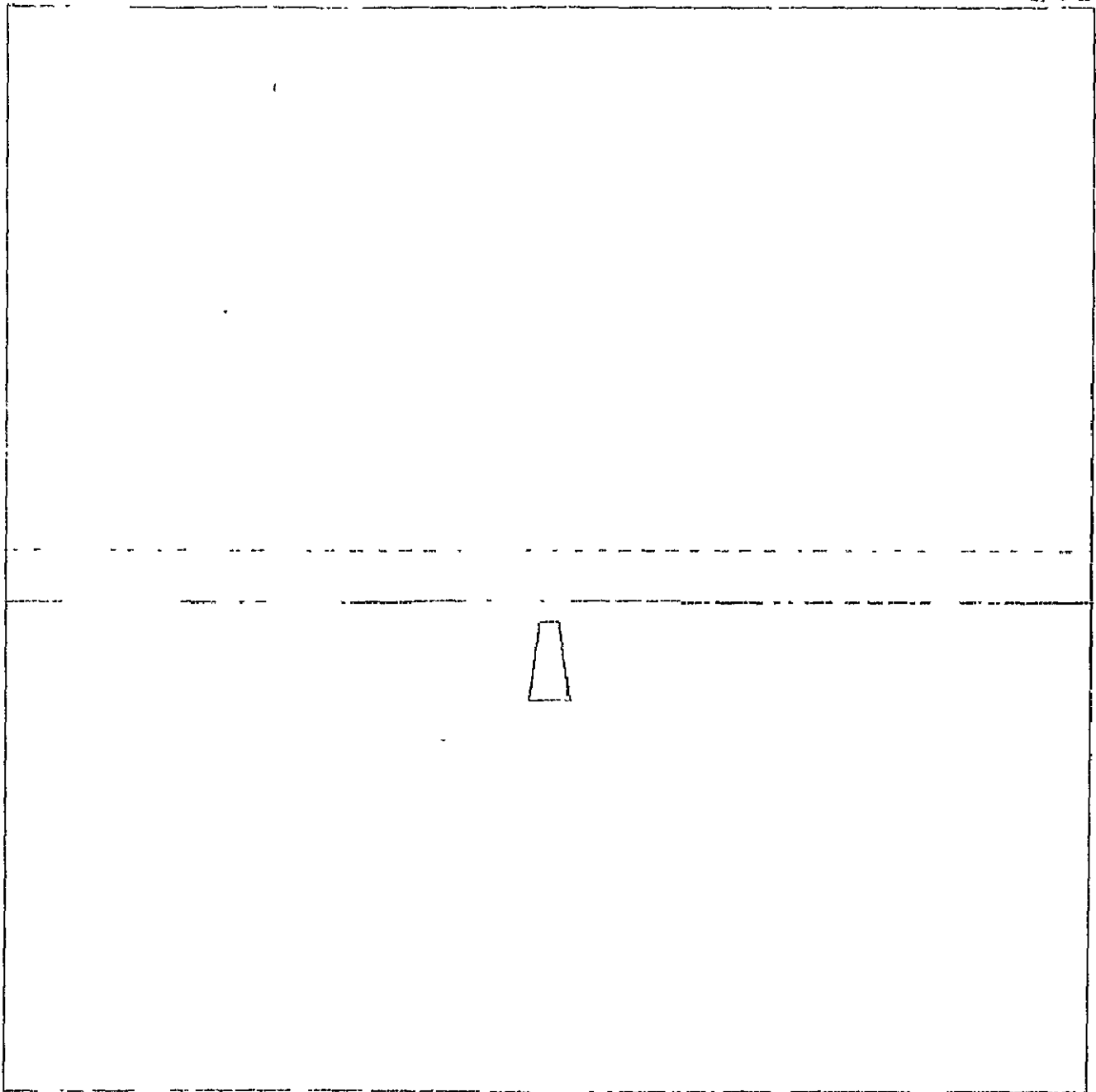
(b) Distance to TD = 1/2 mi.

Figure 12.- Continued.



(c) Altitude = 50 ft.

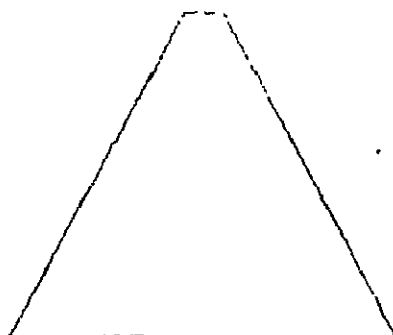
Figure 12.- Concluded.



(a) Distance to TD = 2 mi.

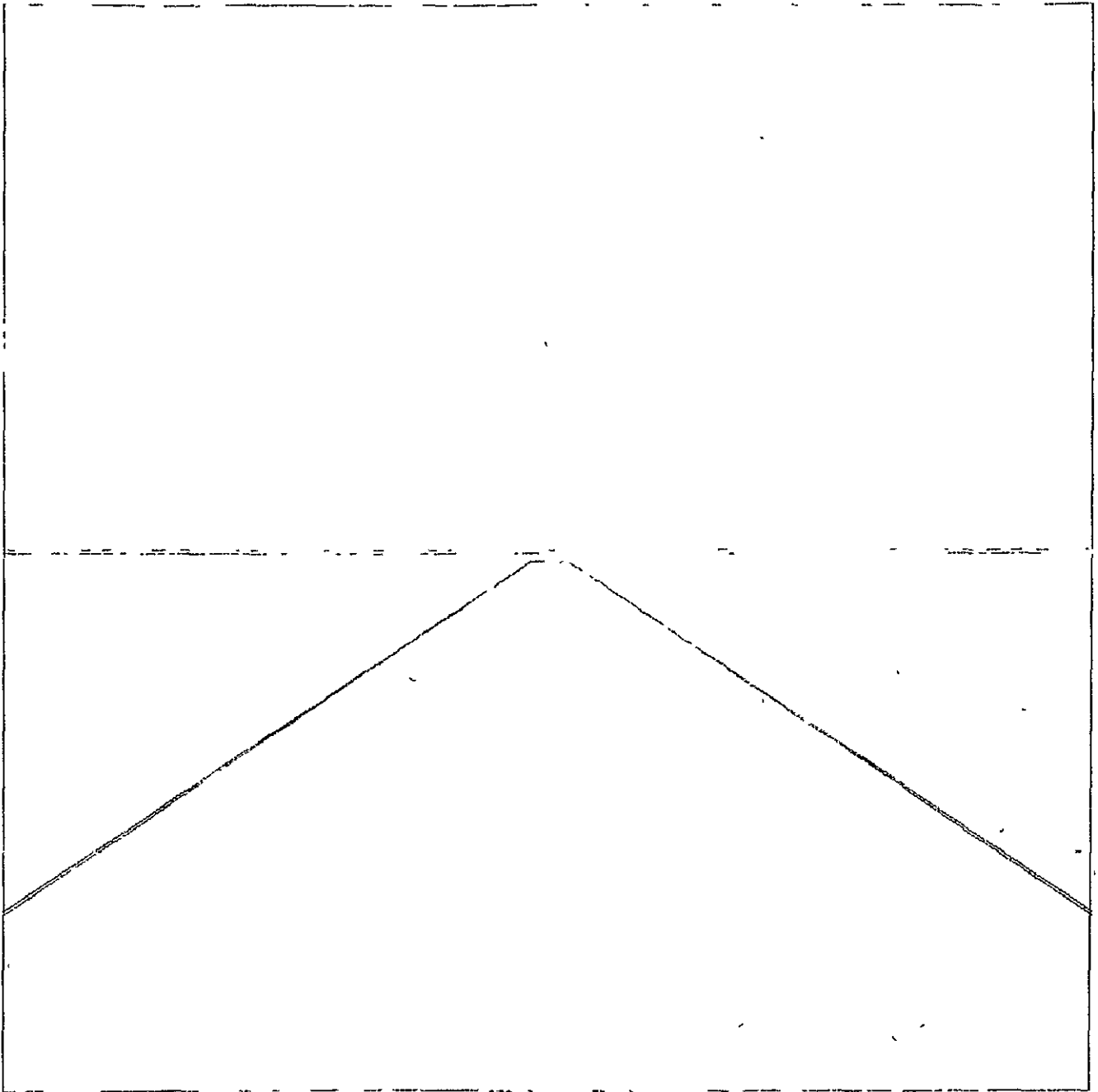
Figure 13.- Scan angle error of 1%, aircraft on glide path.

ORIGINAL PAGE IS
OF POOR QUALITY



(b) Distance to TD = 1/2 mi.

Figure 13.- Continued.



(c) Altitude = 50 ft.

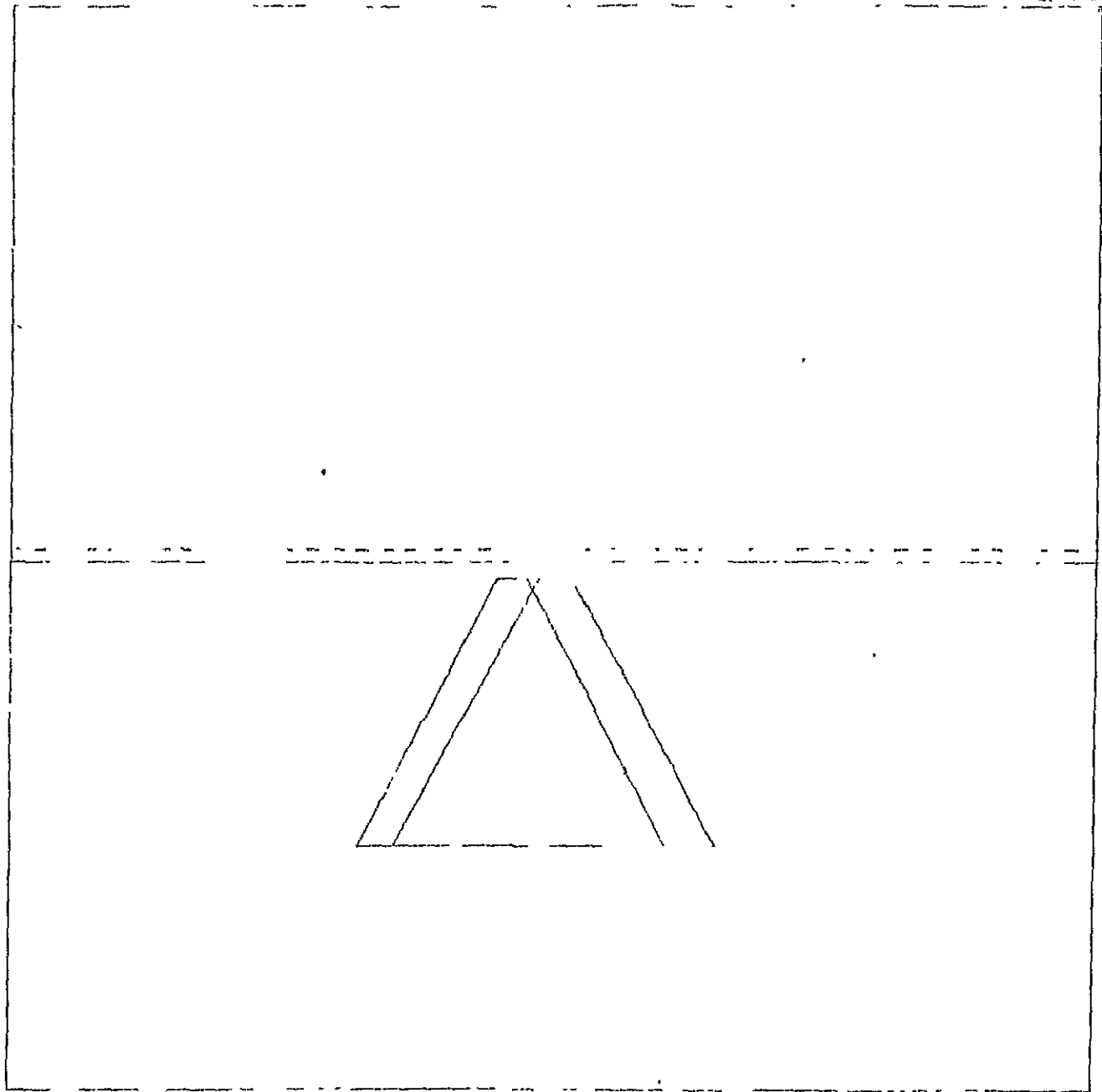
Figure 13.- Concluded.



(a) Distance to TD = 2 mi.

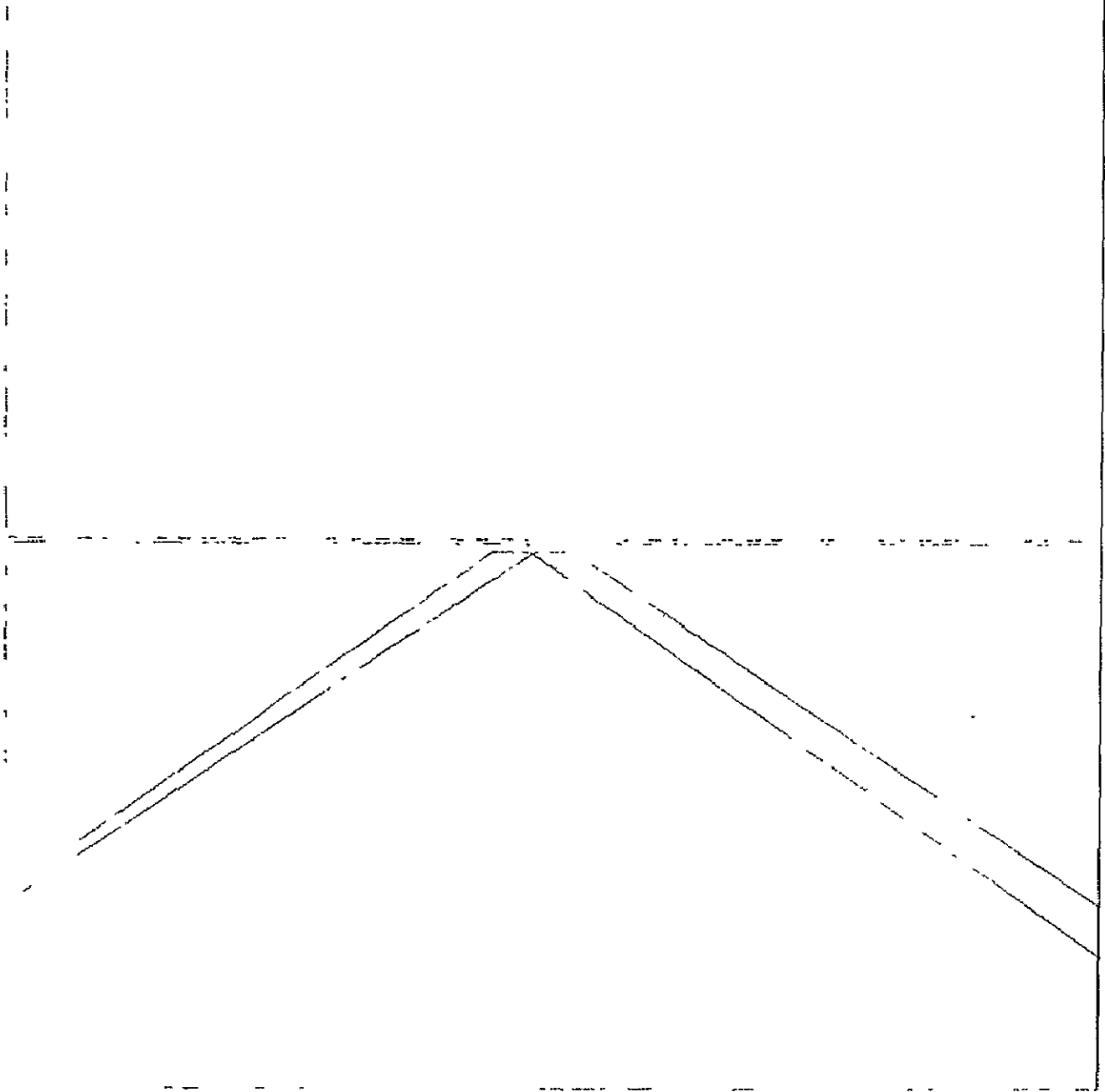
Figure 14.- Scan angle error of $1^\circ \pm 5\%$, aircraft on glide path.

ORIGINAL PAGE IS
OF POOR QUALITY



(b) Distance to TD = $1/2$ mi.

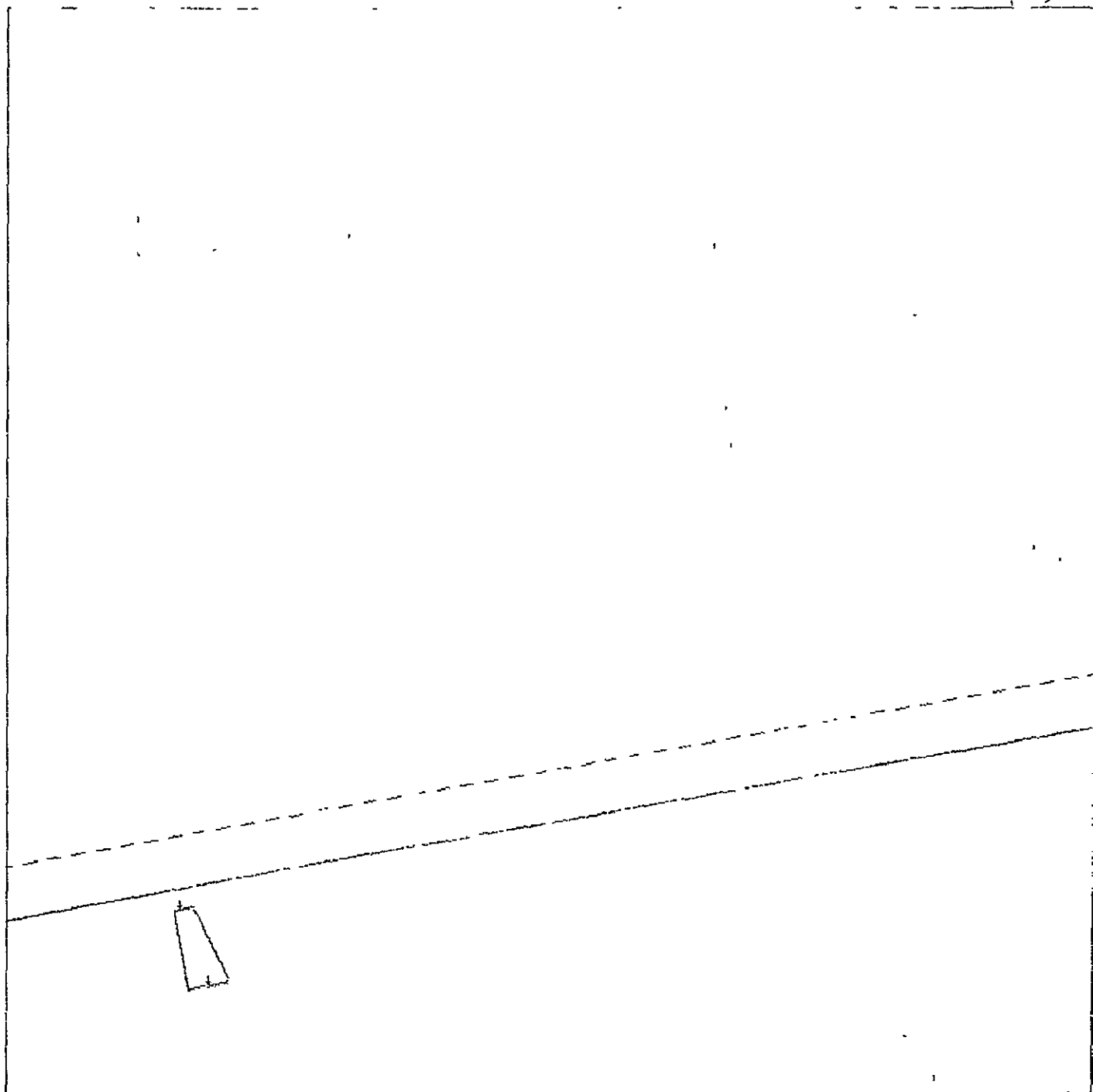
Figure 14.- Continued.



(c) Altitude = 50 ft.

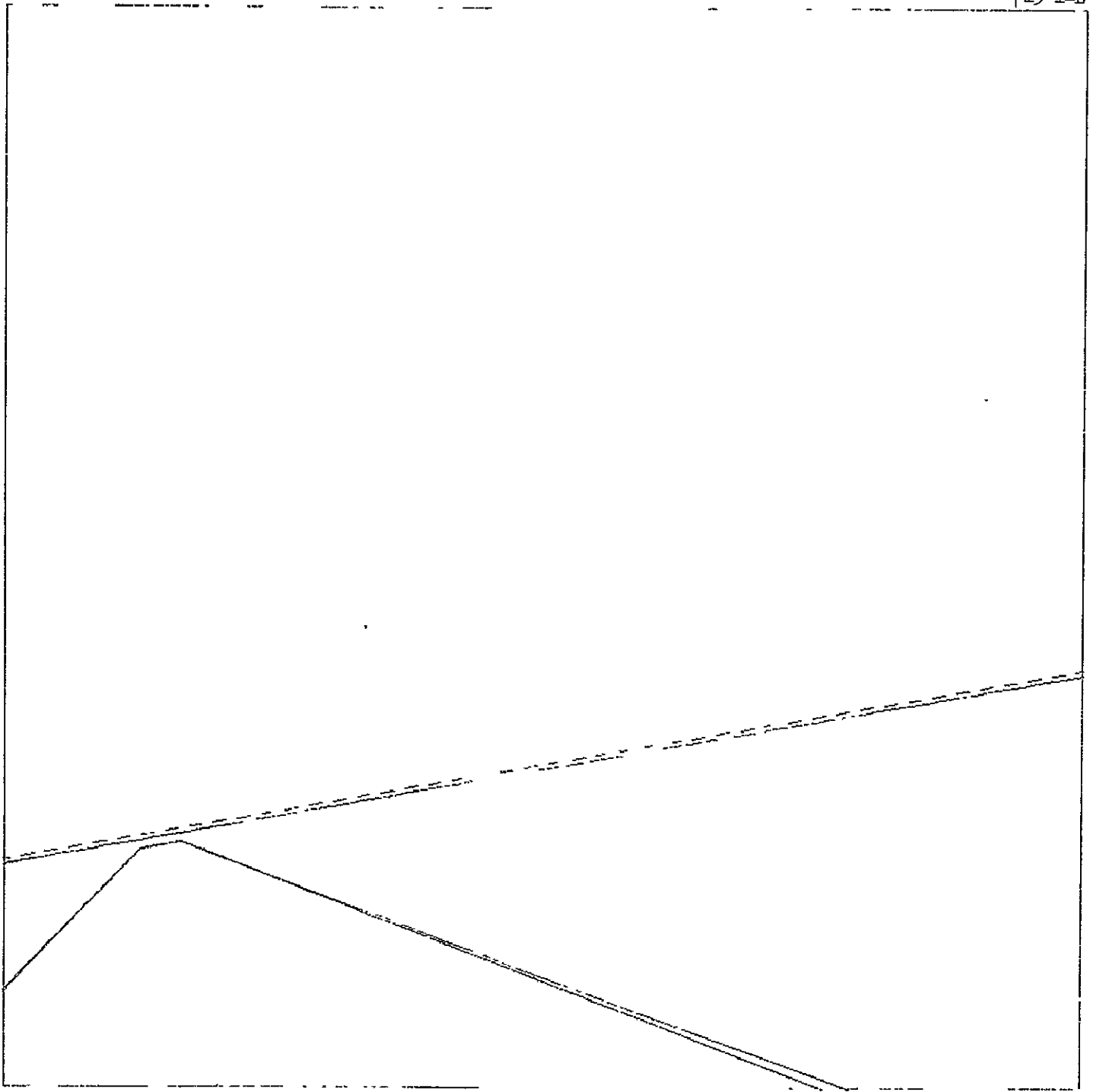
Figure 14.- Concluded.

ORIGINAL PAGE IS
OF POOR QUALITY



(a) Distance to TD = 2 mi.

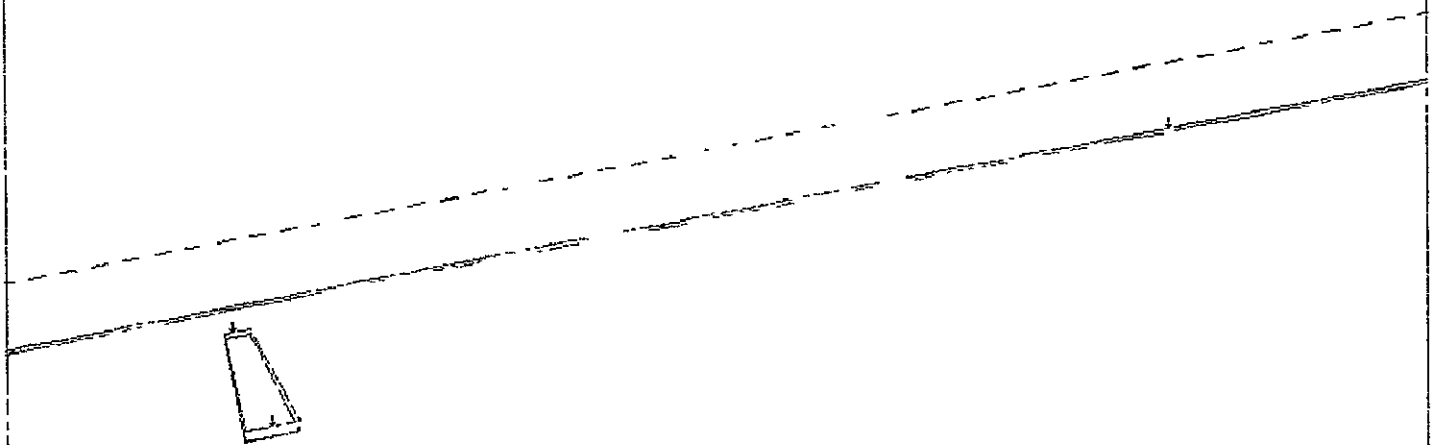
Figure 15 - Range error of 5 ft. + 1%, aircraft off glide path,
 $Y = R = 10^\circ$, $P = 5^\circ$.



(b) Altitude = 50 ft.

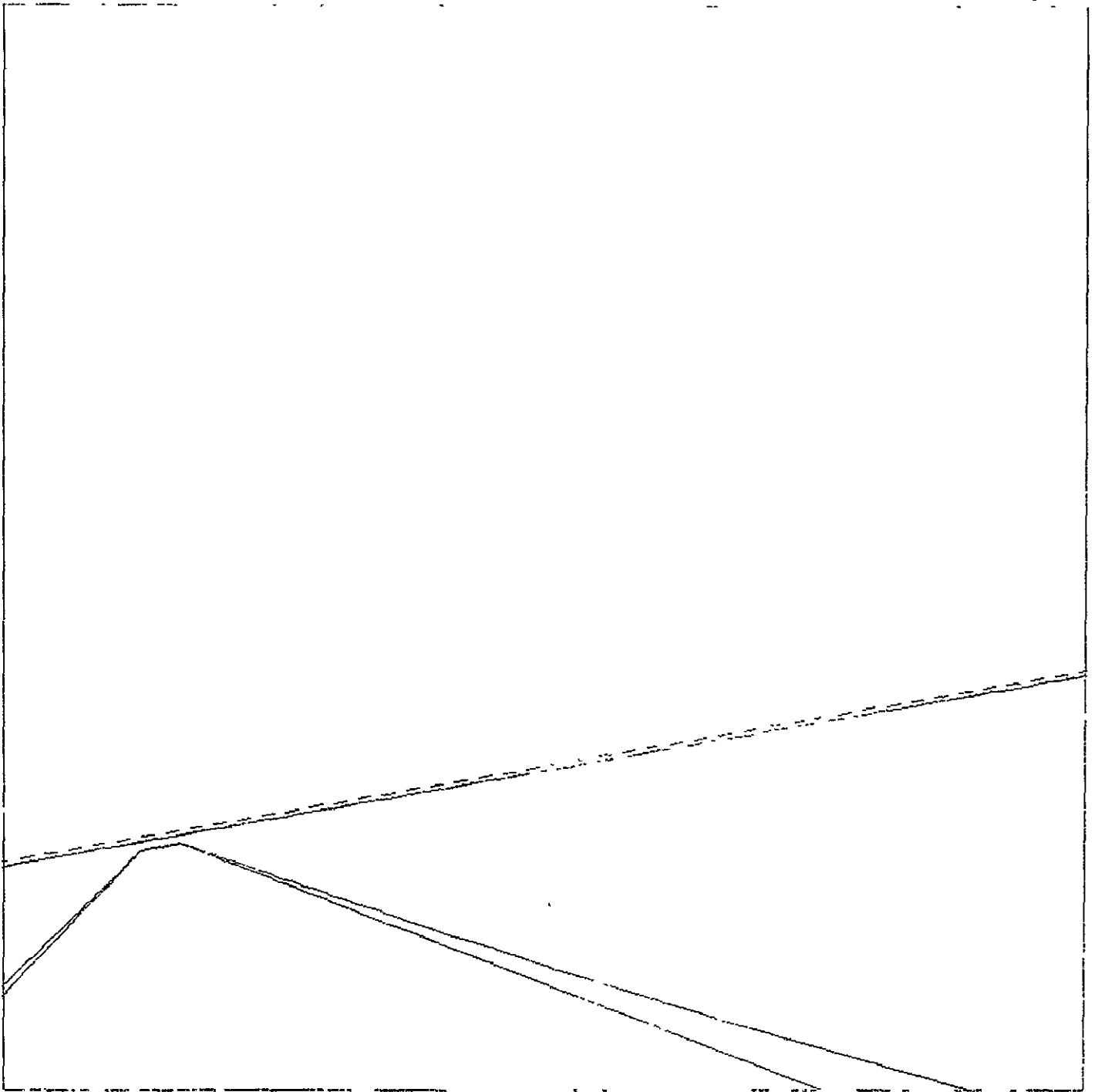
Figure 15.- Concluded.

ORIGINAL PAGE IS
OF POOR QUALITY



(a) Distance to TD = 2 mi.

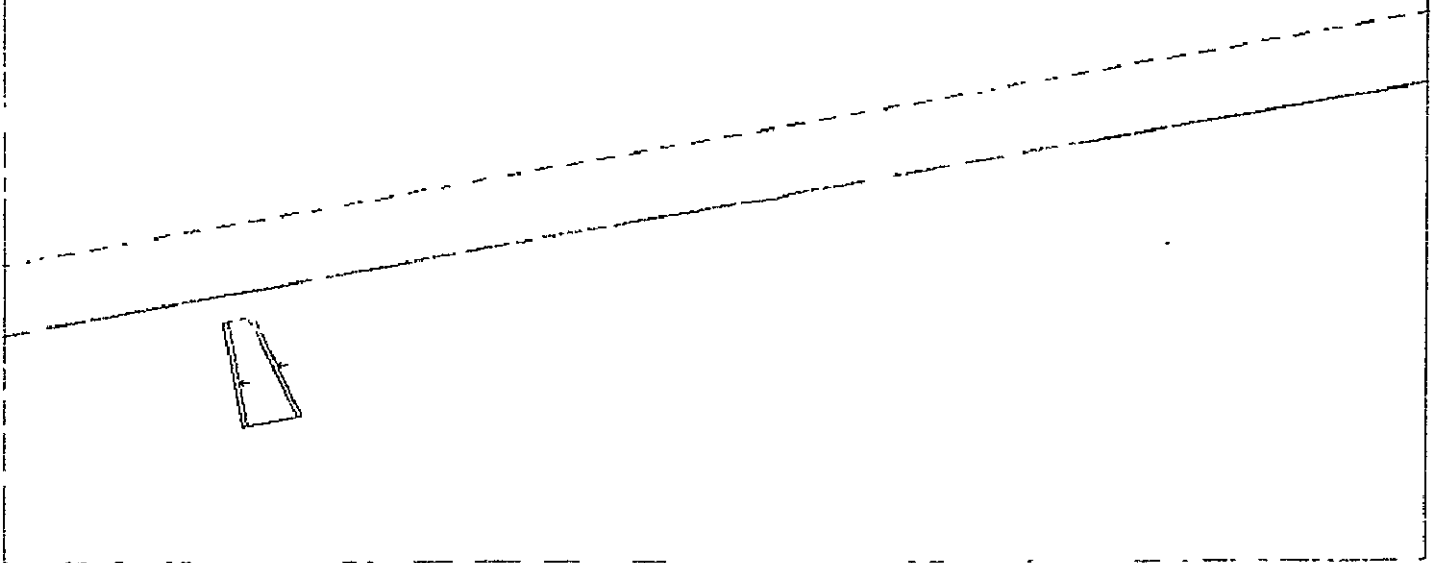
Figure 16.- Range error of 25 ft. + 5%, aircraft off glide path,
 $Y = R = 10^\circ$, $P = 5^\circ$.



(b) Altitude = 50 ft.

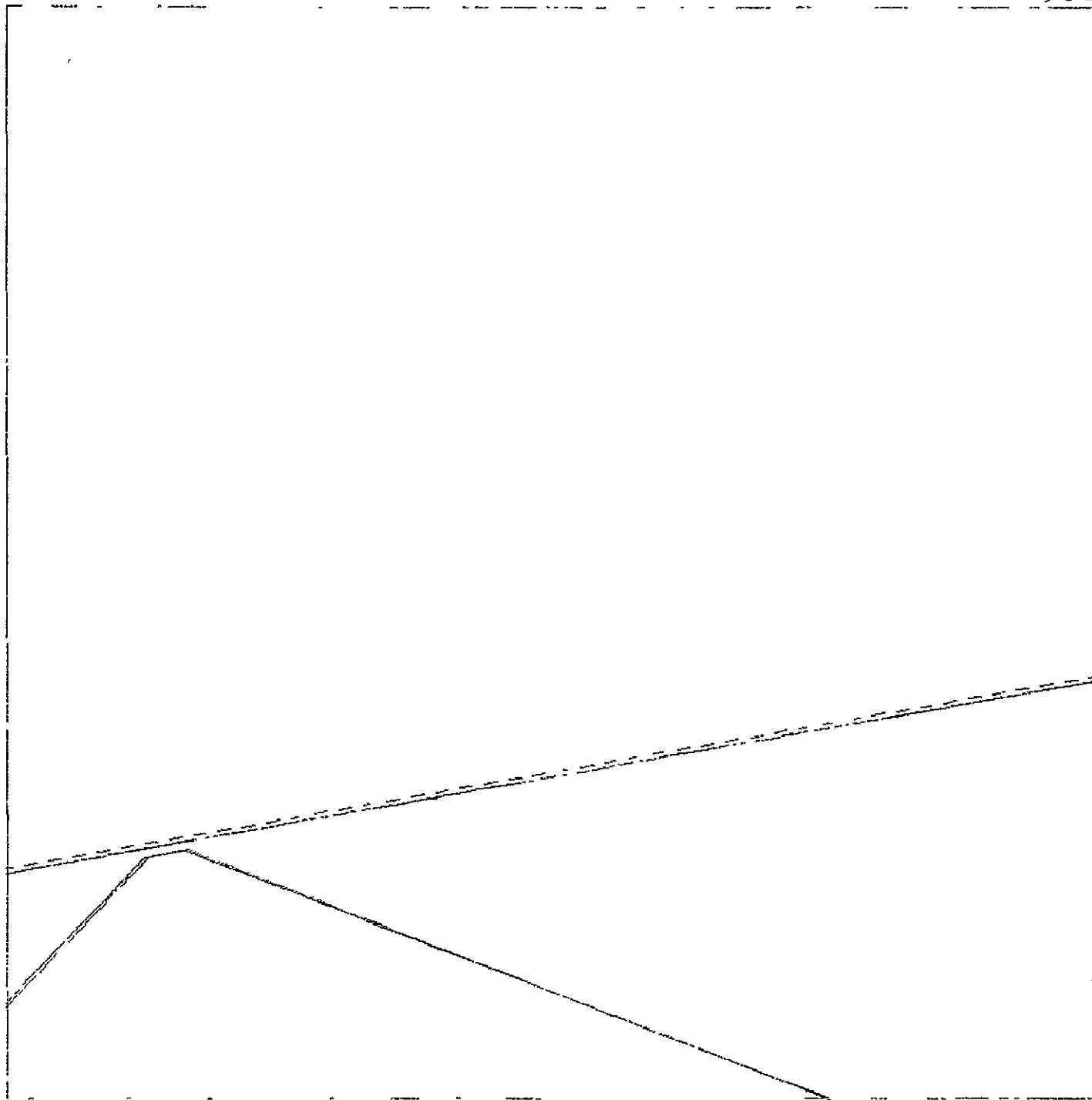
Figure 16.- Concluded.

ORIGINAL PAGE IS
OF POOR QUALITY



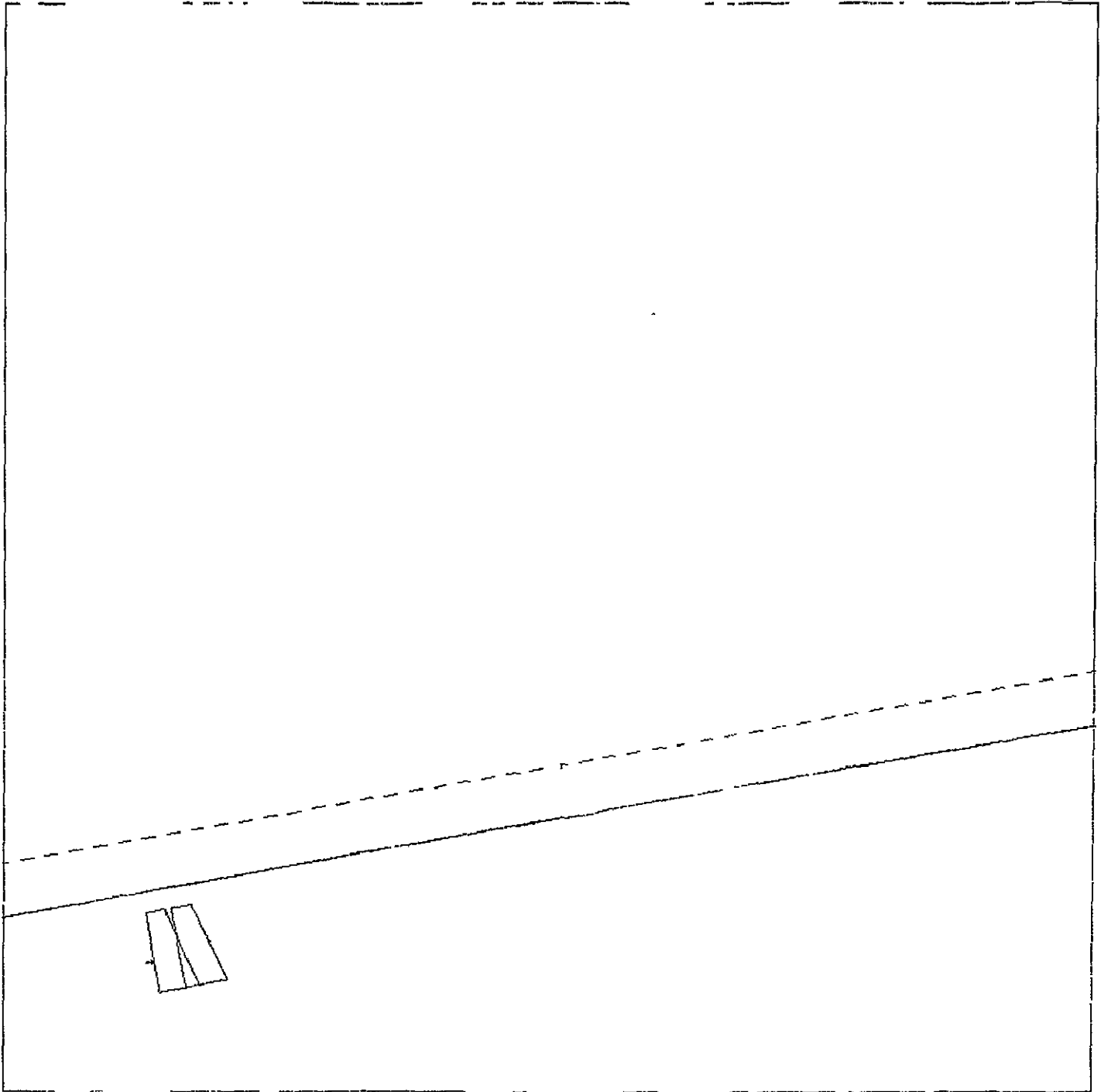
(a) Distance to TD = 2 mi.

Figure 17.- Scan angle error of 1%, aircraft off glide path,
 $Y = R = 10^\circ$, $P = 5^\circ$.



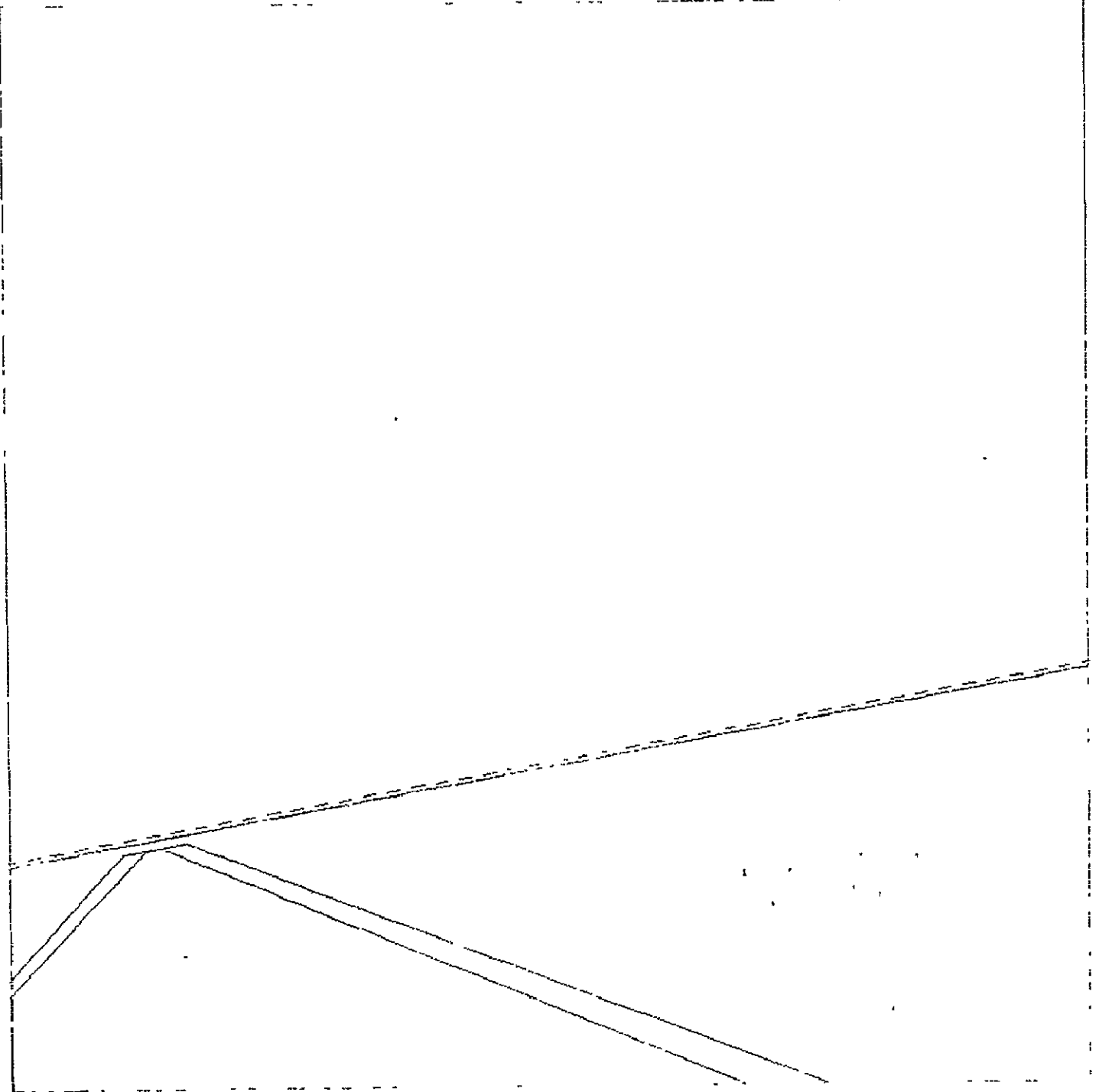
(b) Altitude = 50 ft.

Figure 17.- Concluded.



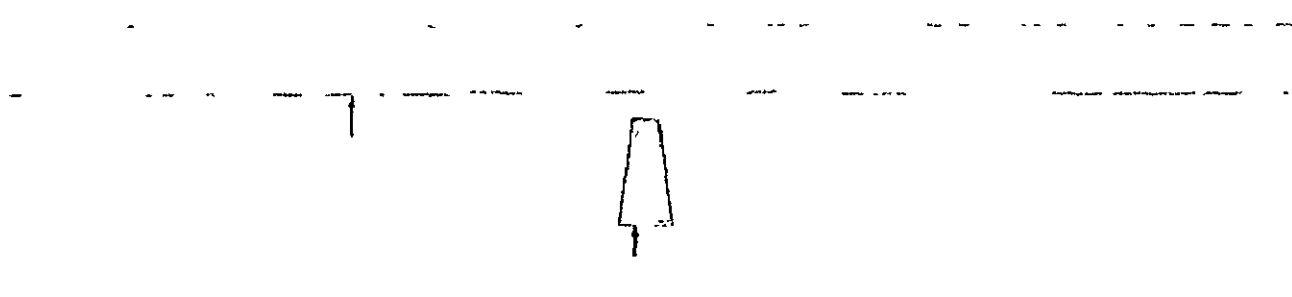
(a) Distance to TD = 2 mi.

Figure 18.- Scan angle error of $1^\circ + 5\%$, aircraft off glide path,
 $Y = R = 10^\circ$, $P = 5^\circ$.



(b) Altitude = 50 ft.

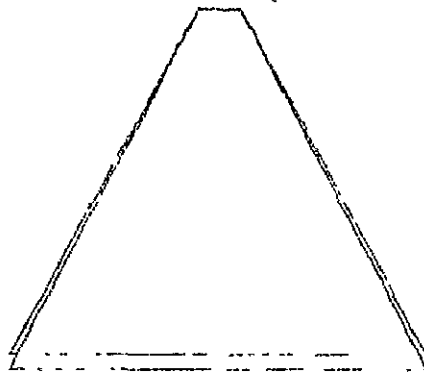
Figure 18.- Concluded.



ORIGINAL PAGE IS
OF POOR QUALITY

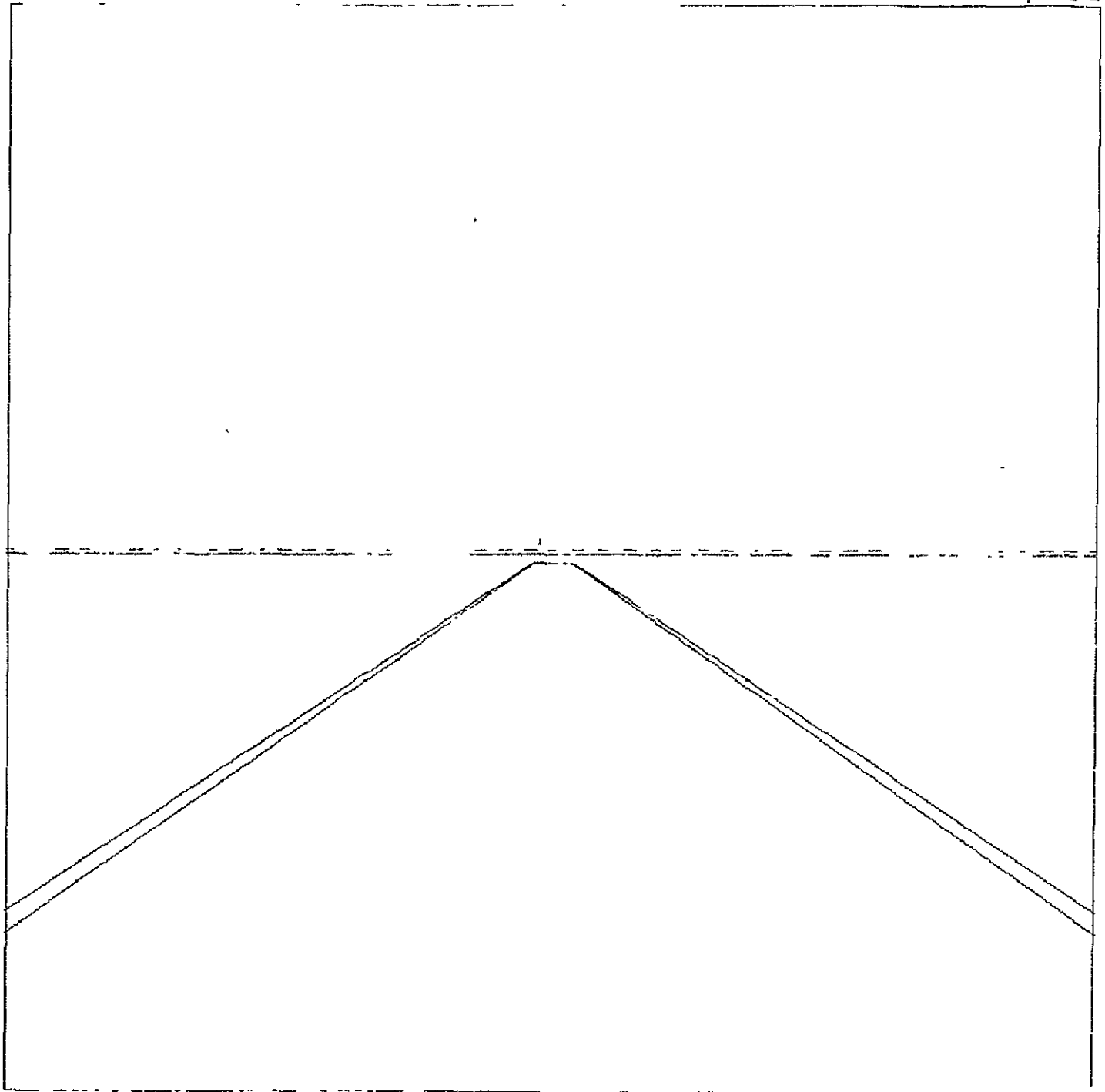
(a) Distance to TD = 2 mi.

Figure 19.- Altitude error of 2 ft. + 2%, aircraft on glide path.



(b) Distance to TD = 1/2 mi.

Figure 19.- Continued.



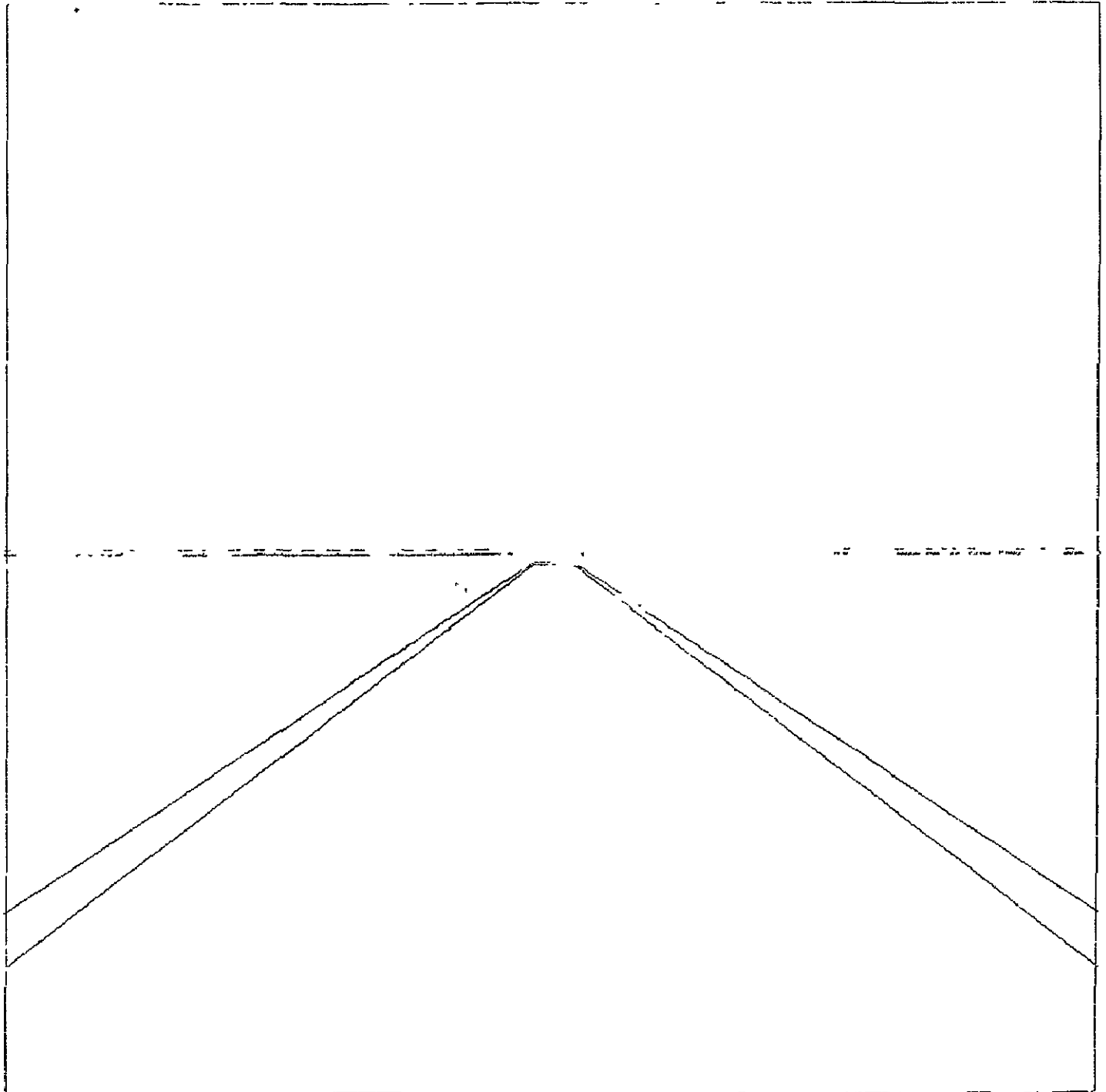
(c) Altitude = 50 ft.

Figure 19.- Concluded.



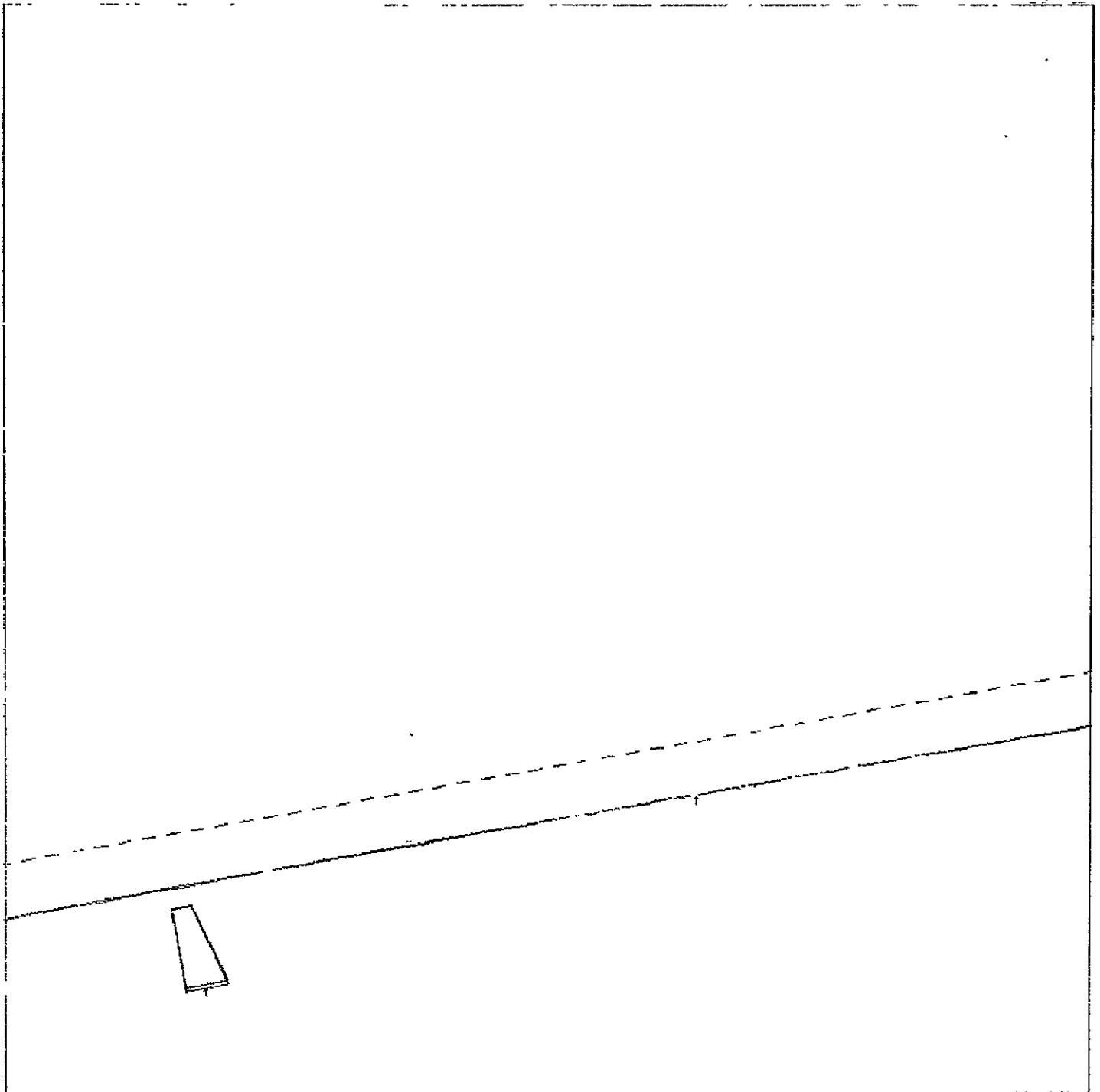
(a) Distance to TD = 2 mi.

Figure 20.- Altitude error of 5 ft. + 5%, aircraft on glide path.



(b) Altitude = 50 ft.

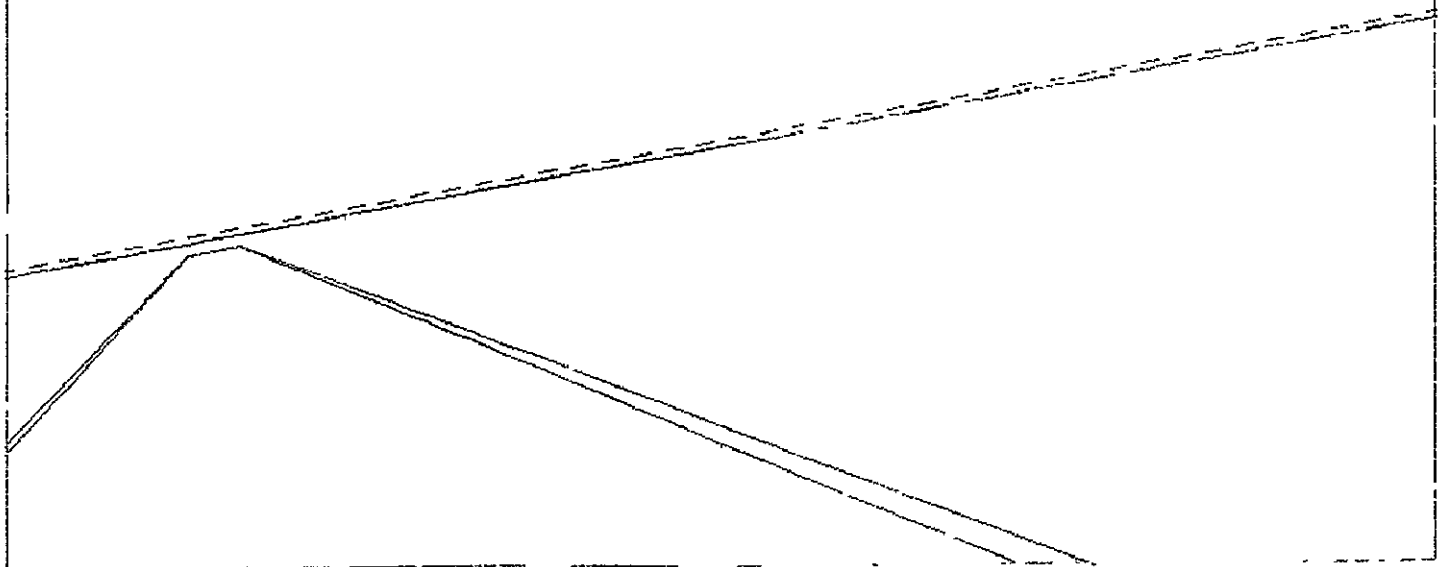
Figure 20.- Concluded.



(a) Distance to TD = 2 ml.

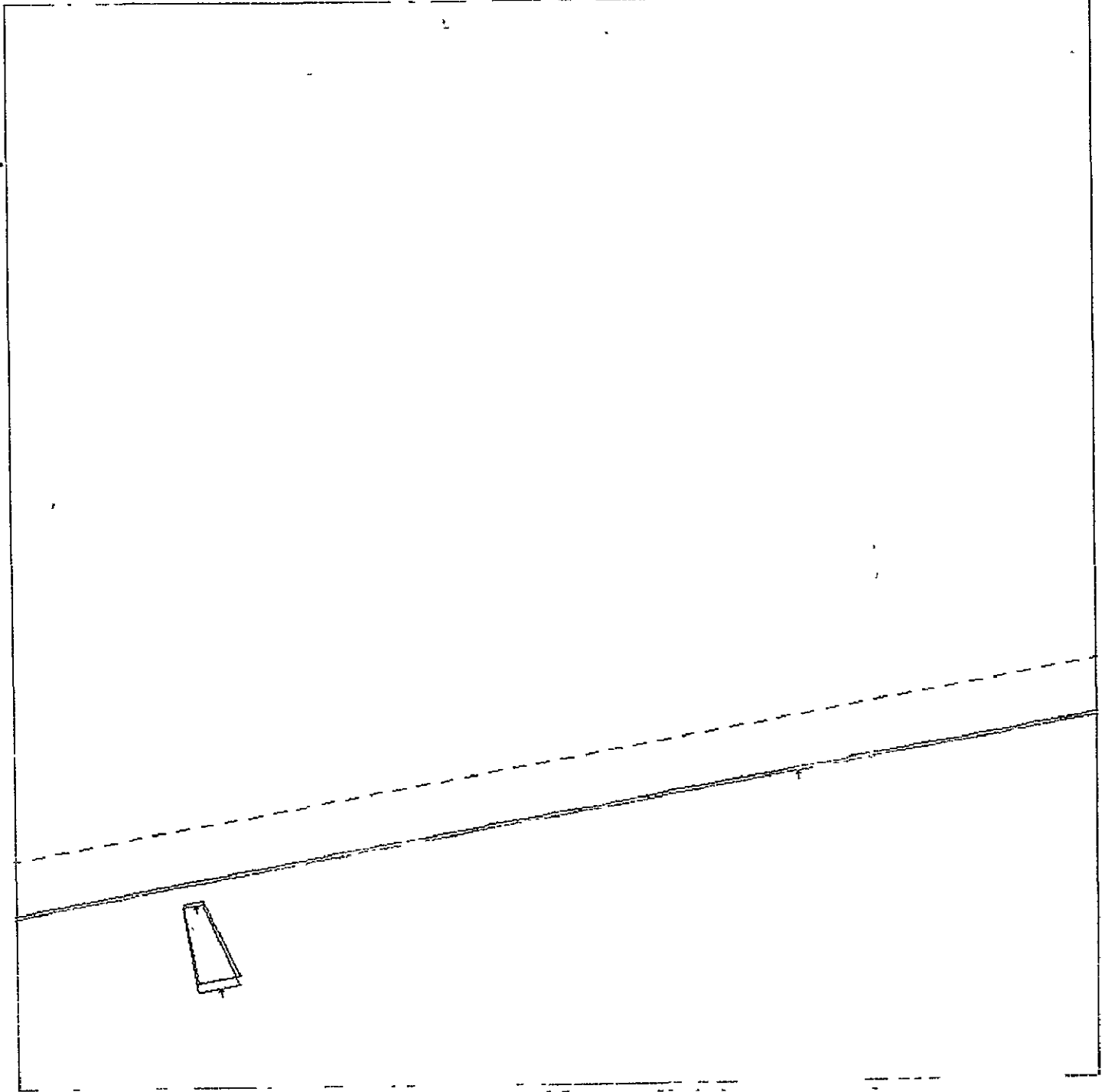
Figure 21 - Altitude error of 2 ft. + 2%, aircraft off glide path,
 $Y = R = 10^\circ$, $P = 5^\circ$.

ORIGINAL PAGE IS
OF POOR QUALITY



(b) Altitude = 50 ft.

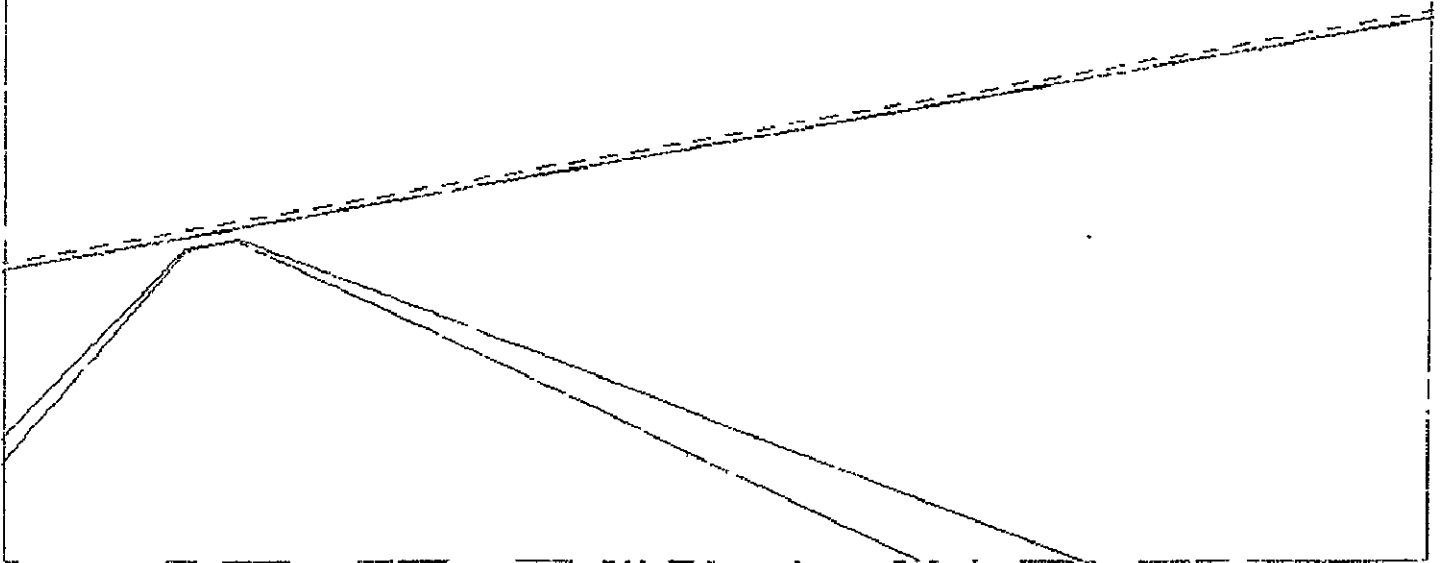
Figure 21.- Concluded.



(a) Distance to TD = 2 mi.

Figure 22.- Altitude error of 5 ft. + 5%, aircraft off glide path,
 $Y = R = 10^\circ$, $P = 5^\circ$.

ORIGINAL PAGE IS
OF POOR QUALITY



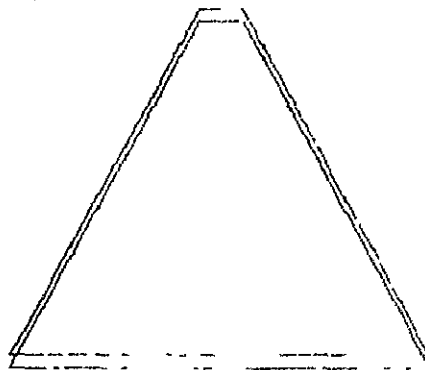
(b) Altitude = 50 ft.

Figure 21.- Concluded.



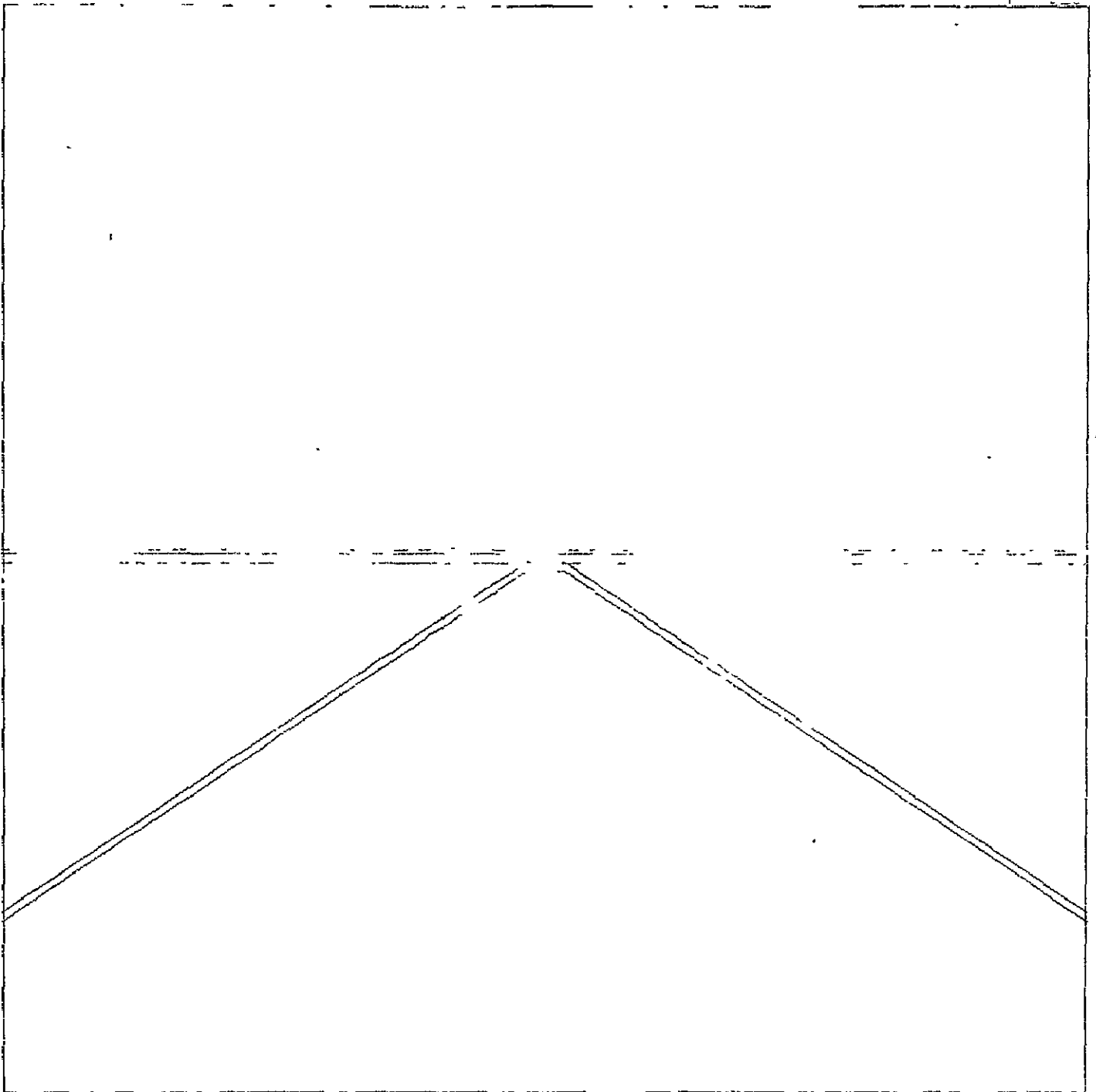
(a) Distance to TD = 2 mi.

Figure 23.- Pitch error of $0.212^\circ + 0.5\%$, aircraft on glide path.



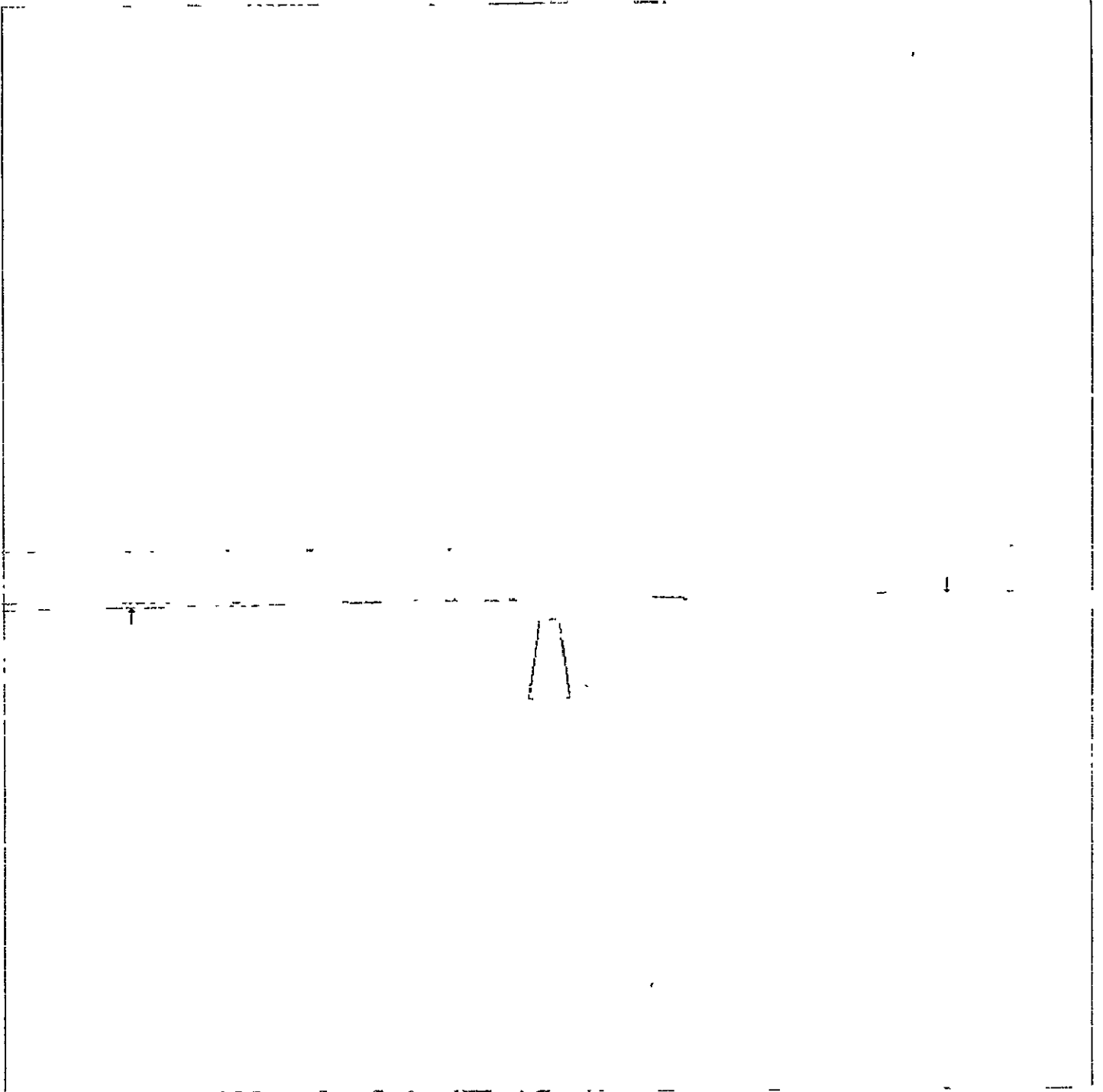
(b) Distance to TD = 1/2 mi.

Figure 23.- Continued.



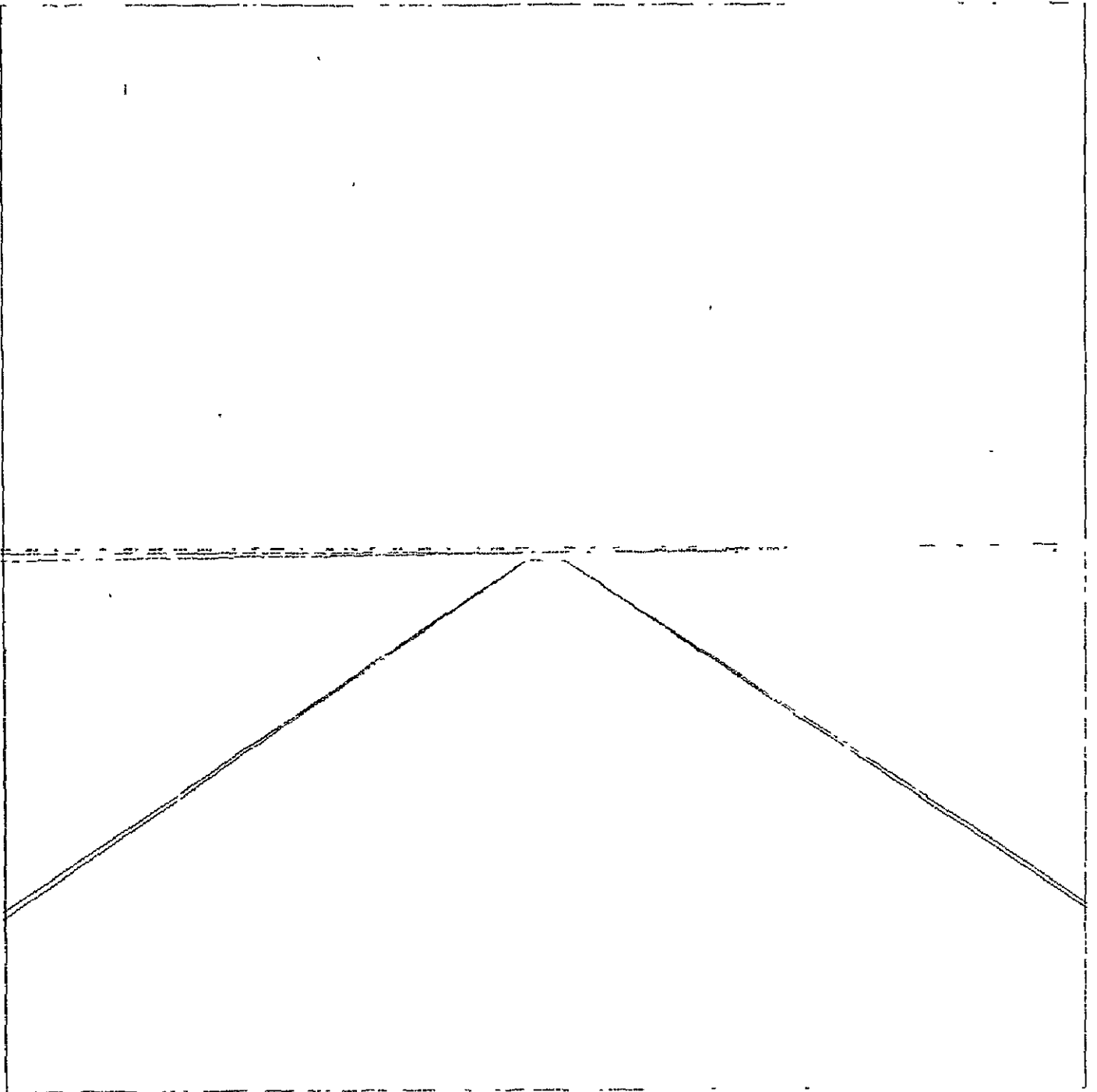
(c) Altitude = 50 ft.

Figure 23.- Concluded.



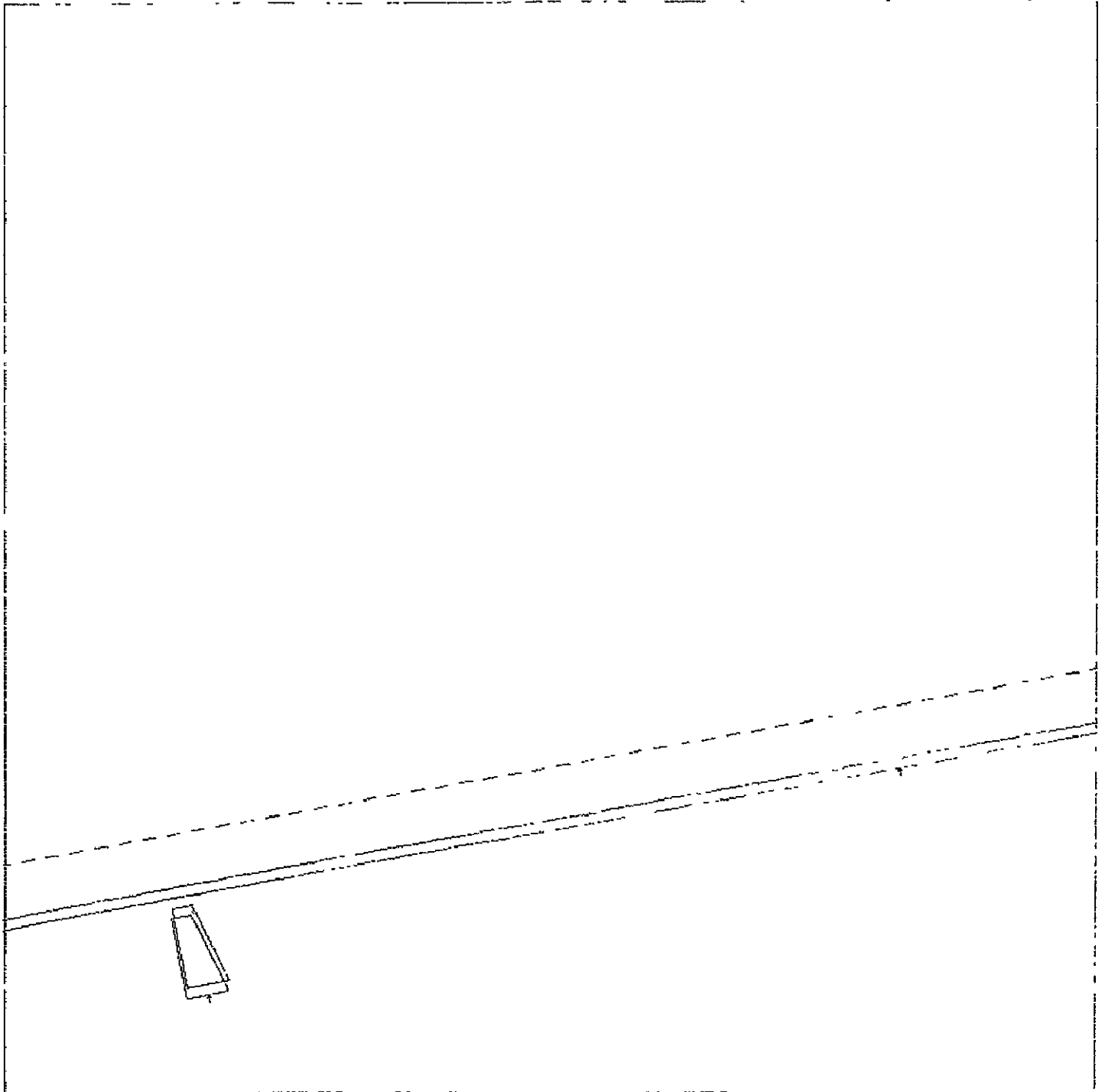
(a) Distance to TD = 2 mi.

Figure 74.- Roll error of $0.707^\circ \pm 0.5\%$, aircraft on glide path.



(b) Altitude = 50 ft.

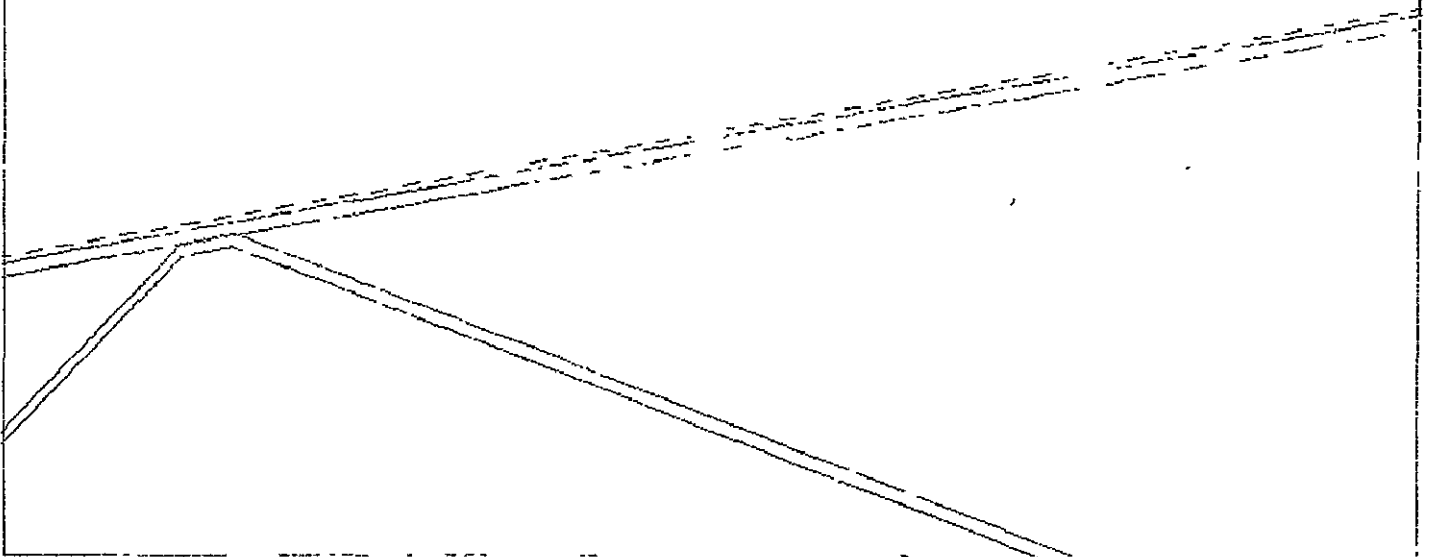
Figure 24.- Concluded.



(a) Distance to TD = 2 ml.

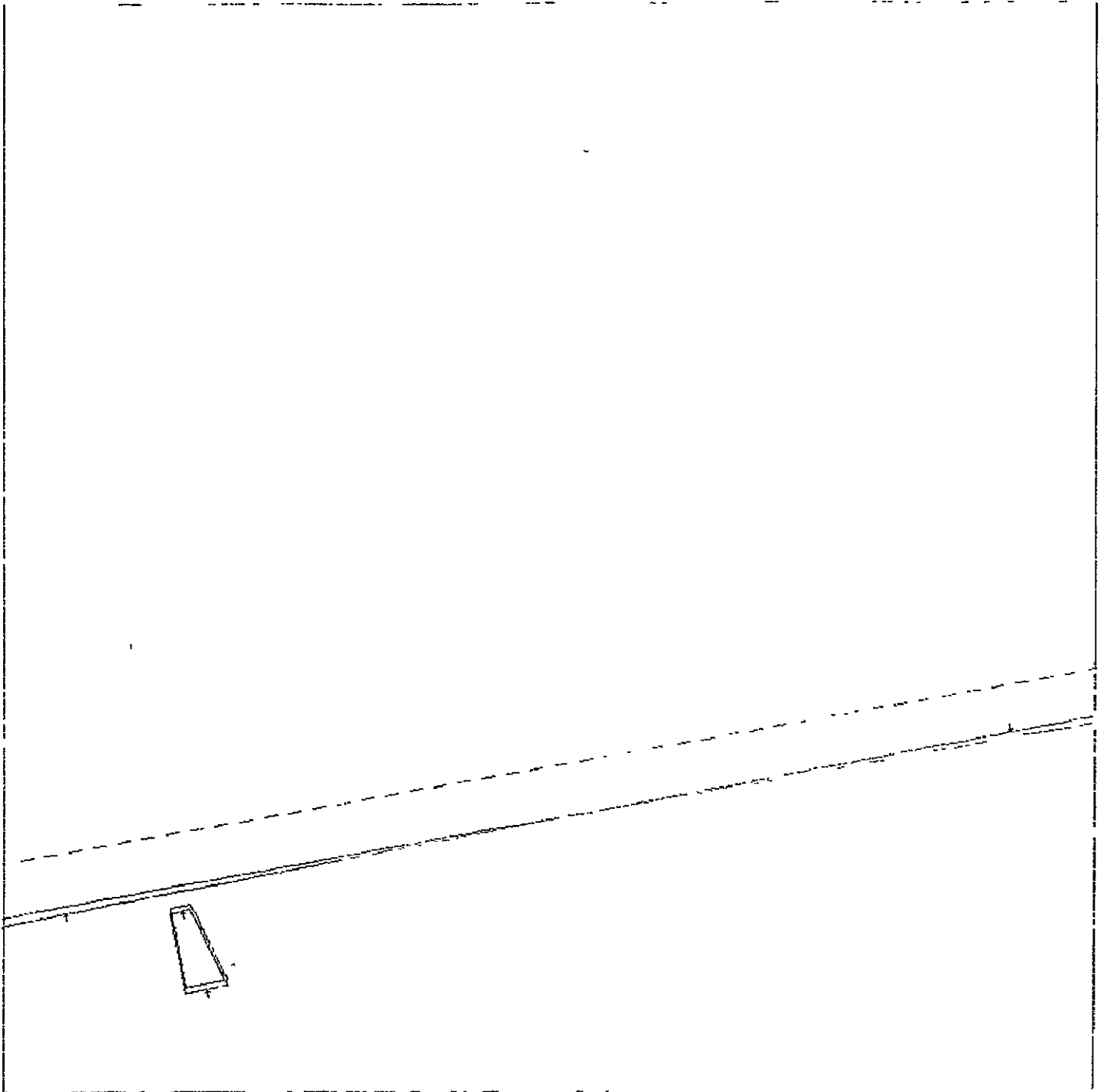
Figure 25.- Pitch error of $0.212^\circ + 0.5\%$, aircraft off glide path,
 $Y = R = 10^\circ$, $P = 5^\circ$.

ORIGINAL PAGE IS
OF POOR QUALITY



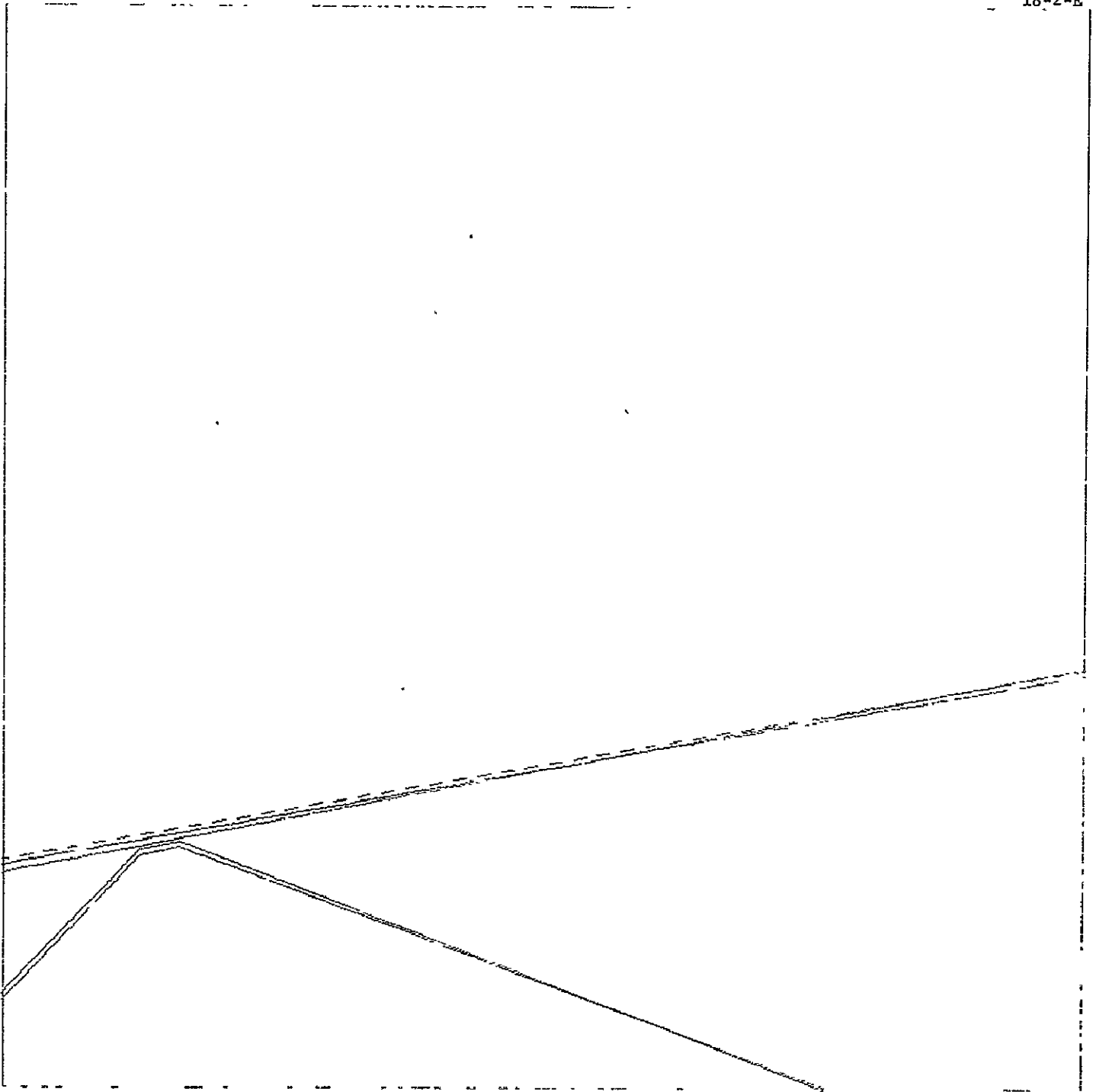
(b) Altitude = 50 ft.

Figure 25.- Concluded.



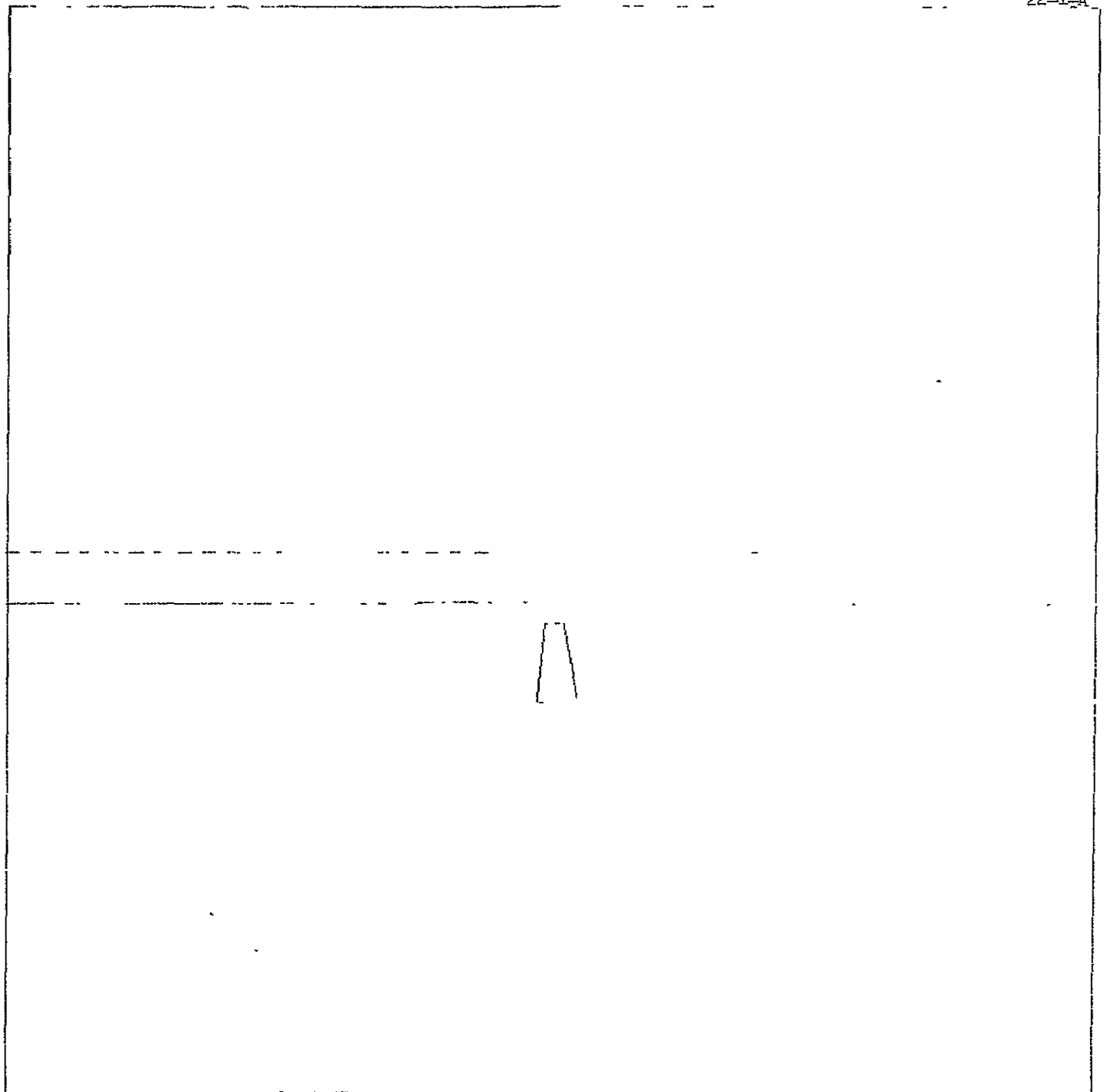
(a) Distance to TD = 2 mi.

Figure 25.- Roll error of $0.707^\circ + 0.5\%$, aircraft off glide path,
 $Y = R = 10^\circ$, $P = 5^\circ$.



(b) Altitude = 50 ft.

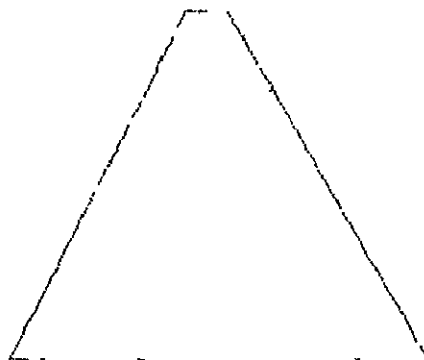
Figure 26.- Concluded.



(a) Distance to TD = 2 mi.

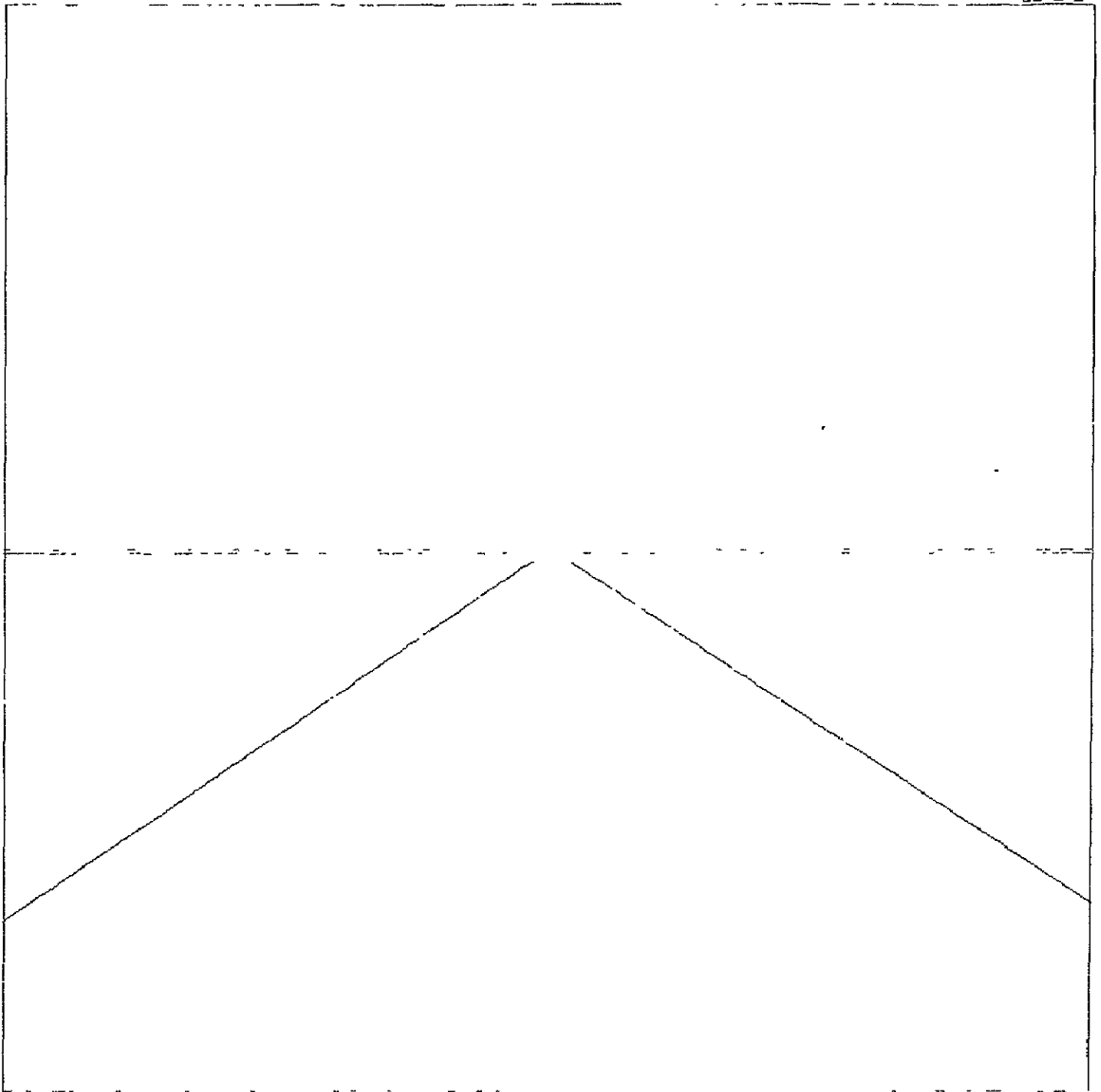
Figure 26.- Small angle approximation with aircraft of 0.117° left of centerline, $Y = P = R = 0^\circ$.

ORIGINAL PAGE IS
OF POOR QUALITY



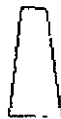
(b) Distance to TD = 1/2 mi.

Figure 27.- Continued.



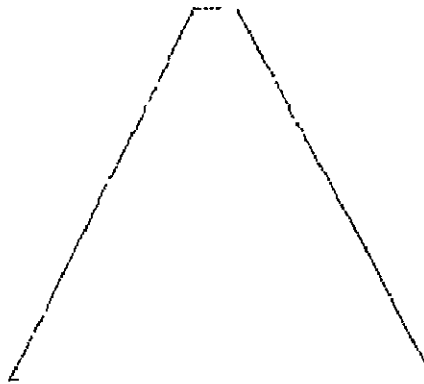
(c) Altitude = 50 ft.

Figure 27.- Concluded.



(a) Distance to TD = 2 mi.

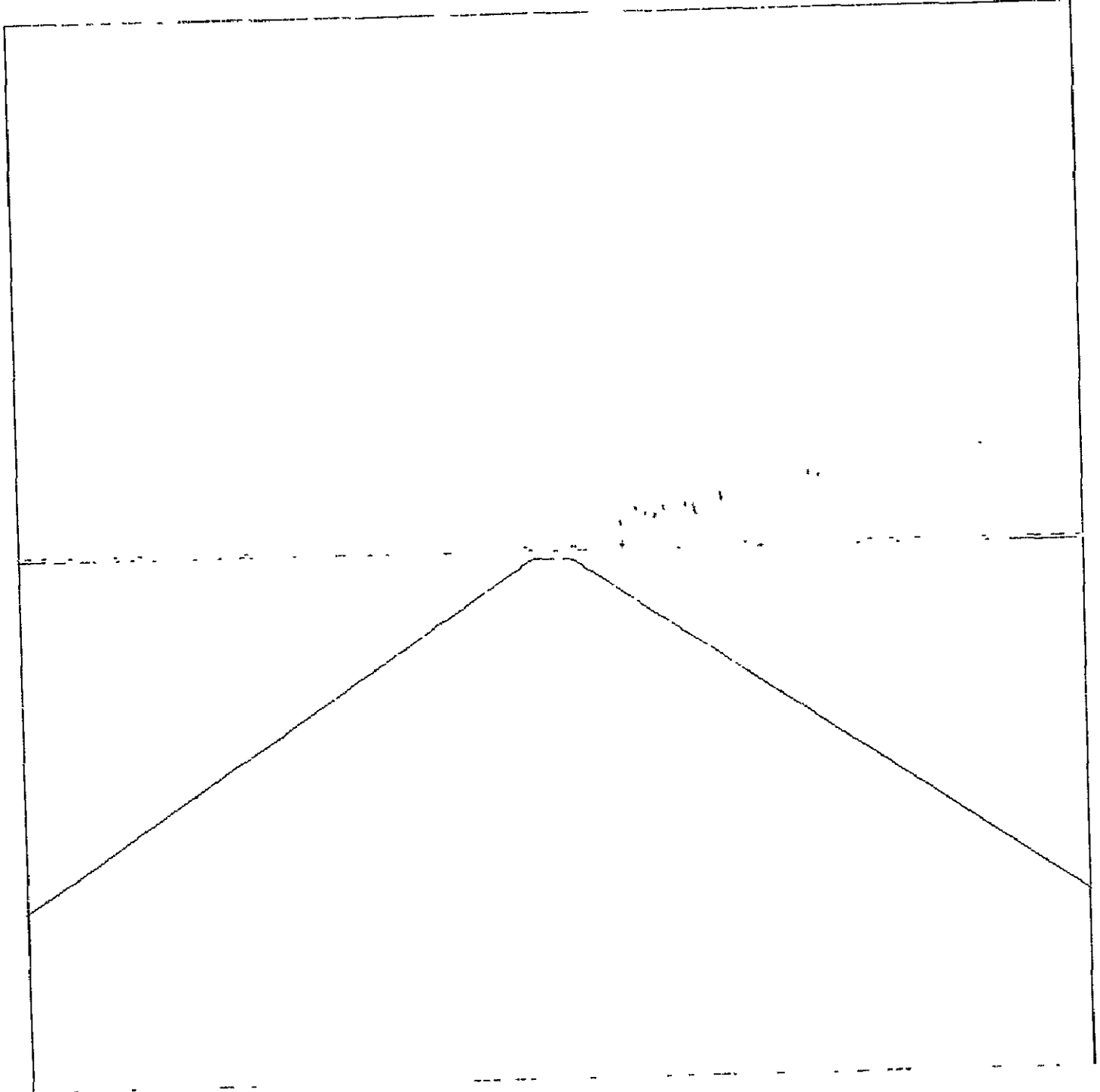
Figure 28.- Small angle approximation with aircraft of 0.17° above 3° glide slope, $Y = P = R = 0^\circ$.



(b) Distance to TD = $1/2$ mi.

Figure 28.- Continued.

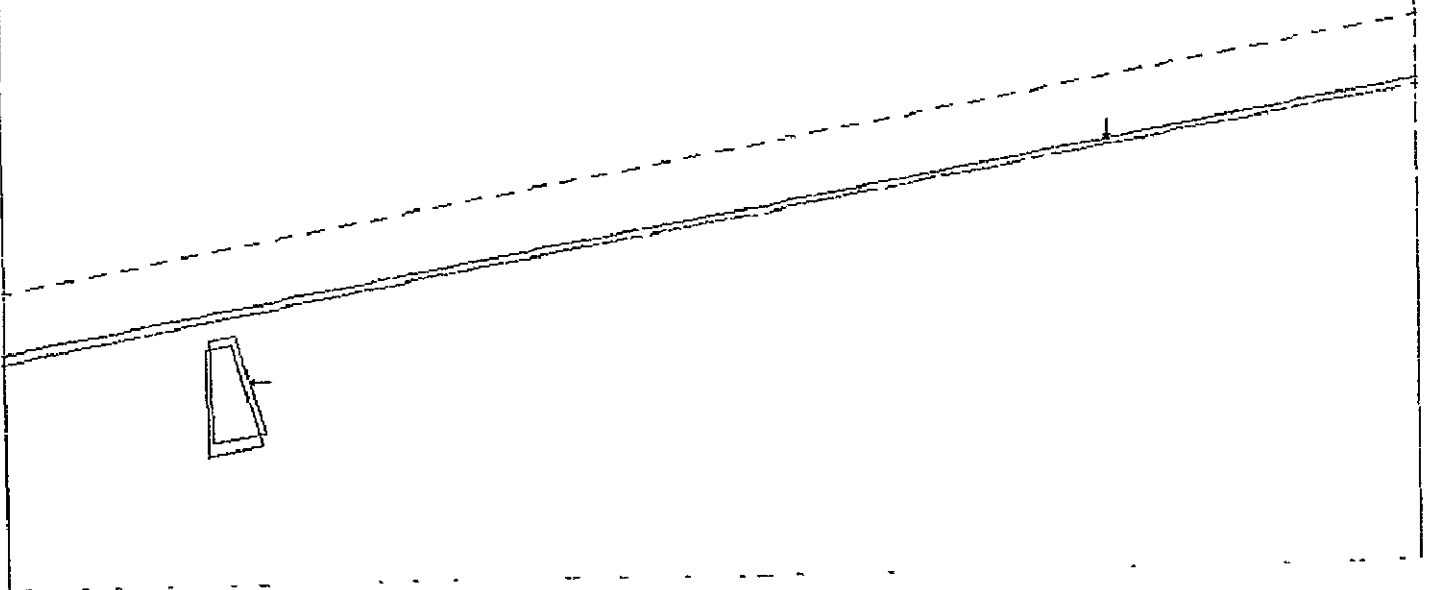
CD



(c) Altitude = 50 ft.

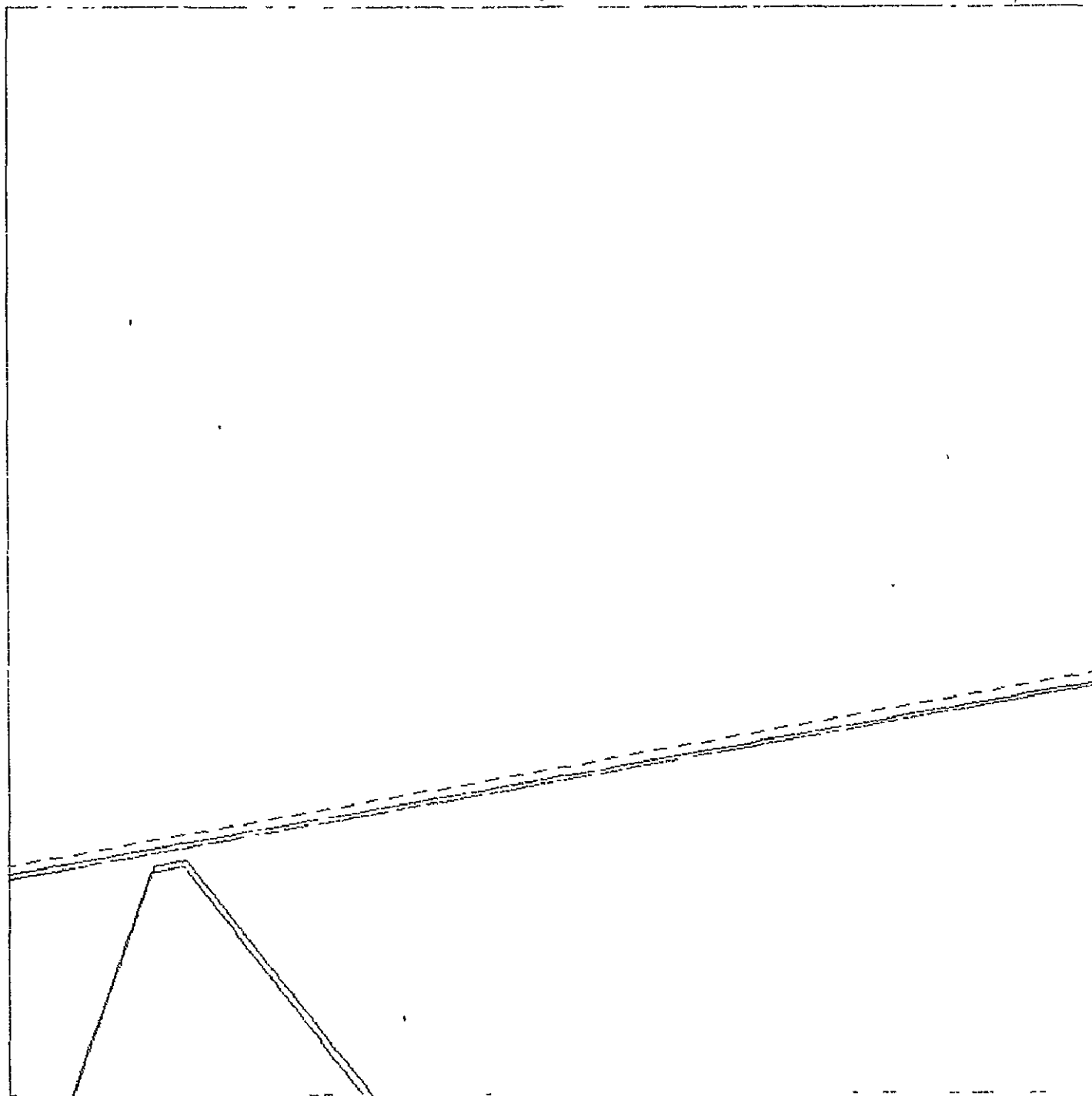
Figure 28.- Concluded.

ORIGINAL PAGE IS
OF POOR QUALITY



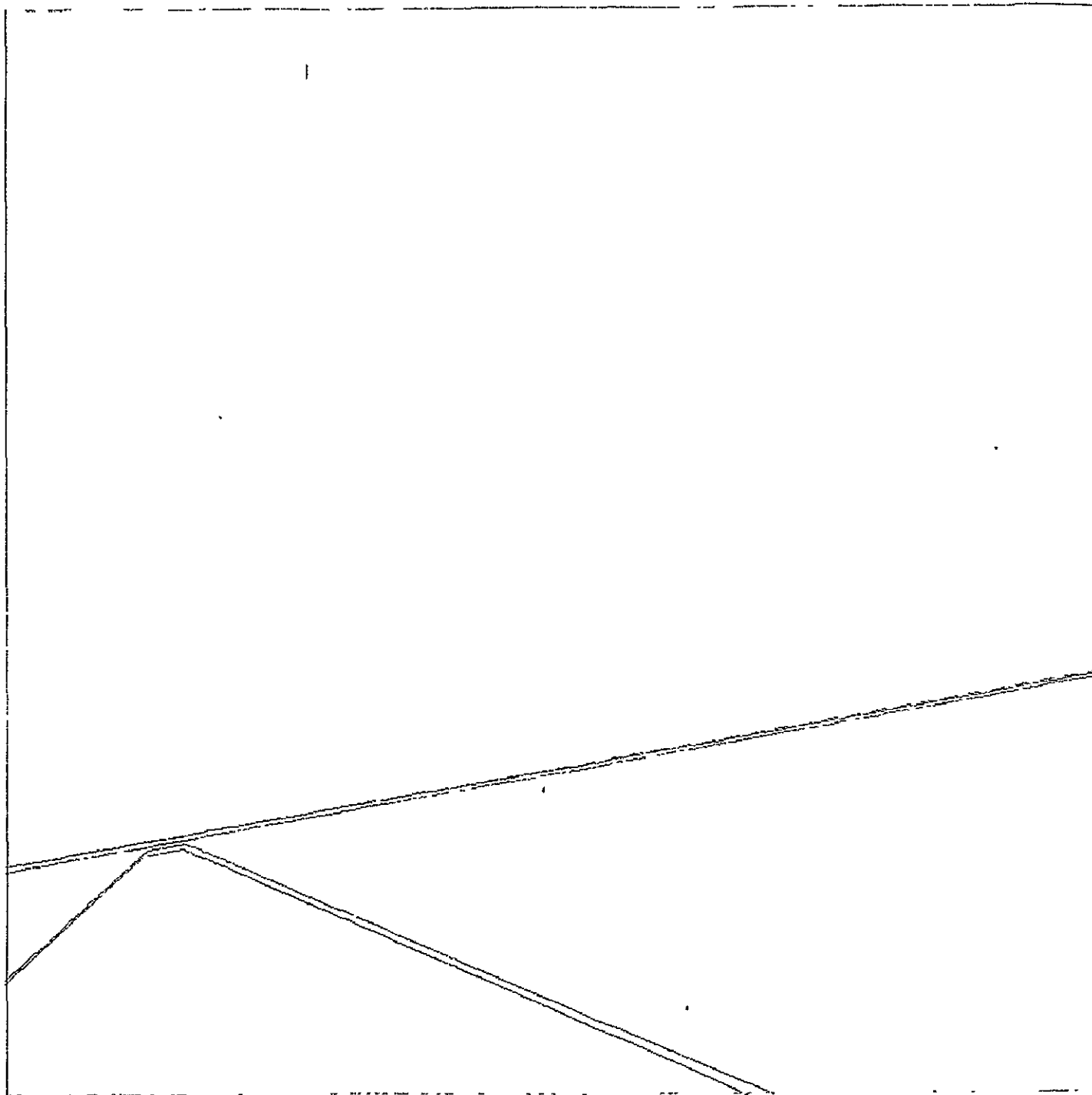
(a) Distance to TD = 2 mi.

Figure 29.- Small angle approximation with aircraft on glide path,
 $Y = R = 10^\circ$, $P = 5^\circ$.



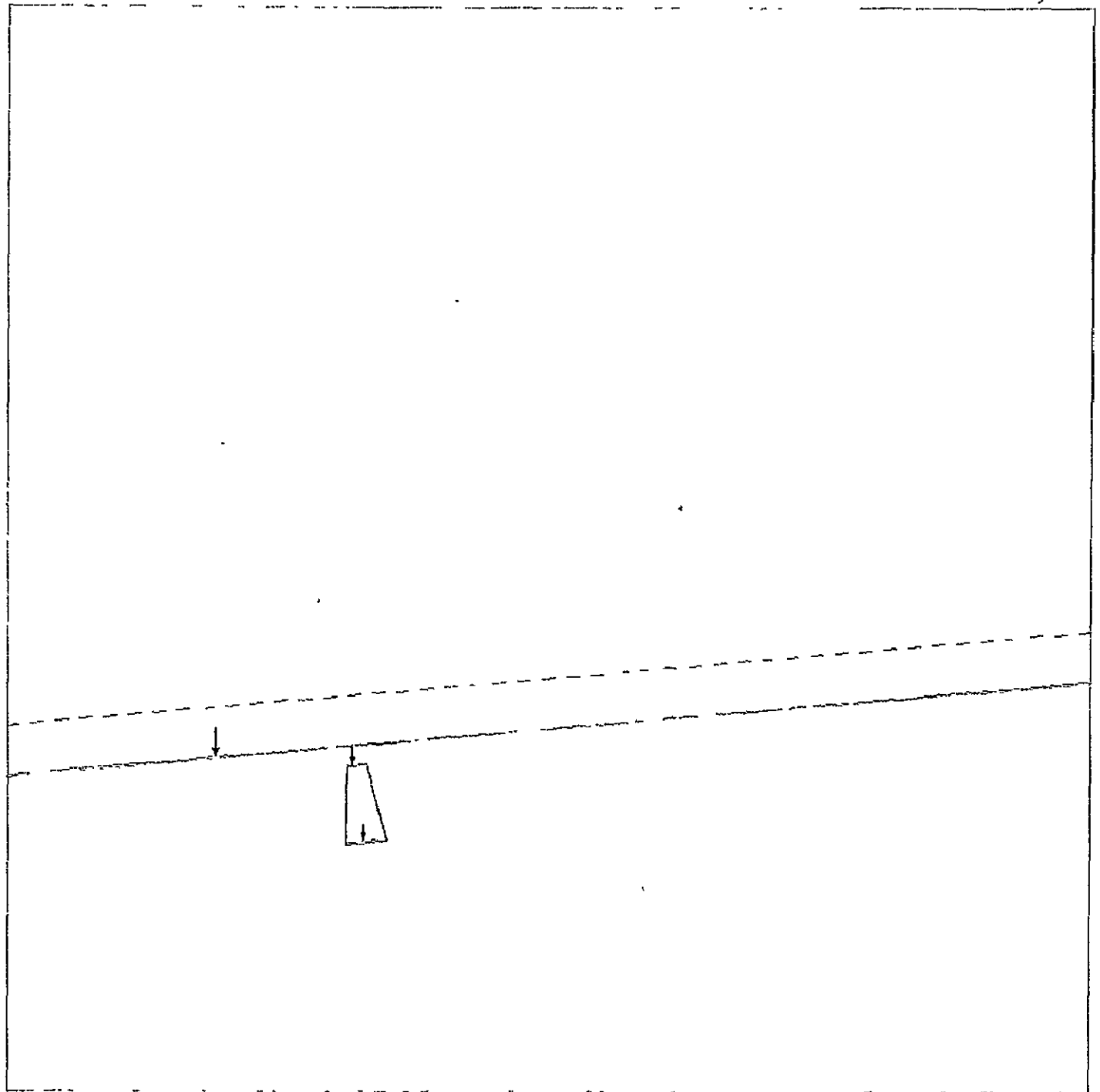
(b) Distance to TD = 1/2 mi.

Figure 29.- Continued.



(c) Altitude = 50 ft.

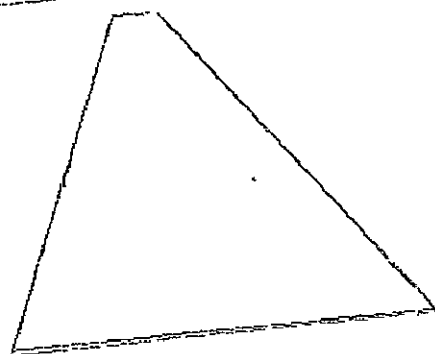
Figure 29.- Concluded.



(a) Distance to TD = 2 mi.

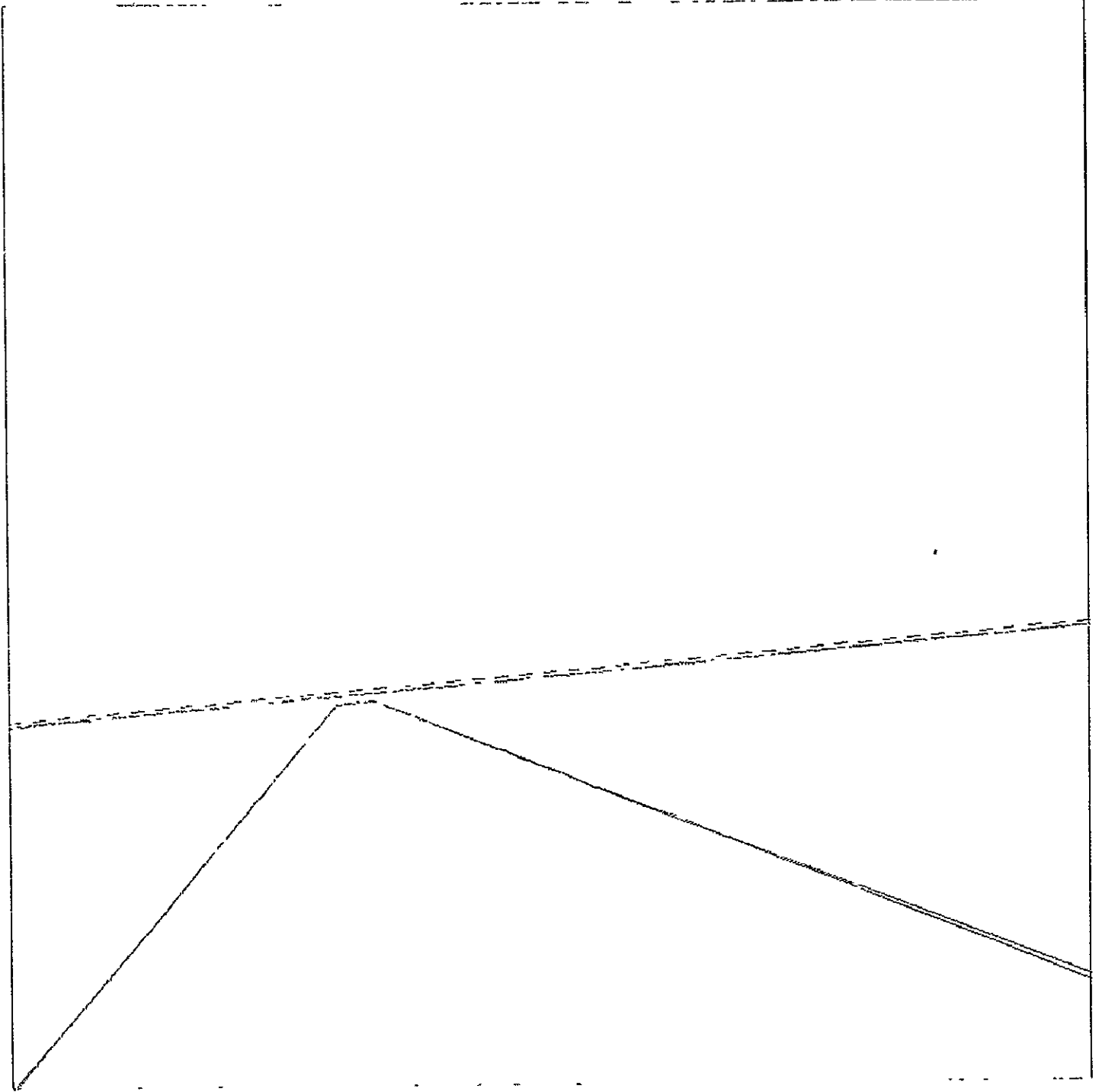
Figure 30.-- Small angle approximation with aircraft 25 ft. left of and 10 ft. below glide path, $Y = R = 5^\circ$, $P = 3^\circ$.

ORIGINAL PAGE IS
OF POOR QUALITY



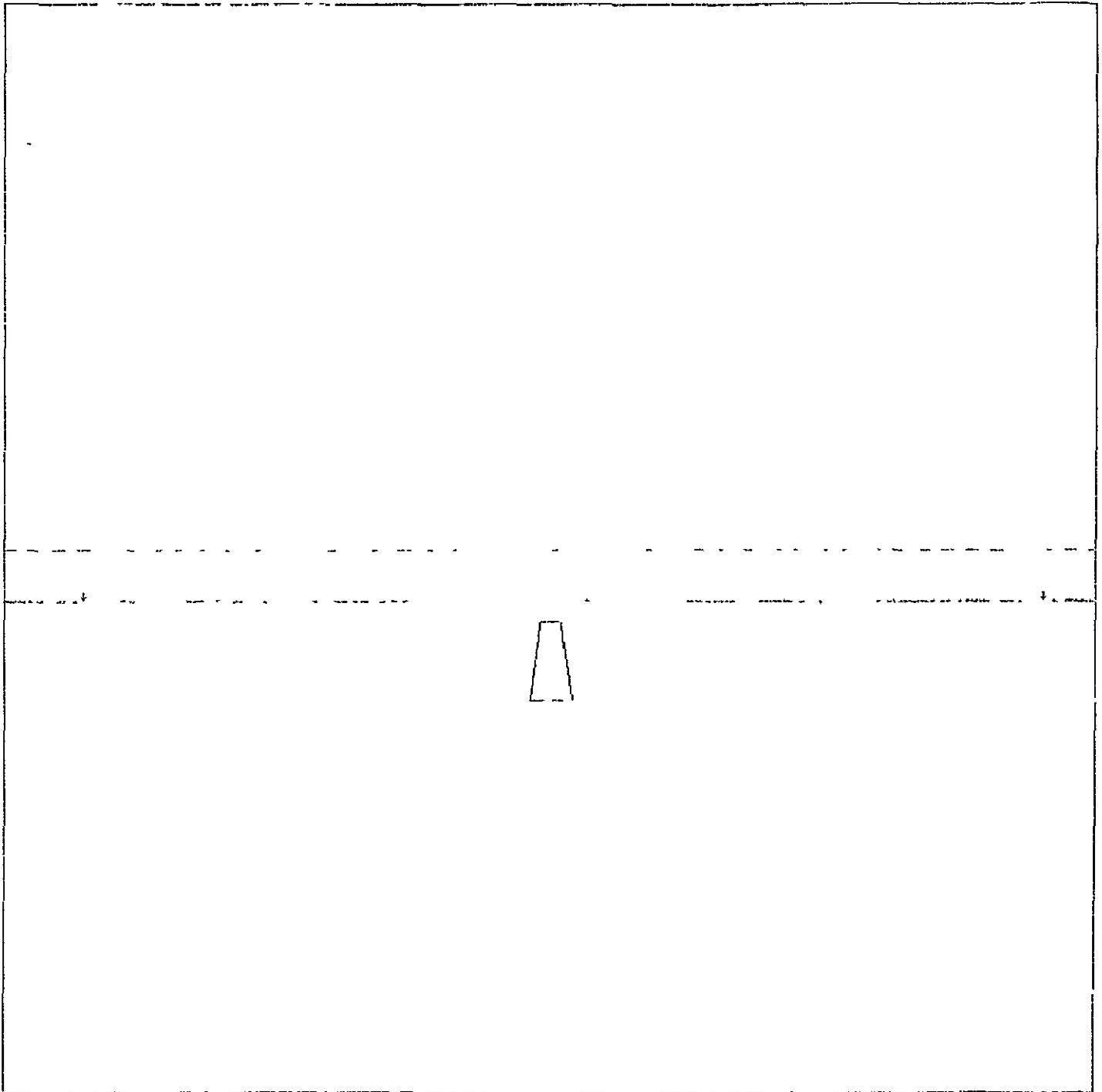
(b) Distance to TD = 1/2 mi.

Figure 30.- Continued.



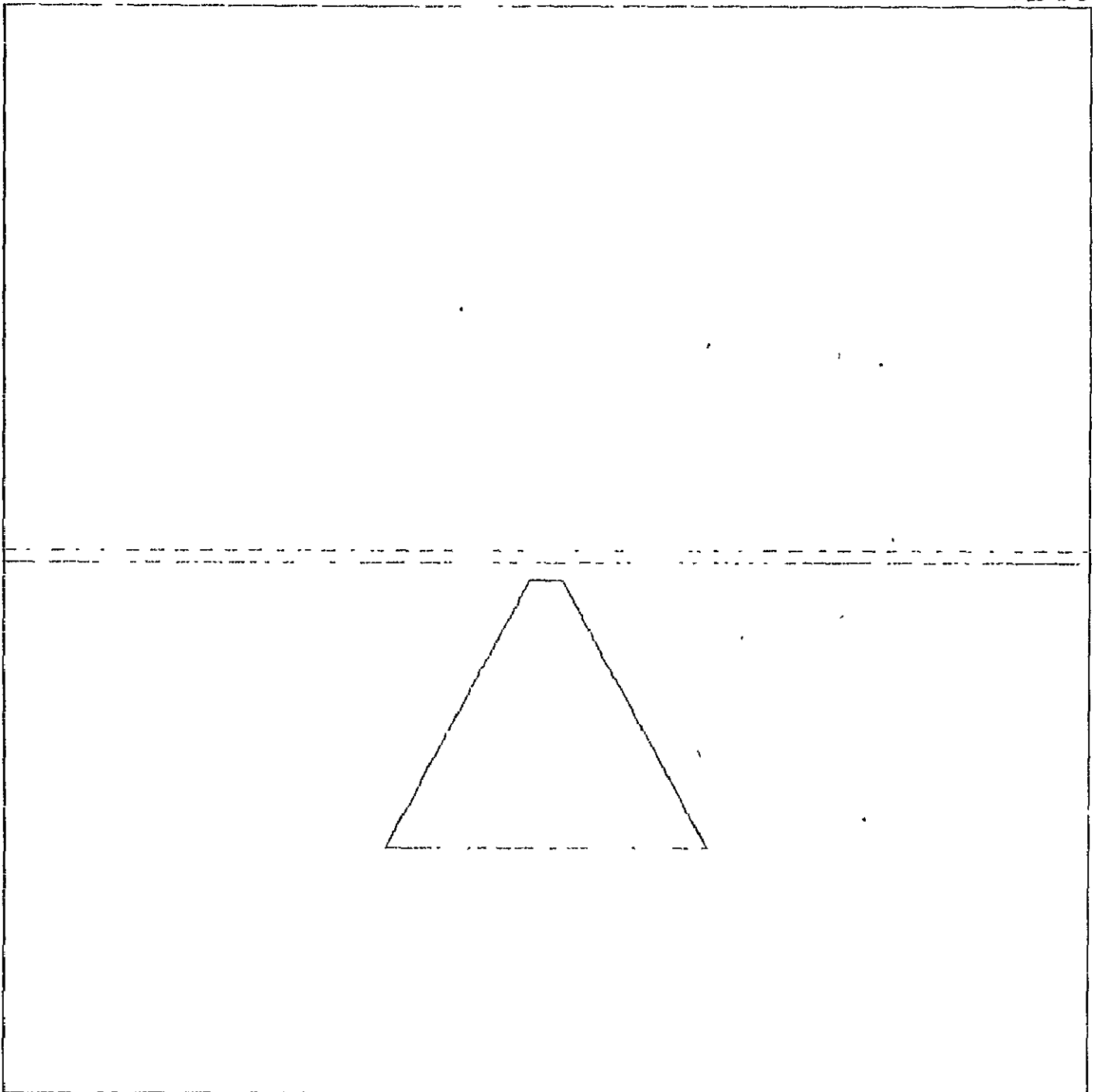
(c) Altitude = 50 ft.

Figure 30.- Concluded.



(a) Distance to TD = 2 mi.

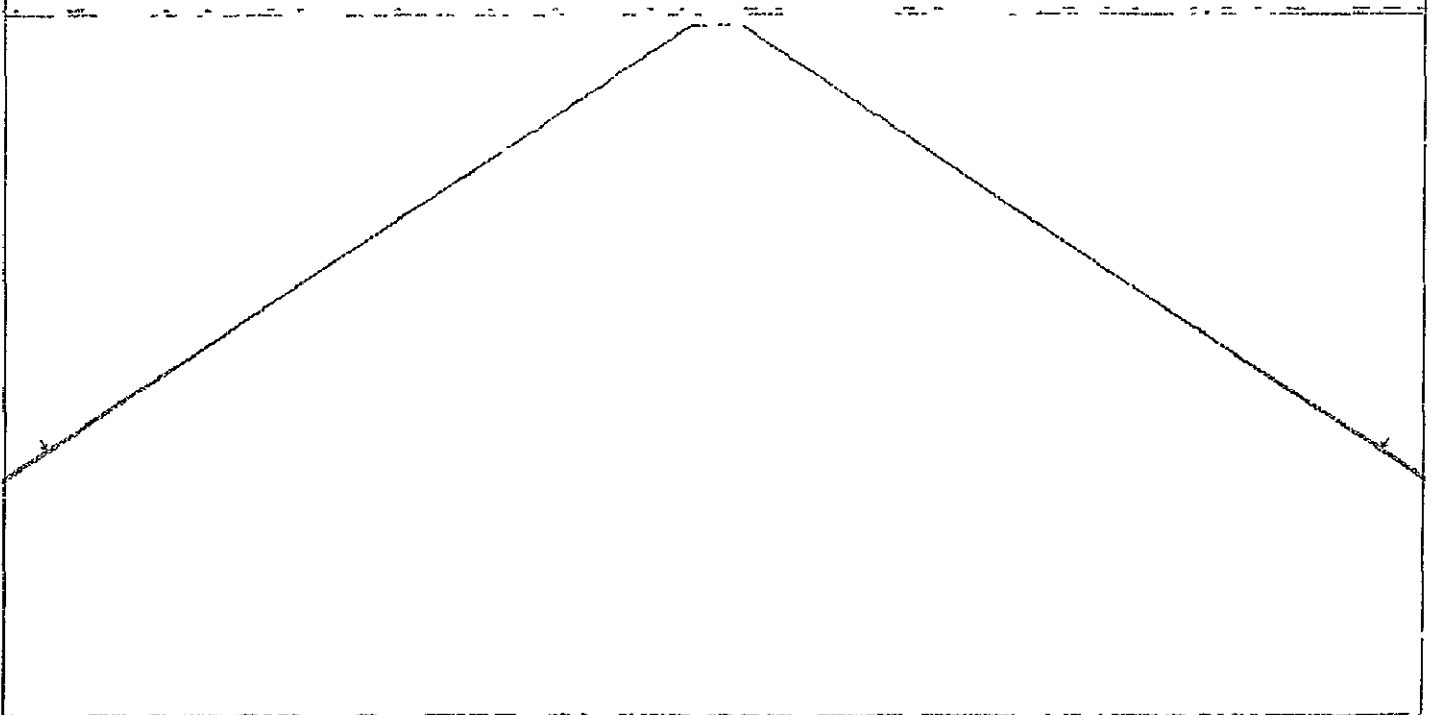
Figure 31.- Unstabilized display with aircraft on glide path,
 $Y = P = R = 0^\circ$.



(b) Distance to TD = $1/2$ mi.

Figure 31.- Continued.

ORIGINAL PAGE IS
OF POOR QUALITY



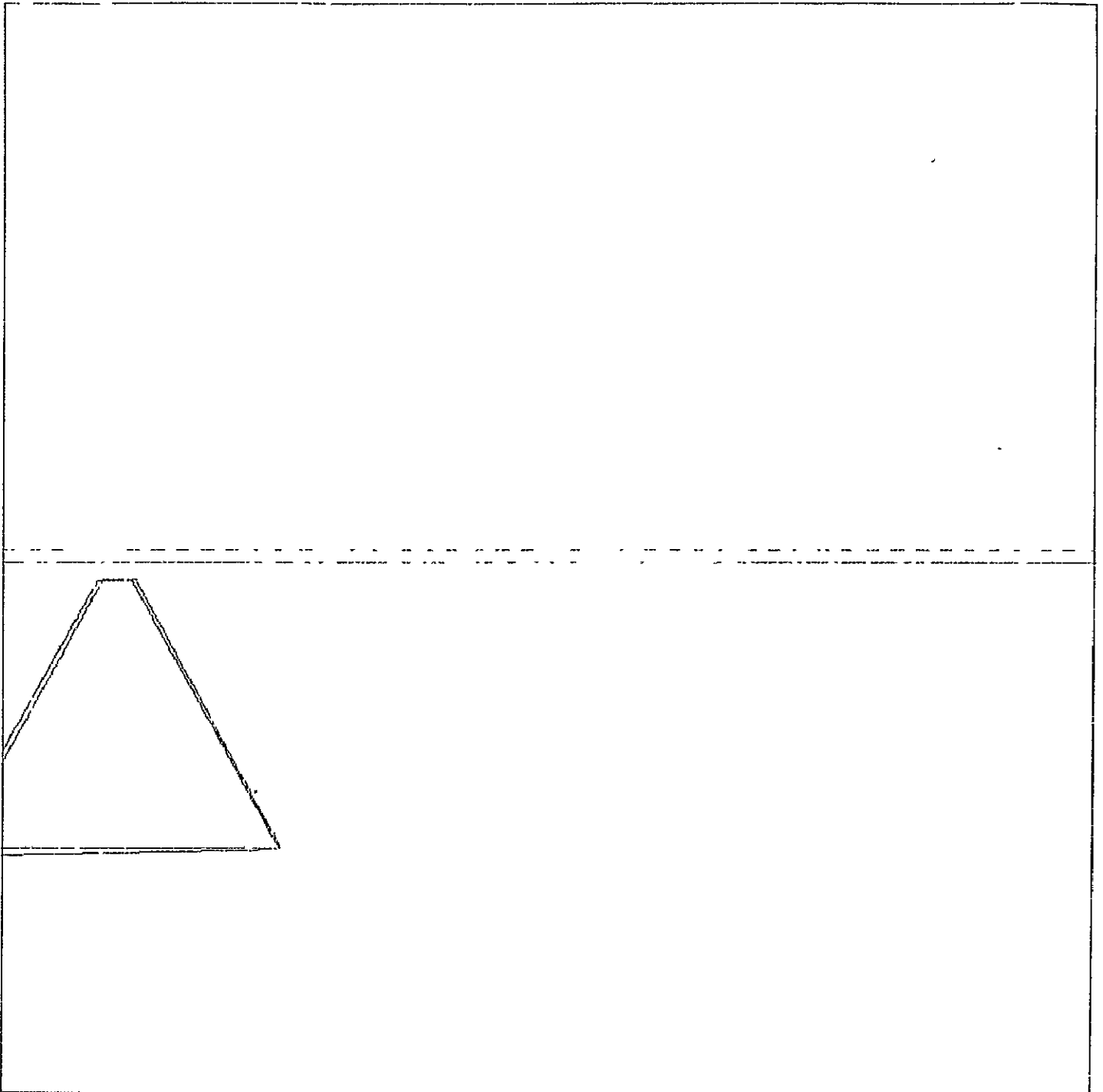
(c) Altitude = 50 ft.

Figure 31.- Concluded.



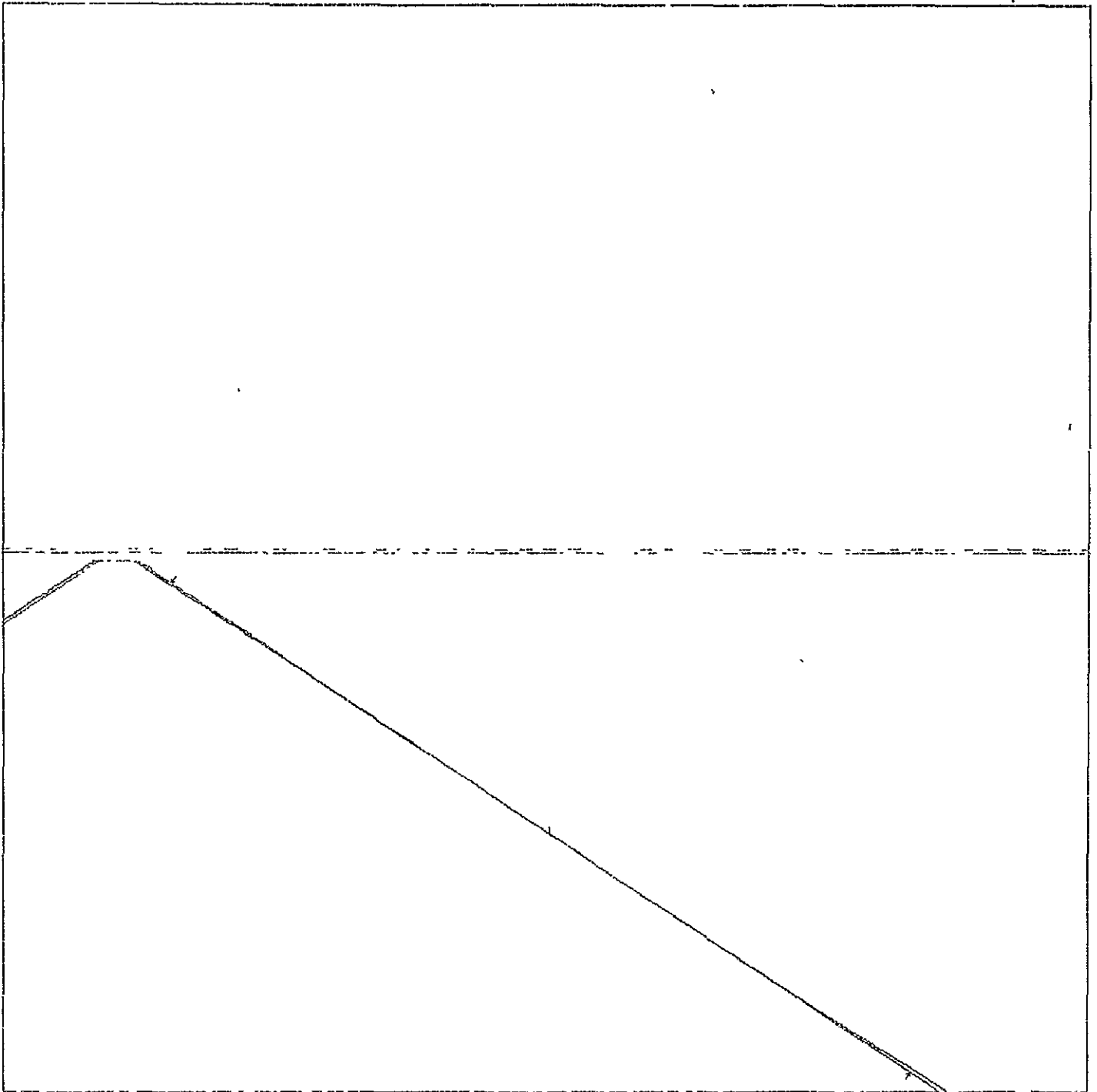
(a) Distance to TD = 2 mi.

Figure 32.- Unstabilized display with aircraft on glide path,
 $Y = 10^{\circ}$, $P = R = 0^{\circ}$.



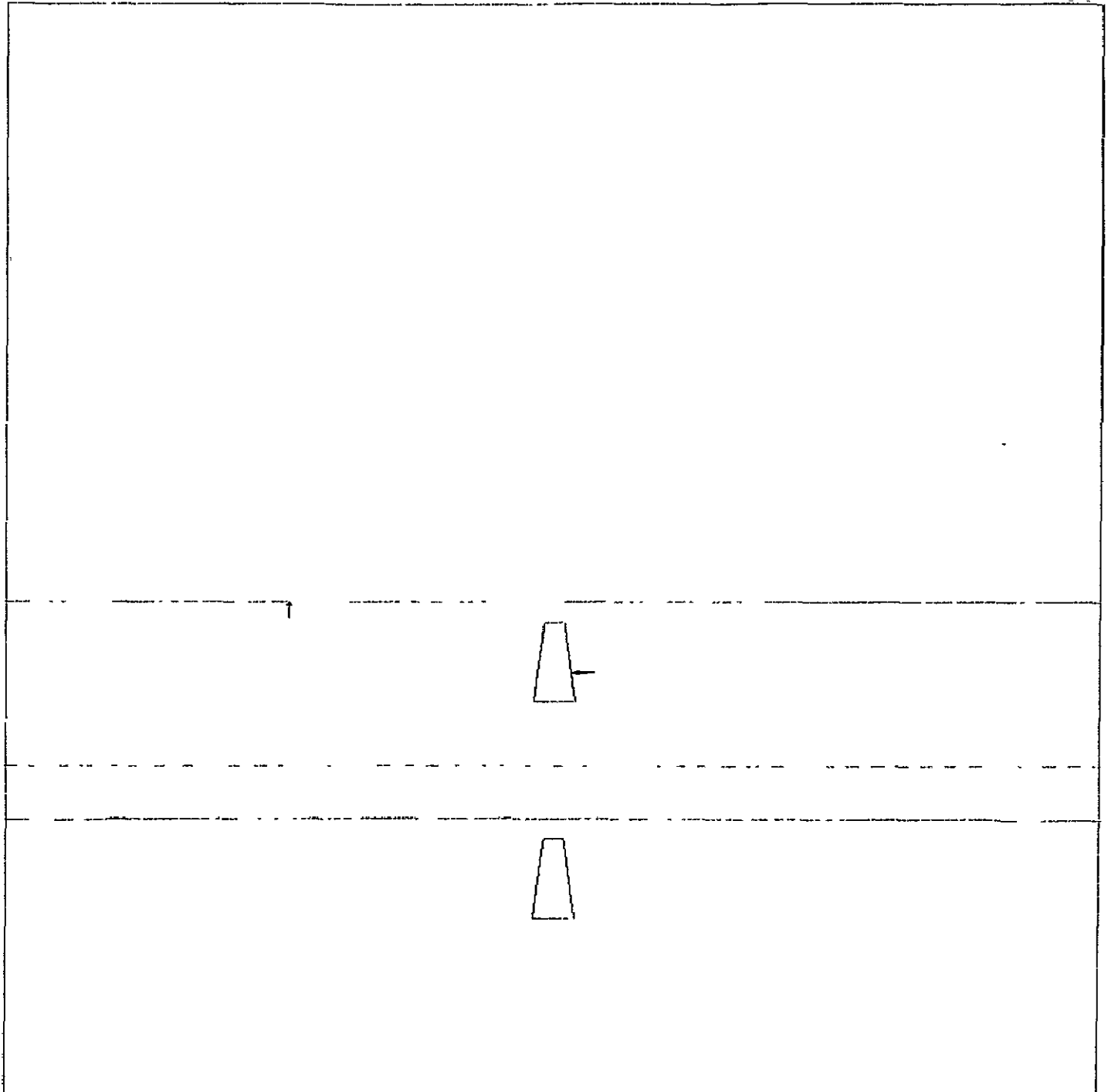
(b) Distance to TD = $1/2$ mi.

Figure 32.- Continued.



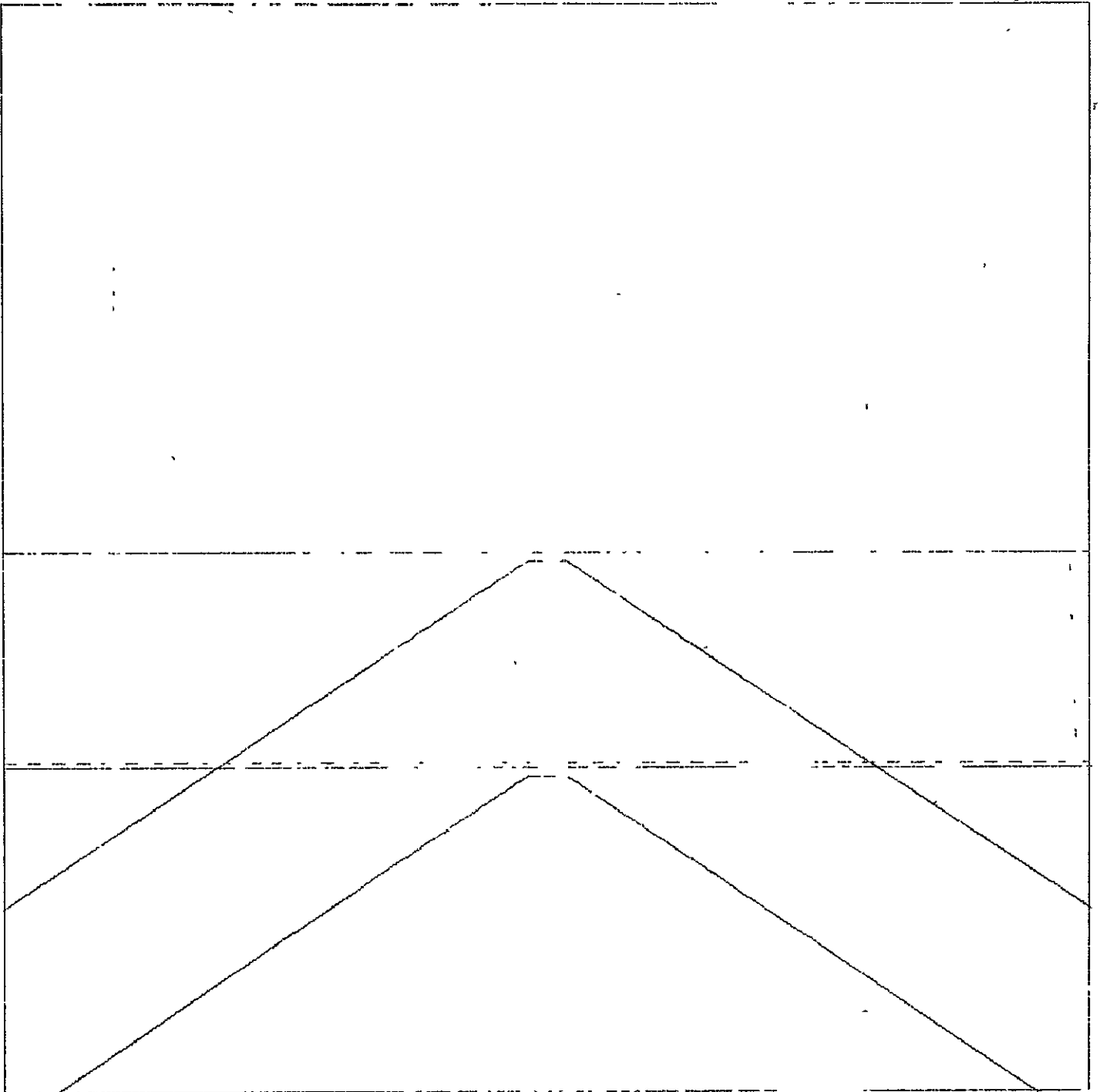
(c) Altitude = 50 ft.

Figure 32.- Concluded.



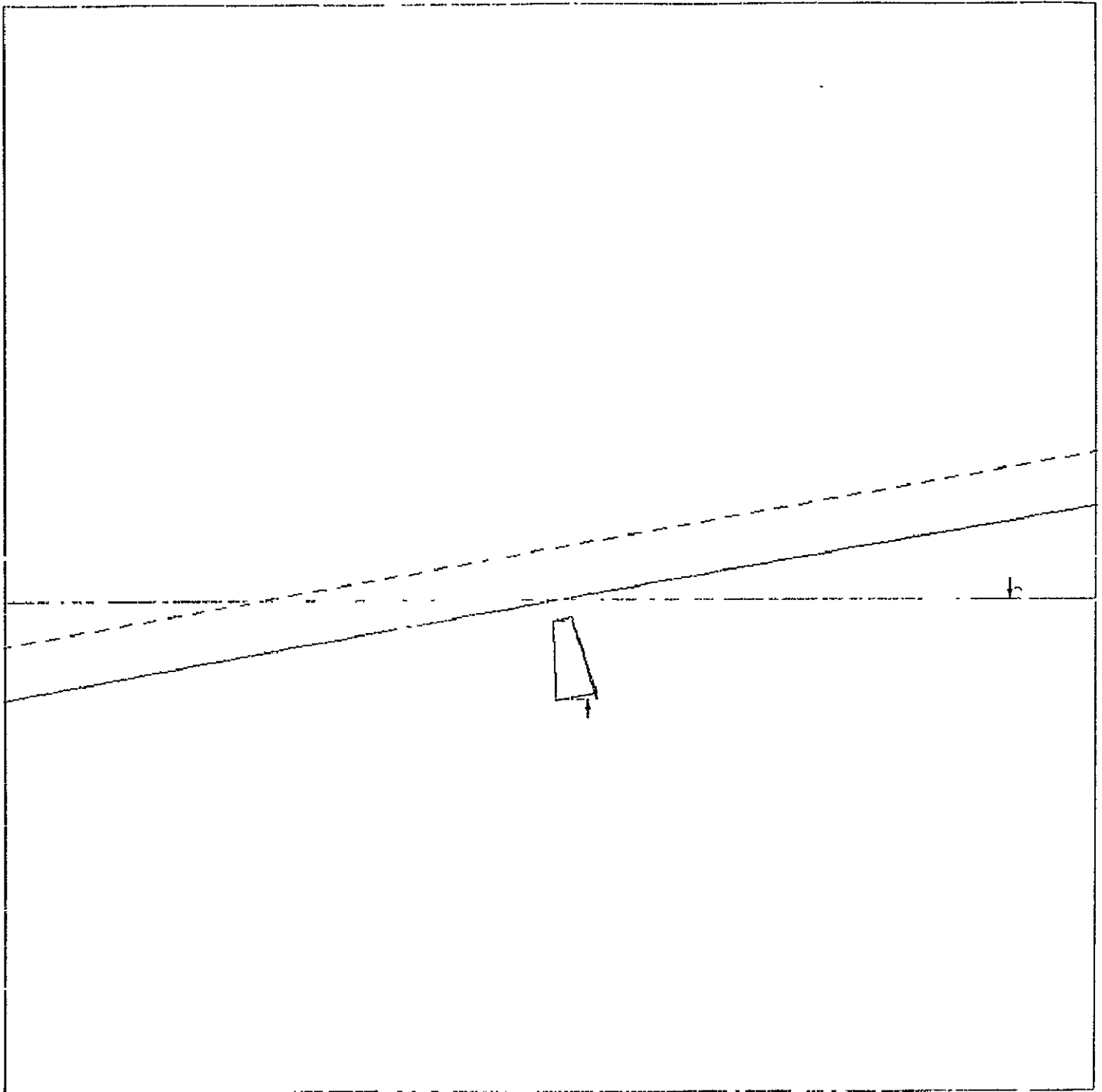
(a) Distance to TD = 2 mi.

Figure 33.- Unstabilized display with aircraft on glide path,
 $P = 5^{\circ}$, $Y = R = 0^{\circ}$.



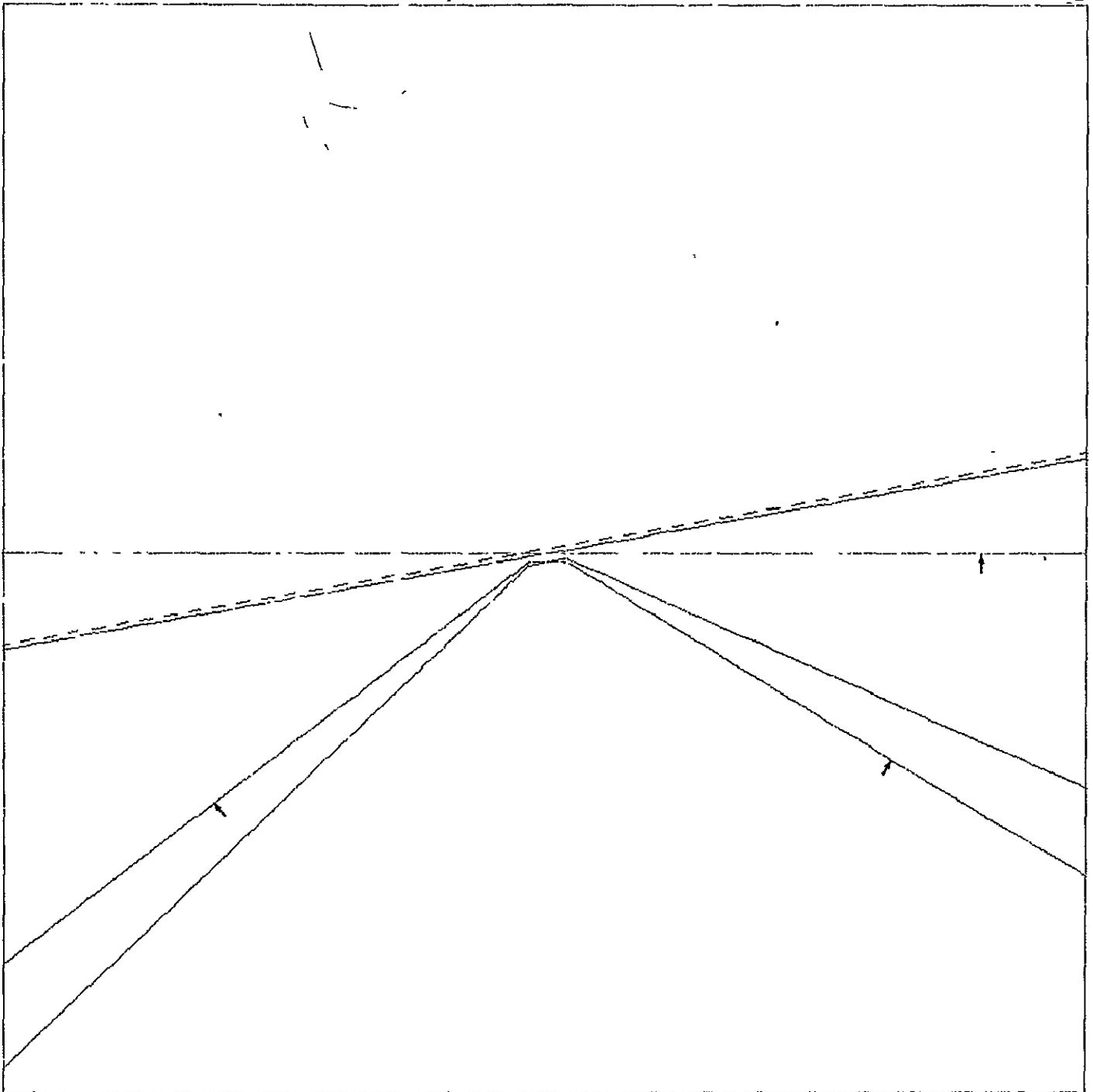
(b) Altitude = 50 ft.

Figure 33.- Concluded..



(a) Distance to TD = 2 mi.

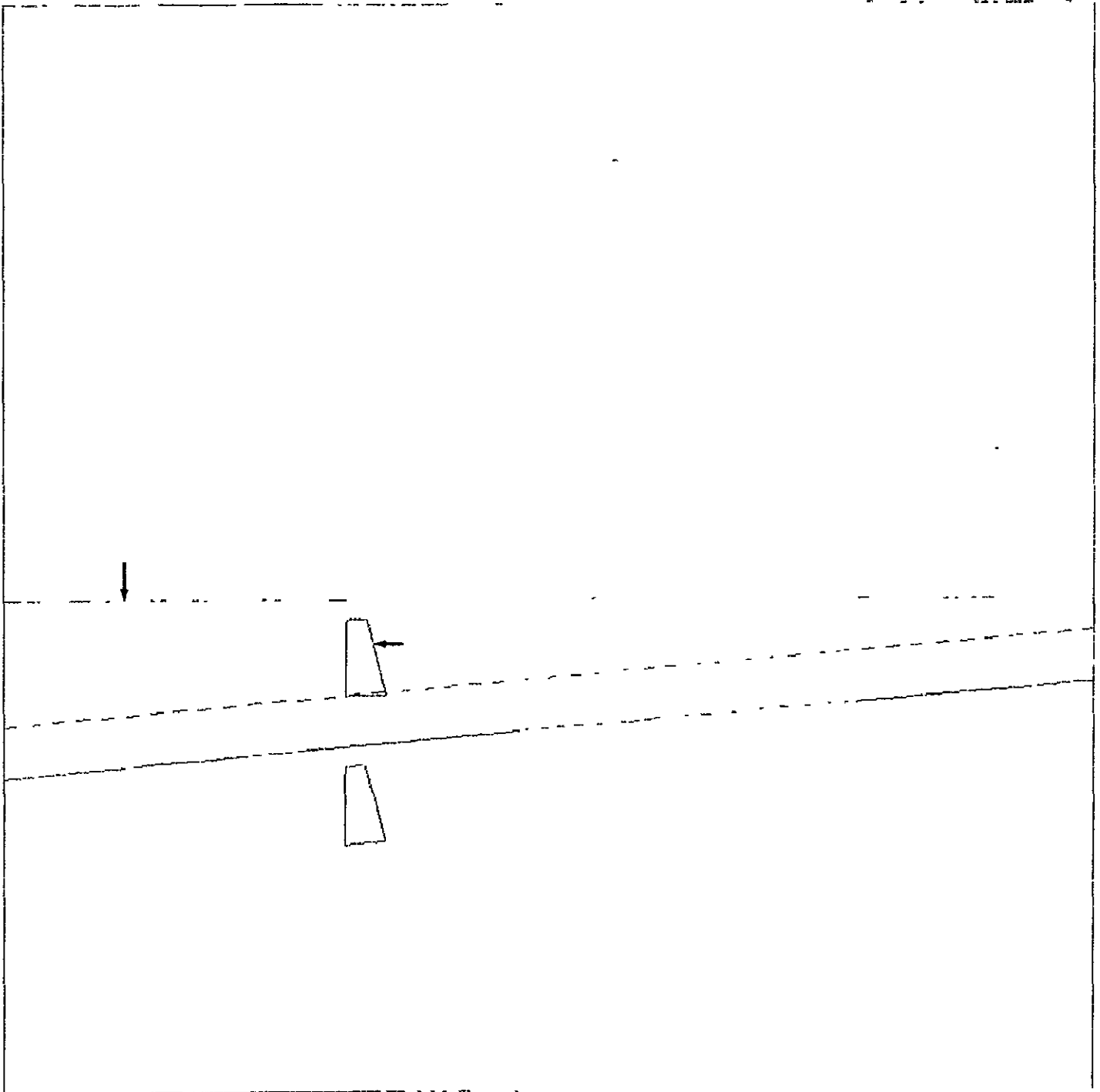
Figure 34.- Unstabilized display with aircraft on glide path,
 $Y = P = 0^\circ$, $R = 10^\circ$.



(b) Altitude = 50 ft.

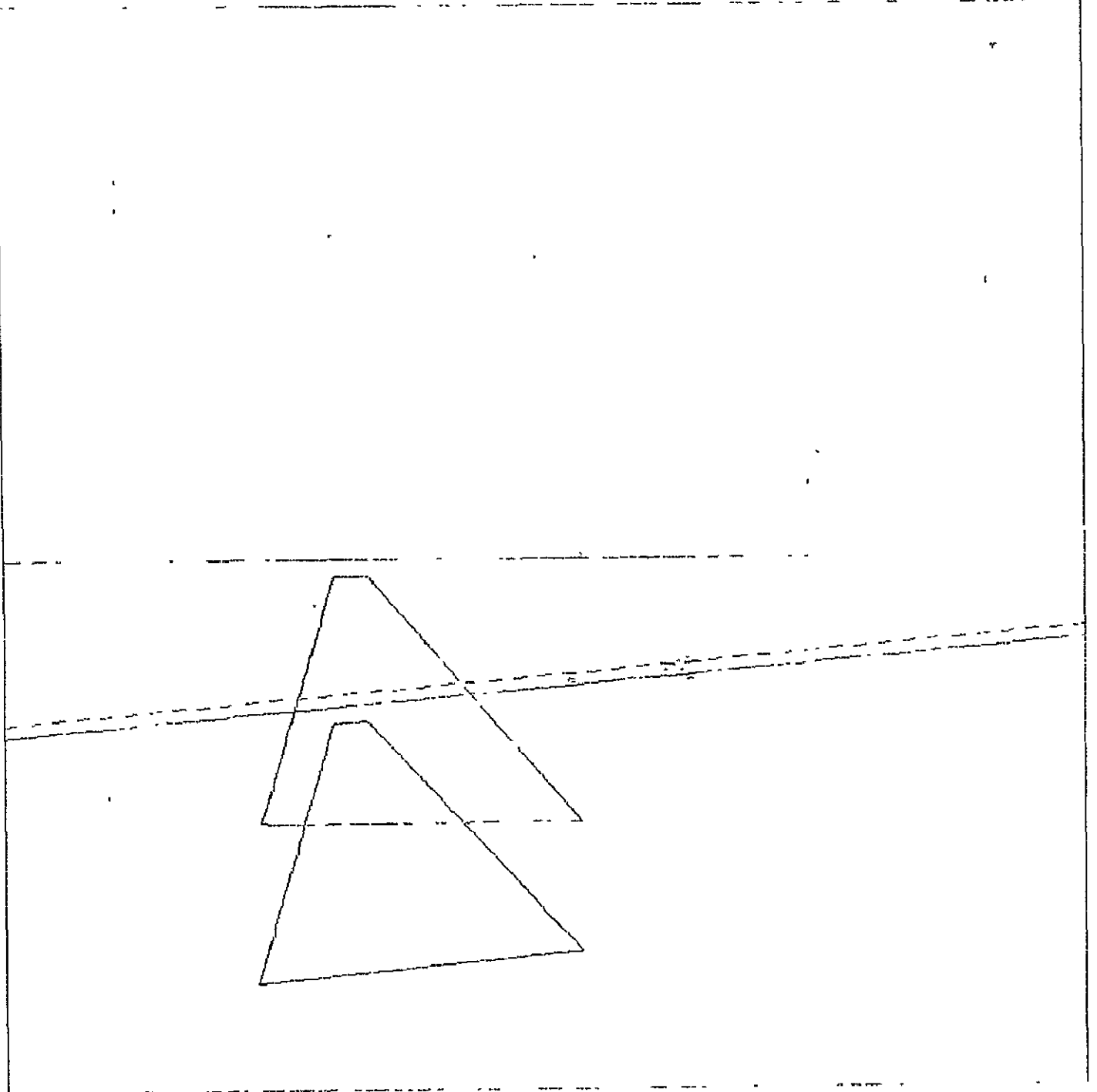
Figure 34.- Concluded.

ORIGINAL PAGE IS
OF POOR QUALITY



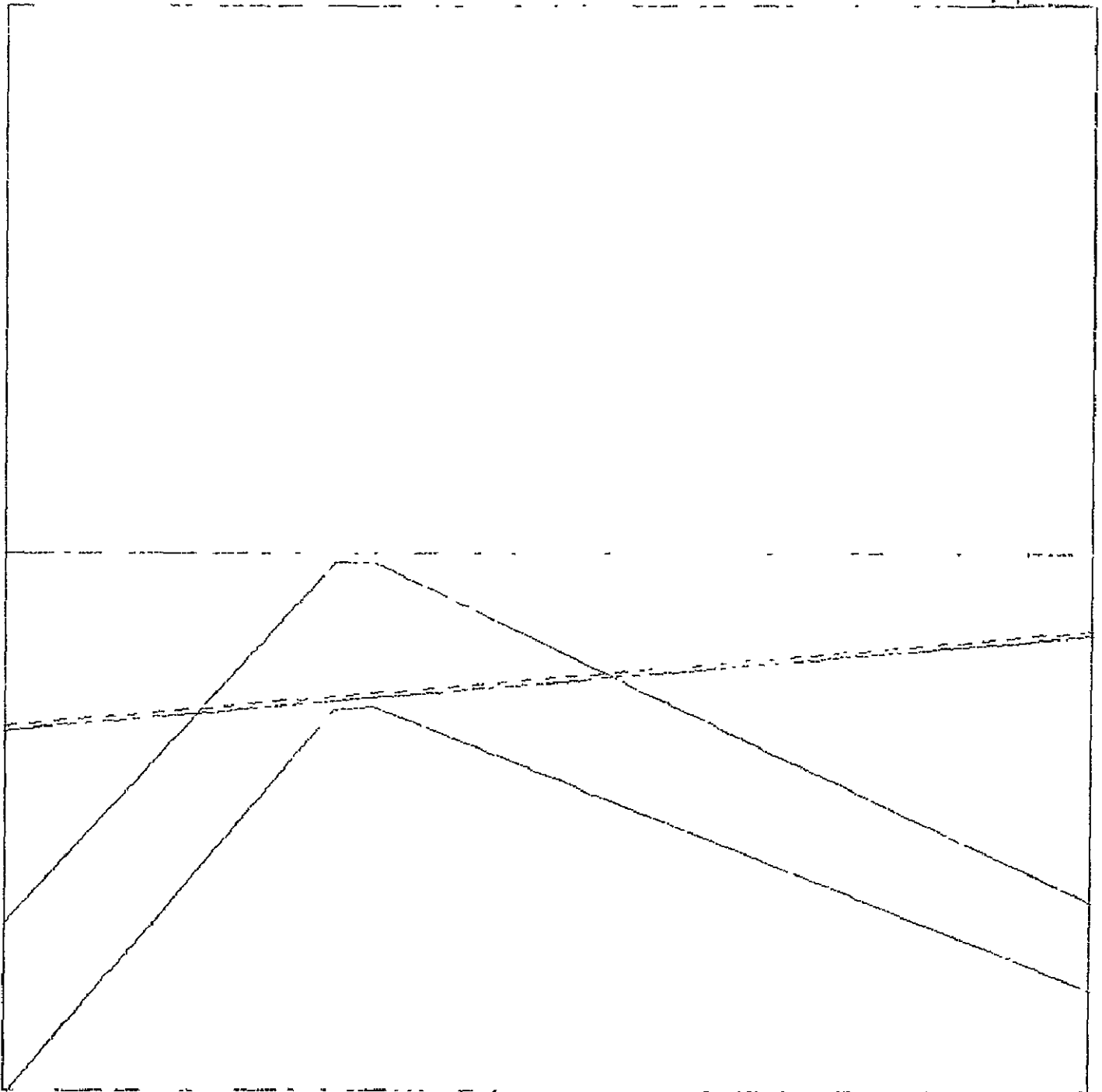
(a) Distance to TD = 2 mi.

Figure 35.- Unstabilized display with aircraft 25 ft. left of and 10 ft. below glide path, $Y = R = 5^\circ$, $P = 3^\circ$.



(b) Distance to TD = 1/2 mi.

Figure 35.- Continued.



(c) Altitude = 50 ft.

Figure 35.- Concluded.

ORIGINAL PAGE IS
OF POOR QUALITY

APPENDIX A

INTRODUCTION

The problem of drawing the radar image of the target (horizon and runway outline) will be solved by transforming a set of points in target space to the corresponding set of points in image space and appropriately connecting the image points by straight line segments.

The transformation of a point in target space to a point in image space will be accomplished through the following series of computations: 1) locate the target point in a set of earth fixed coordinates x, y, z centered in the aircraft; 2) transform from earth coordinates to aircraft fixed coordinates x_3, y_3, z_3 ; 3) transform from aircraft to radar coordinates R, ξ ; 4) introduce measurement errors in the radar coordinates and transform to aircraft coordinates using approximations in the computed transformation; and 5) transform from aircraft to image coordinates y_i, z_i .

Derivation of Transformations

Target space.— Let x, y, z be a Cartesian coordinate system centered in the aircraft with the x -axis parallel to the runway centerline, the z -axis vertically downward, and the y -axis oriented to form a right-handed coordinate system.

This coordinate system and the aircraft-runway geometry are shown in figure A1.

Let the aircraft location be specified by the glide slope ϵ , the azimuth angle δ , the distance y_0 to the left of the glide path, the distance z_0 above the glide path, and the projected distance x_a of the aircraft from the touchdown point. Then the coordinates of any point $P(x,y,z)$ along the outline of the runway are

$$\left. \begin{aligned} x &= x_a - l_a + p \\ y &= y_a \pm w/2 \\ z &= z_a = h \end{aligned} \right\} \quad (A1)$$

where

$$y_a = x_a \tan \delta + y_o \quad (A2)$$

$$z_a = x_a \sec \delta \tan \epsilon + z_o \quad (A3)$$

Earth coordinates to aircraft coordinates transformation.- In transforming from earth to aircraft coordinates it will be assumed that aircraft attitude angles Y (yaw), P (pitch), and R (roll) are measured in the sequence Y, P, R.

Let x_1, y_1, z_1 be a set of aircraft fixed coordinates, originally alined with x, y, z , after a yaw maneuver of angle Y as in figure A2. Then the transformation $T_1: (x, y, z) \rightarrow (x_1, y_1, z_1)$ is defined by

$$\begin{bmatrix} x_1 \\ y_1 \\ z_1 \end{bmatrix} = \begin{bmatrix} \cos Y & \sin Y & 0 \\ -\sin Y & \cos Y & 0 \\ 0 & 0 & 1 \end{bmatrix} \begin{bmatrix} x \\ y \\ z \end{bmatrix} \quad (A4)$$

Now, let x_2, y_2, z_2 be a set of aircraft fixed coordinates, originally alined with x_1, y_1, z_1 , after a pitch maneuver P as in figure A3. Then the transformation $T_2: (x_1, y_1, z_1) \rightarrow (x_2, y_2, z_2)$ is defined by

$$\begin{bmatrix} x_2 \\ y_2 \\ z_2 \end{bmatrix} = \begin{bmatrix} \cos P & 0 & -\sin P \\ 0 & 1 & 0 \\ \sin P & 0 & \cos P \end{bmatrix} \begin{bmatrix} x_1 \\ y_1 \\ z_1 \end{bmatrix} \quad (A5)$$

Let x_3, y_3, z_3 be a set of aircraft fixed coordinates, originally aligned with x_2, y_2, z_2 , after a maneuver through an angle R as in figure A4. Then the transformation $T_3: (x_2, y_2, z_2) \rightarrow (x_3, y_3, z_3)$ is defined by

$$\begin{bmatrix} x_3 \\ y_3 \\ z_3 \end{bmatrix} = \begin{bmatrix} 1 & 0 & 0 \\ 0 & \cos R & \sin R \\ 0 & -\sin R & \cos R \end{bmatrix} \begin{bmatrix} x_2 \\ y_2 \\ z_2 \end{bmatrix} \quad (A6)$$

The transformation T from earth coordinates to aircraft coordinates is then given by

$$T = T_3 T_2 T_1$$

or

$$\begin{bmatrix} x_3 \\ y_3 \\ z_3 \end{bmatrix} = \begin{bmatrix} \cos P \cos Y & \cos P \sin Y \\ (-\cos R \sin Y + \sin R \sin P \cos Y) & (\cos R \cos Y + \sin R \sin P \sin Y) \\ (\sin R \sin Y + \cos R \sin P \cos Y) & (-\sin R \cos Y + \cos R \sin P \sin Y) \end{bmatrix} \begin{bmatrix} x \\ y \\ z \end{bmatrix} \quad (A7)$$

Aircraft coordinates to radar coordinates.- Assume that the forward looking radar scans the target using a phased array antenna with the array axis colinear with the aircraft y_3 axis and centered at the origin of the x_3, y_3, z_3 coordinate system. When the array is scanned at an angle ξ , the radar is pointed at a target (point $P(x_3, y_3, z_3)$ in figure A6) defined by the intersection of the ground and a right cone, whose axis is the y_3 axis, with half apex angle ξ .

The radar coordinates r, ξ of the point P are found from

$$r = \sqrt{x_3^2 + y_3^2 + z_3^2}$$

$$\xi = \cos^{-1} \left(\frac{y_3}{r} \right)$$
(A8)

Radar coordinates to aircraft coordinates.- Consider the point P in figure A7 located on the ground at radar coordinates r, ξ . The y_3 coordinate of P is

$$y_3 = r \cos \xi$$
(A9)

The altitude h , as measured by the aircraft's altimeter, is the distance to the subaircraft point (x_{3h}, y_{3h}, z_{3h}) . From the right triangle OPQ

$$|\vec{r} - \vec{h}|^2 + |\vec{h}|^2 = |\vec{r}|^2$$

or

$$(x_3 - x_{3h})^2 + (z_3 - z_{3h})^2 = r^2 - h^2 - (y_3 - y_{3h})^2 \quad (A10)$$

From right triangle OPU

$$x_3 = \sqrt{r^2 - y_3^2 - z_3^2} \quad (A11)$$

Substituting (A11) into (A10) and rearranging produces

$$-x_{3h} \sqrt{r^2 - z_3^2 - y_3^2} = z_{3h}z_3 + y_{3h}y_3 - h^2 \quad (A12)$$

Square equation (A12) and rearrange to obtain a quadratic in z_3 .

$$\begin{aligned} (x_{3h}^2 + z_{3h}^2) z_3^2 + 2z_{3h}(y_{3h}y_3 - h^2)z_3 \\ + x_{3h}^2(y_3^2 - r^2) + (y_{3h}y_3 - h^2)^2 = 0 \end{aligned} \quad (A13)$$

Then

$$z_3 = \frac{-b \pm \sqrt{b^2 - 4ac}}{2a} \quad (A14)$$

where

$$a = x_{3h}^2 + z_{3h}^2 \quad (A15a)$$

$$b = 2z_{3h}(y_{3h}y_3 - h^2) \quad (A15b)$$

$$c = x_{3h}^2 (y_3^2 - r^2) + (y_{3h} y_3 - h^2)^2$$

The altitude h is known and y_3 is known from equation (A9). To find x_{3h} , y_{3h} , z_{3h} consider that the earth coordinates of the subaircraft point Q are $(0, 0, h)$. Applying the transformation T (eq. (A7)) to the coordinates of Q , we obtain

$$\left. \begin{aligned} x_{3h} &= -h \sin P \\ y_{3h} &= h \sin R \cos P \\ z_{3h} &= h \cos R \cos P \end{aligned} \right\} \quad (A16)$$

All of the quantities required to compute z_3 are now known.

The remaining aircraft coordinate x_3 of the point P can now be calculated using equation (A11).

Aircraft coordinates to image coordinates.— Consider the CRT screen centered on and perpendicular to the x_3 -axis at a distance d from the origin as shown in figure A8. For a magnification ratio of unity the location (y_i, z_i) of the image P_i of a target point P must lie at the intersection of the radius vector \vec{r} and the CRT screen. It is a simple problem in geometry to find that

$$\left. \begin{aligned} y_i &= \frac{y_3}{x_3} d \\ z_i &= \frac{z_3}{x_3} d \end{aligned} \right\} \quad (A17)$$

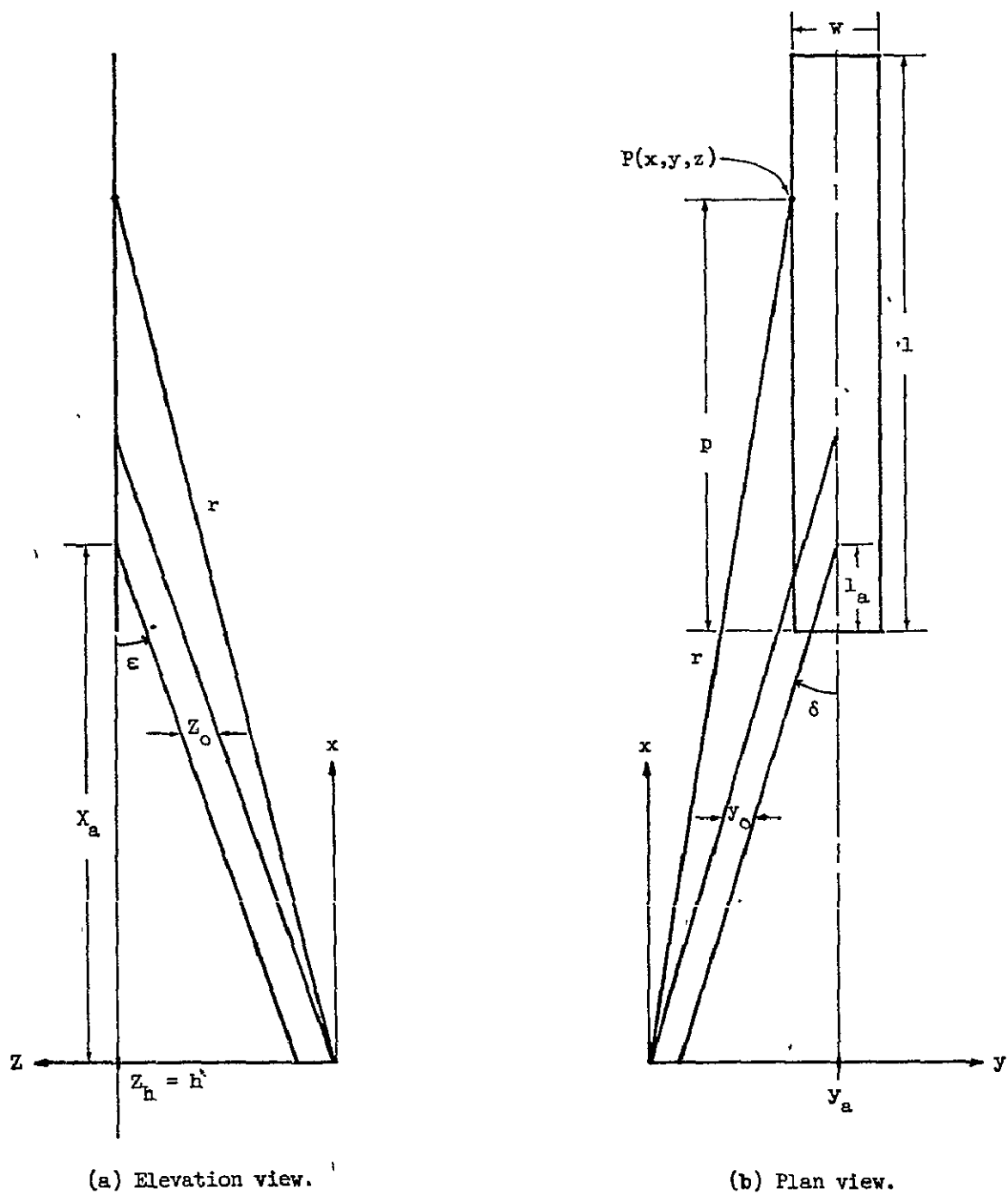


Figure A1.- Aircraft-runway geometry in earth coordinates.

ORIGINAL PAGE IS
OF POOR QUALITY

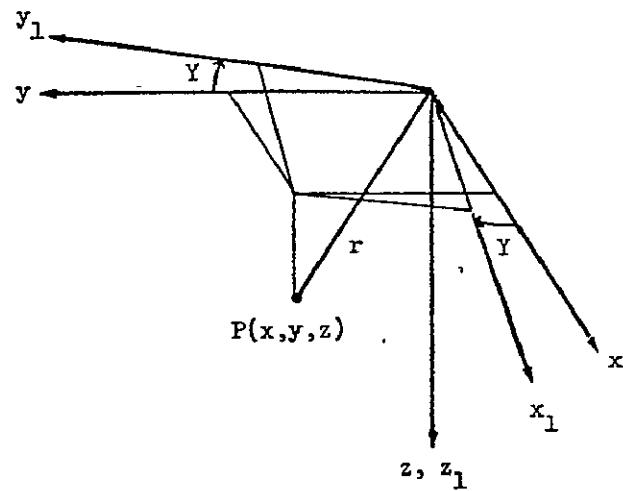


Figure A2.- Coordinate geometry after yaw maneuver.

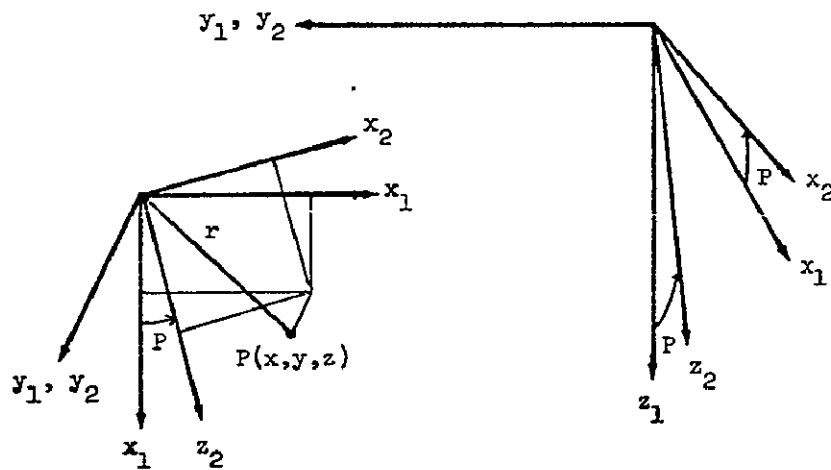


Figure A3.- Coordinate geometry after pitch maneuver.

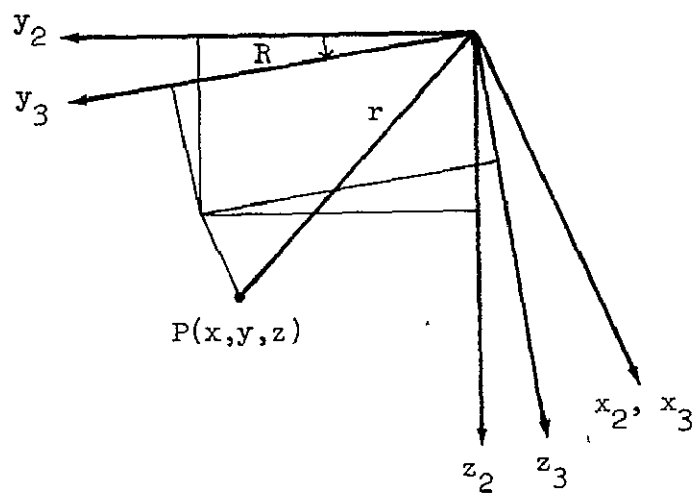


Figure A4.- Coordinate geometry after roll maneuver.

ORIGINAL PAGE IS
OF POOR QUALITY

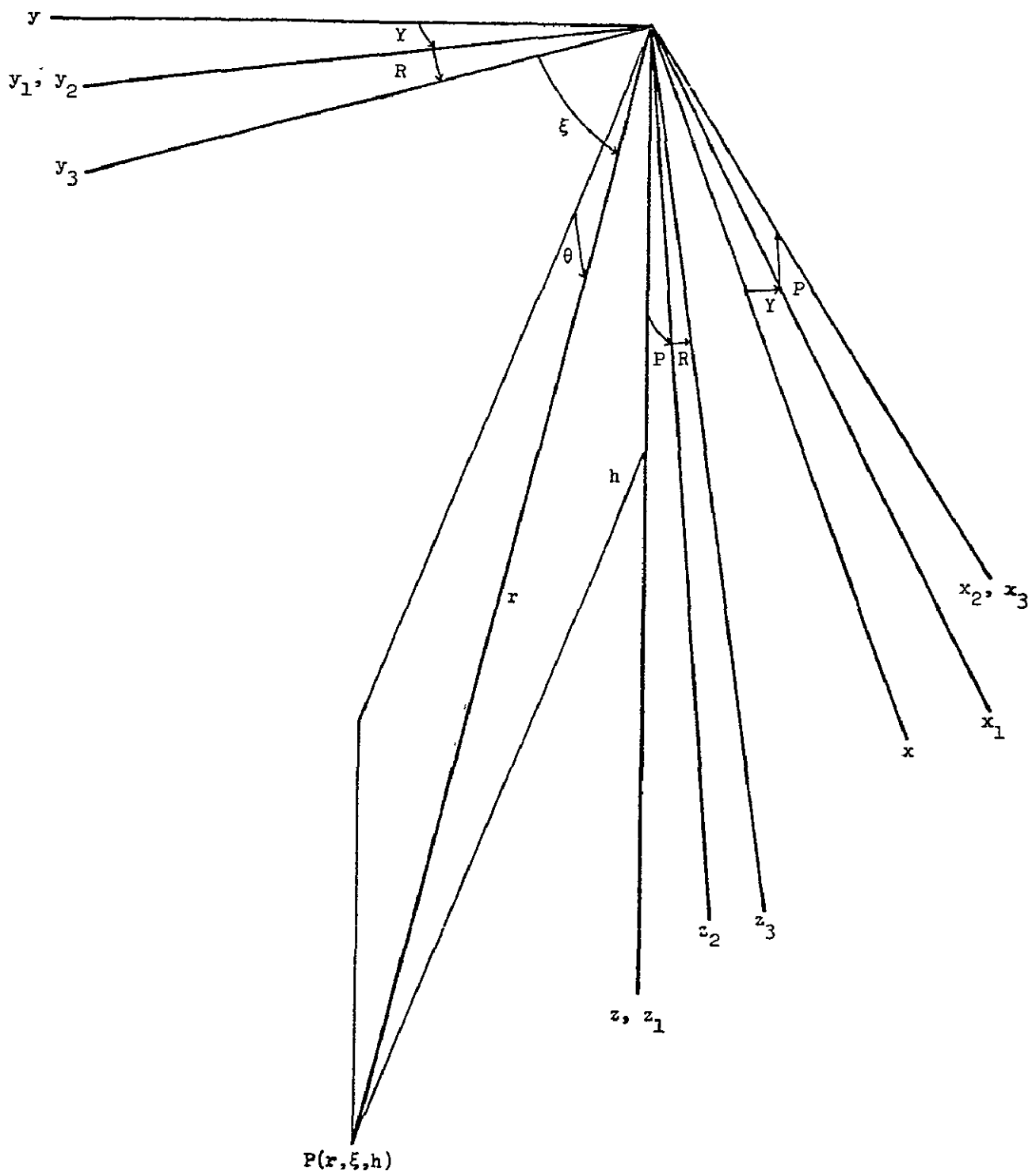


Figure A5.- Earth coordinate to aircraft coordinate geometry.

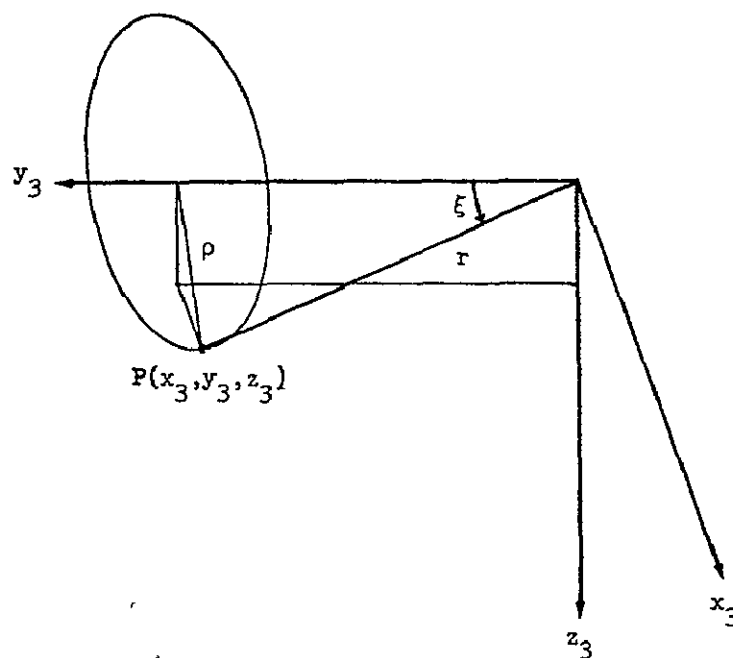
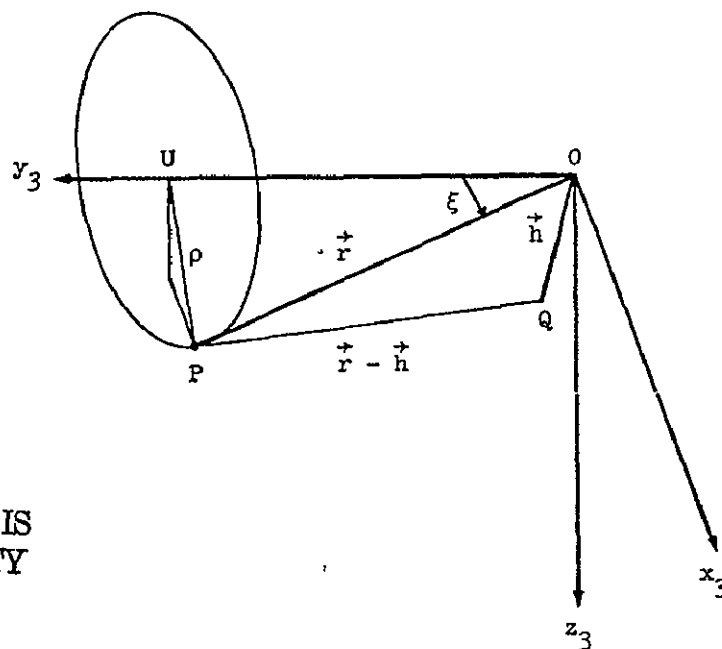


Figure A6.- Aircraft coordinate to radar coordinate transformation geometry.



ORIGINAL PAGE IS
OF POOR QUALITY

Figure A7.- Radar coordinate to aircraft coordinate transformation geometry.

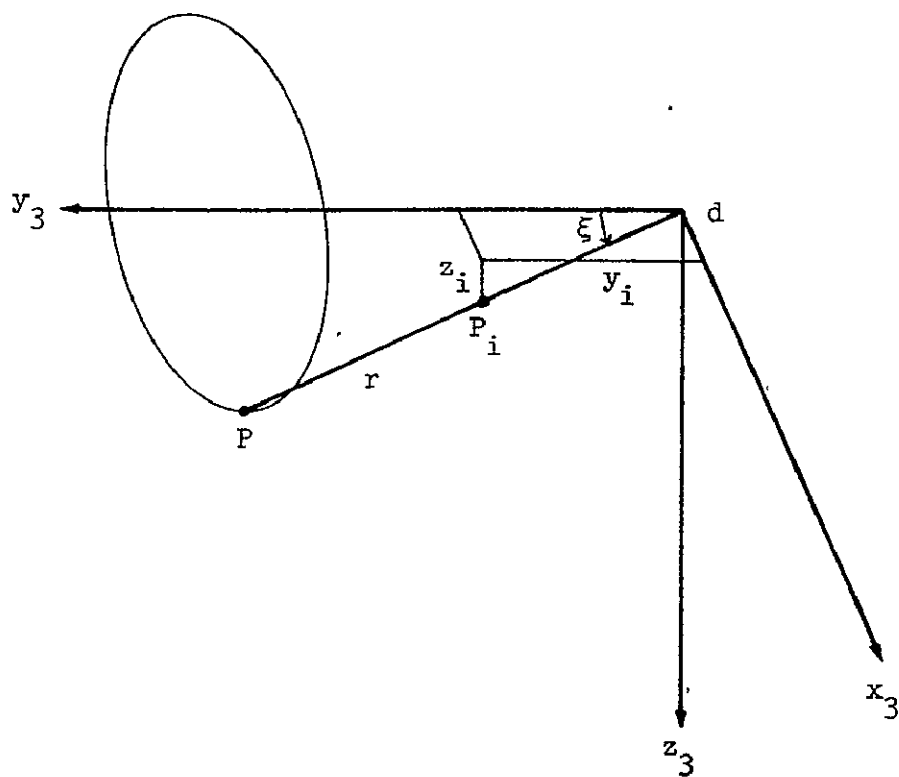


Figure A8.- Radar coordinate-image coordinate geometry.

APPENDIX B

APPROXIMATIONS TO THE RADAR TO AIRCRAFT COORDINATES TRANSFORMATION

INTRODUCTION

In Appendix A we derived the transformation which converts the radar coordinates of a point P to the aircraft coordinates for that point. To perform this computation in the radar requires the knowledge (measurement) of aircraft altitude and attitude and requires computer facilities capable of performing square root and trigonometric computations. The attitude measurement and computational requirements can be reduced by using certain approximations in the transformation. Two such approximations are described in this appendix.

Unstabilized Display

An unstabilized display is one on which the image is constructed without knowledge of the aircraft's attitude. In other words, it is assumed that the aircraft is flying straight and level with the result that

$$z_3 = h \tag{B1}$$

A further approximation is that

$$\cos \xi = \sin\left(\frac{\pi}{2} - \xi\right)$$

$$\approx \frac{\pi}{2} - \xi \tag{B2}$$

Then from equation (A9)

$$\begin{aligned}y_3 &= r \cos \xi \\&\approx r\left(\frac{\pi}{2} - \xi\right)\end{aligned}\tag{B3}$$

and from equation (A11)

$$\begin{aligned}x_3 &= \sqrt{r^2 - y_3^2 - z_3^2} \\&= \sqrt{r^2 \sin^2 \xi - z_3^2} \\&\approx \sqrt{r^2 - h^2}\end{aligned}\tag{B4}$$

where $\sin^2 \xi \approx 1$

It is obvious that the above approximations are good only when aircraft roll and pitch are very small and when the radar is scanning close to forward ($\xi \approx \frac{\pi}{2}$). Even then the image may not be adequate for some applications, such as attitude determination.

Small Angle Approximations

Using small angle approximations to the trigonometric functions does not eliminate the requirement to measure aircraft attitude, but it does reduce the computational workload. The applicable approximations are

$$\left. \begin{aligned} \sin \xi &= 1 \\ \cos \xi &= \frac{\pi}{2} - \xi \\ \sin P &= P \\ \sin R &= R \\ \cos P &= \cos R = 1 \end{aligned} \right\} \quad (B5)$$

With these approximations the coefficients used in computing z_3 (eqs. (A14) - (A16)) become

$$\left. \begin{aligned} a &= h^2(P^2 + 1) \\ b &= 2h^2[r(\frac{\pi}{2} - \xi)R - h] \\ c &= -r^2h^2P^2 + h^2[rR(\frac{\pi}{2} - \xi) - h]^2 \end{aligned} \right\} \quad (B6)$$

Equations (B3) and (B4) are used to calculate y_3 and x_3 , respectively.

APPENDIX C

COMPUTATION OF HORIZON IMAGE

Actual Horizon

In level flight ($R = P = 0$) the horizon is imaged along the y_i -axis ($z_i = 0$) independent of altitude and yaw angle Y . (See line (1), fig. C1.) After a pitch up through an angle P , the equation for the horizon image is

$$z_i = d \tan P \quad (C1)$$

where d is the distance from the origin along the x_3 -axis to the CRT screen as in Appendix A, figure A8. (See line (2), fig. C1.)

If the pitch up maneuver is followed by a roll through an angle R , the horizon image intercepts the z_i -axis ($y_i = 0$) at

$$z_{i0} = d \cdot \tan P / \cos R \quad (C2)$$

and the slope of the image line is

$$\begin{aligned} m &= \frac{dz_i}{dy_i} \\ &= - \tan R \end{aligned} \quad (C3)$$

The equation describing the horizon image, as shown by line (3) in fig. C1, is then

$$z_i = -y_i \tan R + d \cdot \tan P / \cos R \quad (C4)$$

Radar Horizon

Assume that the maximum range of the radar is r_{\max} . The problem is to locate the locus of points on the ground (called the radar horizon) corresponding to $r = r_{\max}$ and to find the image of this locus on the CRT screen. The problem will be solved by determining in earth coordinates the locus of points for $r = r_{\max}$. The image is then found by employing the series of coordinate transformations described in Appendix A.

The locus of points for $r = r_{\max}$ is a circle centered on the sub-aircraft point and described by

$$x^2 + y^2 = r_{\max}^2 - h^2 \quad (C5)$$

However, only the segment of that circle whose image lies on the CRT screen is of interest.

Let the segment of interest lie within an azimuth angle $\pm\phi_{\max}$ about the aircraft heading, where ϕ_{\max} is yet to be determined. Then the y-coordinate of a point P on the radar horizon is

$$y = x \tan (Y - \phi) \quad (C6)$$

where ϕ is the azimuth angle of P relative to the aircraft heading. (See fig. C2.) Combining equations (C5) and (C6), we find the x-coordinate to be

$$x = \sqrt{\frac{r_{\max}^2 - h^2}{1 + \tan^2(Y - \phi)}} \quad (C7)$$

To determine ϕ_{\max} , consider that the maximum angle subtended by the image of the radar horizon would occur when the aircraft attitude is such that the image line is a diagonal of the screen. Then

$$\phi_{\max} = \tan^{-1} \left(\frac{1}{2} \sqrt{y_{\text{CRT}}^2 + z_{\text{CRT}}^2} \right) \quad (C8)$$

ORIGINAL PAGE IS
OF POOR QUALITY

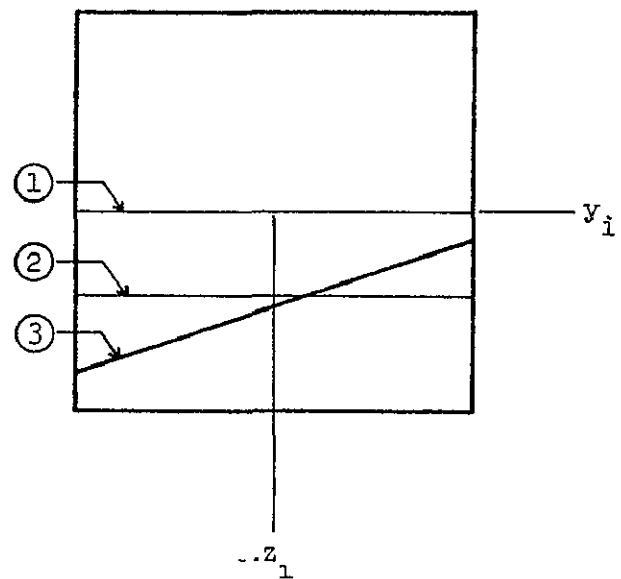
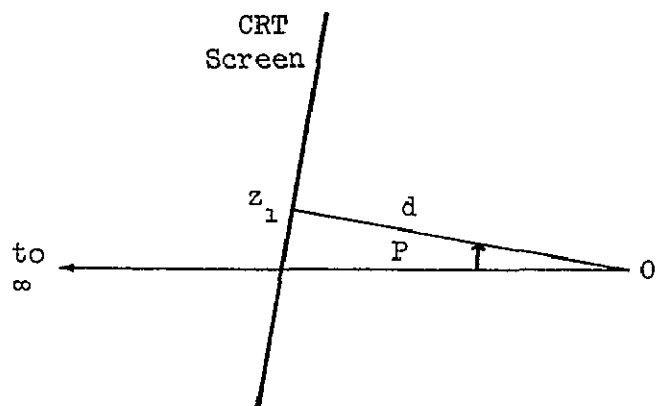


Figure C1.- Geometry for determining horizon image position.

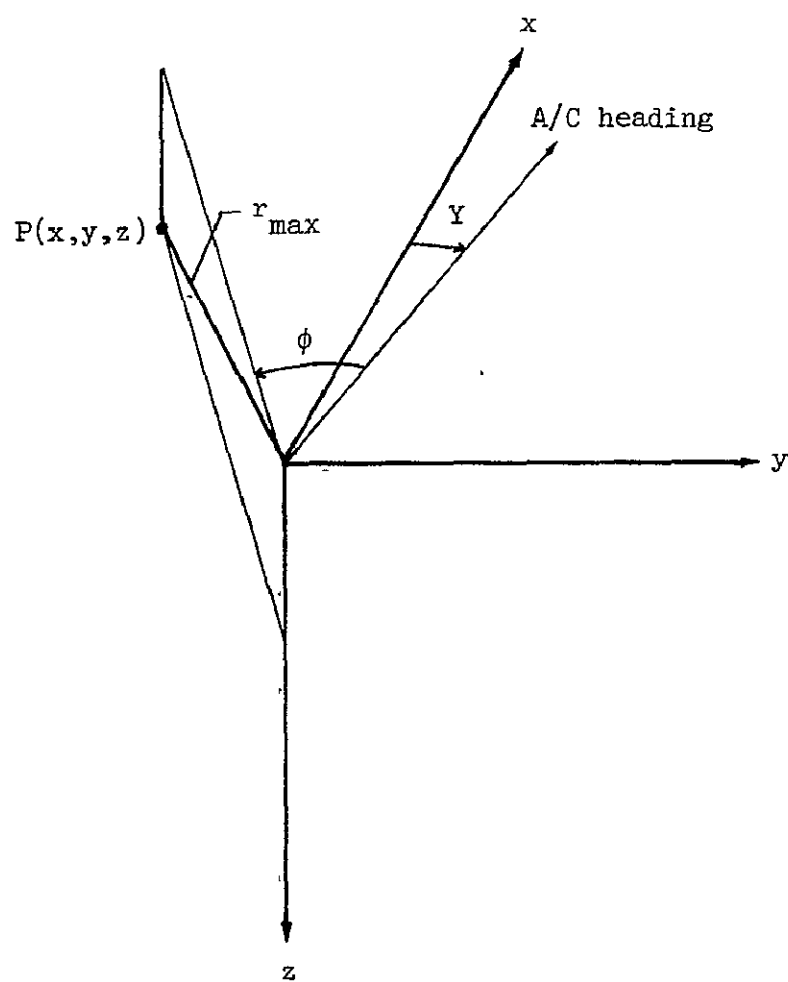


Figure C2.- Geometry for drawing radar horizon.

APPENDIX D

COMPUTER PROGRAM DISPLAY

A computer program named DISPLAY was written to perform the calculations described in Appendices A-C and to produce outline drawings of the radar image. Three versions of the program were utilized. The first version produced a set of radar images from a set of input data describing the aircraft position and attitude. The second version produced two overlayed radar images from two sets of input data. This program could be used to compare the images obtained from slightly different aircraft positions or attitudes to determine what changes in aircraft state could be detected on the images. The third version of the program produced two overlayed radar images from one set of input data with one image being exact and the other being distorted by computational approximations and/or by measurement errors. This program could be used to determine the effect on the image of the approximations described in Appendix B and the effect of measurement errors in the radar, attitude, and altitude data. It is this third version that will be described in this appendix.

The general outline of the program operation can be obtained from examination of the comment statements in the accompanying program printout. A few specific items will be described in more detail.

Images of the radar horizon and the runway outline were obtained by computing the position in earth coordinates of a number of points on the target and then converting these points in image coordinates using the series of transformations described in Appendices A and B. The image was then drawn by connecting these points with straight line segments.

Plots, or images, were normally produced on the Varian plotter, which has a resolution of .01 inches. The frame size for each image (or overlaid pair) was established at 8.87 in. square, and the plotting system automatically suppressed any portion of the image which was outside the frame limits. The outline of the CRT screen was drawn as a 8.85 in. square. Thus the frame size essentially limited the image to the area on the CRT screen.

The radar horizon was drawn by computing image points at 100 equally spaced angular intervals between the azimuth angle limits of $\pm\phi_{\max}$ and connecting this point with straight line segments.

Each side of the runway image was obtained by computing the image of 70 points along the side of the runway. The spacing between points was varied as follows: the near one-fourth of the runway was divided into 40 equally spaced intervals, the next one-fourth of the runway was divided into 20 equal intervals, and the top half was divided into 10 equal intervals. This technique was used to grossly approximate a constant angular spacing between the points.

The transformation from radar coordinates to aircraft coordinates to image coordinates was accomplished in a subroutine. This was done to allow different approximations to the transformation, as described in Appendix B, to be utilized by simply substituting subroutines. One of these subroutines was used to introduce measurements errors into the computations. This was done by replacing the measured variable, say h , by h' in the computations, where

$$h' = h + h_{mul} + h_{er}$$

and

h_{mul} = percentage error

h_{er} = bias error

Other variables treated in this manner were:

r = radar range, ft.

ξ = radar scan angle, rad.

Y = aircraft yaw, rad.

P = aircraft pitch, rad.

R = aircraft roll, rad.

```

PROGRAM DISPLAY(INPUT,OUTPUT,TAPES=INPUT)
C
C      THIS PROGRAM COMPARES EXACT PERSPECTIVE WITH PERSPECTIVE
C      GENERATED WITH ANGLE APPROXIMATIONS
C
      DIMENSION XR(5),XCR(5),YXCR(5),XXH(2),YYH(2),XXI(212),YYI(212)
      DIMENSION X,RHI(101),YYRHI(101)
      DIMENSION X,RHI(101),YYRHI(101),XXIA(212),YYIA(212)
      COMMON YI,XI,P,R,ACR,YAWER,PER,PER,HFR,HMUL,RANGFER,RANGMUL,XSTER,
      XSIMUL,YSIMUL,PMUL,IMUL
C
C      INITIALIZE GRAPHIC SYSTEM
C      READ DATA
C      CONVERT TO RADIAN
C
      CALL PDEFUN
500  READ 1000,Y0,P0,P0,EP50,DEFIA,Y0,Z0
1000  FORMAT(1/F10.3)
      IF (F0F.5) 9H.04
98   CALL CALPLT(0.0,0.0,0.999)
      STOP
99   PI=3.1415926
      READ 1004,YWER,YAWMUL,PER0,PMUL,PER0,RMUL,HFR,HMUL,RANGFER,
      RANGMUL,XSIMUL,XSIMUL
1004  FORMAT(12F5.2)
      DT=PI/10.
      YAW=Y0+DT*R
      P=P0+DT*R
      R=R0+DT*R
      EPS=EP50+DT*R
      DEFIA=DEFIA+DT*R
      YAWER=YAWER+DT*R
      PER=PER0+DT*R
      PER=PER0+DT*R
      XSTER=XSTER+DT*R
C
C      STORE COORDINATES
C      CALCULATE A/C RANGE FOR EACH PICTURE
C
12  NP=70
11  RI=10000.
10  A=150.
9   RT=1500.
8   XCR=70.
7   YCR=4.87
6   /CR=8.87
5   RP(1)=10560.
4   RP(2)=5240.
3   RP(3)=2640.
2   RP(4)=(100.0-70)/TAN(EP5)

```

ORIGINAL PAGE IS
OF POOR QUALITY

```

      PR(5)=(50.0-Z0)/TAN(EPS)
C
C      PRINT DATA
C
      PRINT 1001,X0,P0,W0,FB50,DELTD,Y0,Z0,RI,RTD,XCRT,YCRT,ZCRT
1001  FORMAT(1H1,'Y0'=#,F7.3,5X*P0=#,F7.3,5X*RI=#,F7.3,1X*EPS0=#,
1H7.3,5X*DELTD=#,F7.3,5X*Y0=#,F7.1,5X*Z0=#,F7.1,1X*RI=#,F7.0
2,5X*RTD=#,F7.0,1X*XCRT=#,F7.2,5X*YCRT=#,F7.2,5X*ZCRT=#,F7.2,
3//)
      PRINT 1002,X0,XMUL,PMUL,RMUL
1002  FORMAT(1X*Y0,XMUL=#,F8.4,5X*PMUL=#,F8.4,5X*RMUL=#,F8.4/)
      PRINT 1003,X0,FB0,PEPD,PERD,HER,HMUL,PARAMETER,RANGMUL,XSIEDD,XSIMUL
1003  FORMAT(1X*Y0,XMUL=#,F8.4,5X*PEPD=#,F8.4,5X*PERD=#,F8.4,5X*HER
1=#,F8.4,5X*H=#,F8.4,1X*PARAMETER=#,F8.4,5X*RANGMUL=#,
2F8.4,5X*XSIEDD=#,F8.4,5X*XSIMUL=#,F8.4//)
C
C      ITERATE OVER EACH AXI POSITION ALONG GLUE PATH
C
      DO 100 J=1,N
      NXH=0
      TX3H=0
C
C      CALCULATE AND DRAW CRT SCREEN
C
      XXCRT(1)=0.1,YYCRT(1)=0.1
      XXCRT(2)=0.1,YYCRT(2)=0.1
      XXCRT(3)=XXCRT(2)+YYCRT(2)
      XXCRT(4)=XXCRT(3)+YYCRT(4)=YYCRT(1)
      XXCRT(5)=XXCRT(1)+YYCRT(5)=YYCRT(1)
      CALL DRAW(XXCRT,YYCRT,5)
C
C      ESTABLISH NEW ORIGIN
C
      CALL CALPLI(YLCR/2.0,ZCRT/2.0,-1)
C
C      CALCULATE AND DRAW SUBROUTINE
C
      YIL=-YCRT/2.0
      ZIL=TAN(R)*YCRT/2.0+XCRT*TAN(P)/COS(R)
12  YIR=YCRT/2.0
11  ZIR=-TAN(R)*YLCR/2.0+XCRT*TAN(P)/COS(R)
10  XXH(1)=YIL  YYH(1)=-ZIL
9   XXH(2)=YIR  YYH(2)=-ZIR
8   CALL DGSUB(XXH(1),YYH(1),XXH(2),YYH(2),1,1)
7   C
6   C      PRINT RESULTS AND HEADINGS
5   C
4   PRINT 1002,PR(1),YIL,ZIL,YIR,ZIR
3   1002  FORMAT(1H1,'*PR'=#,F6.1,1X*YIL=#,F6.2,5X*ZIL=#,F6.2,5X*YIR=#,
2F6.2,5X*ZIR=#,F6.2,1X*XXH(1),1X*YYH(1),1X*XXH(2),1X*YYH(2),
3X*PARAMETER,1X*XSIEDD,1X*XSIMUL,1X*//)

```

ORIGINAL PAGE IS
OF POOR QUALITY

```

C
C      COMPUTE RADAR HORIZON
C      COMPUTE EARTH COORDINATES OF EXTREME LEFT POINT
C
      OMAX=0.052+0.
      OMAX=ATAN2(YCMT,XCPT*SQRT(2.0))+0.02
      Z=OP(1)+TA*(FPS)/COS(DELTA)+ZC
      H=Z
      X=SQRT((P1AX**2-H**2)/(1.0+TAN(YAW-OMAX)**2))
      Y=X*TAN(YAW-OMAX)
C
C      TRANSFORM TO A/C COORDINATES
C
      TX3=COS(P)*COS(YAW)
      TY3=COS(P)*SIN(YAW)
      TZ3=-SIN(P)
      TX3=-COS(R)*SIN(YAW)+SIN(R)*SIN(P)*COS(YAW)
      TY3=COS(R)*COS(YAW)+SIN(R)*SIN(P)*SIN(YAW)
      TZ3=SIN(R)*COS(P)
      TX3=SIN(R)*SIN(YAW)+COS(R)*SIN(P)*COS(YAW)
      TY3=-SIN(R)*COS(YAW)+COS(R)*SIN(P)*SIN(YAW)
      TZ3=COS(R)*COS(P)
      X3=TX3*X+TY3*Y+TZ3*Z
      Y3=TX3*Y+TY3*Z+TZ3*X
      Z3=TX3*Z+TY3*X+TZ3*Y
C
C      TRANSFORM TO RADAR COORDINATES
C
      RANGE=SQRT(Z3**2+Y3**2+X3**2)
      XSI=ACOS(Y3/RANGE)
C
C      CALCULATE IMAGE COORDINATES AND PLOT COORDINATES
C
      CALL COORI(P,GE,(RI,H,YI,ZI))
      XPHI(1)=YI
      YPHI(1)=-ZI
      CALL COORIA(RANGE,XSI,H,YIA,ZIA)
      XPHI(1)=YIA
      YPHI(1)=-ZIA
12
C
11
C      ITERATE ALONG HORIZON
10
C
9
      DEL0=OMAX/5.
7
      17400=1.100
6
C
5
C      COMPUTE EARTH COORDINATES
4
C
3
      X=SQRT((P1AX**2-H**2)/(1.0+TAN(YAW-OMAX+N*DEL0)**2))
2
      Y=X*TAN(YAW-OMAX+N*DEL0)
1
      Z=H

```



```

C
C      TRANSFORM TO A/C COORDINATES
C
      X3=TXX3*X+TYX3*Y+T7X3*Z
      Y3=TXY3*X+TY Y3*Y+T7Y3*Z
      Z3=TXZ3*X+TYZ3*Y+T7Z3*Z
C
C      TRANSFORM TO RADAR COORDINATES
C
      RANGE=SQRT(X3**2+Y3**2+Z3**2)
      ASI=ACOS(Y3/RANGE)
C
C      CALCULATE IMAGE COORDINATES AND PLOT COORDINATES
C
      CALL COORDI(RANGE,XS1,H,YI,ZI)
      XXRH1(1)=YI
      YYRH1(1)=-ZI
      CALL COORDI(RANGE,YI,H,YIA,ZIA)
      XXRHIA(1)=YI
      YYRHIA(1)=-ZIA
400  CONTINUE
C
C      PRINT RESULTS
C
      PRINT 1000
1000  FORM AT(1X,'X3=',10X,'Y3=',10X,'Z3=',10X,'XRH1=',10X,'XXRHIA=',10X,'YYRH1A=',10X)
      PRINT 1001,(X,RH1(I),YYRH1(I),XXRHIA(I),YYRHIA(I),I=1,10),20)
1001  FORM AT(1X,4(F10.3,5X))
C
C      DRAW RADAR HOPEZON
C
      CALL DRA (XXRH1,YYRH1,101)
      CALL DRA(XXRHIA,YYRHIA,101)
C
C      CALCULATE RTH COORDINATES OF NEAR LEFT CORNER OF RUNWAY
C
      XA=RK(1)
      YA=XA*TAN(DEF1A)+Y0
      ZA=XA*TAN(EP5)/COS(DEF1A)+Z0
12  H=Z0
11  X=XA-XTD
10  Y=Y0-XTD
9  Z=Z0
C
C      TRANSFORM TO A/C COORDINATES
C
      X3=TXX3*X+TYX3*Y+T7X3*Z
      Y3=TXY3*X+TY Y3*Y+T7Y3*Z
      Z3=TXZ3*X+TYZ3*Y+T7Z3*Z
      IF(X3.LE.0.0)NX3L=NX3L+1
C

```

```

C          TRANSFORM TO RADAR COORDINATES
C
      RANGE=SQRT(X3**2+Y3**2+Z3**2)
      XSI=ACOS(Y3/RANGE)
      XSID=XSI/DTOR
C
C          CALCULATE IMAGE COORDINATES AND PLOT COORDINATES
C
      CALL COORI(RANGE,XSI,H,YI,ZI)
      XX(1)=YI
      YY(1)=-ZI
      PRINT 1003,X,Y,Z,X3,Y3,Z3,RANGE,XSID,YI,ZI
1003  FORMAT(1XF10.3,9(2XF10.3))
      CALL COORI(RANGE,XSI,H,YIA,ZIA)
      XX(1)=YIA
      YY(1)=-ZIA
      PRINT 1004,YIA,ZIA
1004  FORMAT(9XF10.3,2XF10.3)
C
C          ITERATE ALONG LEFT SIDE OF RUNWAY
C
      DO 101 N=1,1P
C
C          DETERMINE X-INCREMENT AND COMPUTE EARTH COORDINATES OF P(X,Y,Z)
C
      IF(N-NP*4/7)10,10,11
10    DX=RL/4.0/(NP*4.0/7.0)
      GO TO 14
11    IF(N-NP*6/7)12,12,13
12    DX=RL/4.0/(NP*2./7.)
      GO TO 14
13    DX=RL/2.0/(NP/7.)
14    CONTINUE
      X=X+DX
C
C          TRANSFORM TO A/C COORDINATES
C
      X3=TXX3*X+TXX3*Y+TX3*Z
      Y3=TXY3*X+TTY3*Y+TY3*Z
12    Z3=TXZ3*X+TYZ3*Y+TZ3*Z
11    IF(X3.LE.0.0)NX3L=NX3L+1
10    C
C          TRANSFORM TO RADAR COORDINATES
C
      RANGE=SQRT(X3**2+Y3**2+Z3**2)
      XSI=ACOS(Y3/RANGE)
      XSID=XSI/DTOR
C
C          COMPUTE IMAGE COORDINATES AND PLOT COORDINATES
C
      CALL COORI(RANGE,XSI,H,YI,ZI)

```

```

      XXI(N+1)=YI
      YYI(N+1)=-ZI
      CALL COOR1A(RANGE,XSI,H,YIA,ZIA)
      XXIA(J+1)=YIA
      YYIA(N+1)=-ZIA
      IF(N.NE.NP)GO TO 101
      PRINT 1003,X,Y,Z,X3,Y3,Z3,RANGE,XSID,YI,ZI
      PRINT 1004,YIA,ZIA
101  CONTINUE
      C
      C      COMPUTE TOP OF RUNWAY
      C
      Y=Y+W
      C
      C      TRANSFORM TO A/C COORDINATES
      C
      X3=TXX3+X+TYX*Y+TZ*Z
      Y3=TXY3+X+TY*Y+TZ*Z
      Z3=TXZ3+X+TY*Y+TZ*Z
      C
      C      TRANSFORM TO RADAR COORDINATES
      C
      RANGE=SQRT(X3**2+Y3**2+Z3**2)
      XSI=ACOS(Y3/RANGE)
      XSID=XSI/DTW
      C
      C      CALCULATE EARTH COORDINATES AND PLOT COORDINATES
      C
      CALL COOR1(P/RANGE,XSI,H,YI,ZI)
      XXI(NP+2)=YI
      YYI(NP+2)=-ZI
      PRINT 1003,X,Y,Z,X3,Y3,Z3,RANGE,XSID,YI,ZI
      CALL COOR1A(RANGE,XSI,H,YIA,ZIA)
      XXIA(NP+2)=YIA
      YYIA(NP+2)=-ZIA
      PRINT 1004,YIA,ZIA
      C
      C      ITERATE DOWN RIGHT SIDE OF RUNWAY
      C
102  N=1.0
11  C
10  C      DETERMINE X-INCREMENT AND COMPUTE EARTH COORDINATES OF P(X,Y,Z)
1  C
1  IF(N-NP/7)GOTO 21
1  X=R1/2.0/(NP/7.)
1  GO TO 24
1  IF(N-NP/3)GOTO 22,22,23
1  X=R1/4.0/(NP/2./7.)
1  GO TO 24
1  X=R1/4.0/(NP*4./7.)
1  CONTINUE
24

```

ORIGINAL PAGE IS
OF POOR QUALITY

```

      X=X-UX
C
C      TRANSFORM TO A/C COORDINATES
C
      X3=TXX3*X+TXX3*Y+TXZ3*Z
      Y3=TXY3*X+TTY3*Y+TZY3*Z
      Z3=TXZ3*X+TYZ3*Y+TZZ3*Z
      IF(X3.GT.0.)NX3R=N
C
C      TRANSFORM TO RADAR COORDINATES
C
      R=SQRT(X3**2+Y3**2+Z3**2)
      AS1=ACOS(Y3/R/GE)
      XS1D=XS1/R
C
C      CALCULATE IMAGE COORDINATES AND PLOT COORDINATES
C
      CALL COOR1(M,N,XS1,H,YI,ZI)
      X1(N+NP+1)=YI
      Y1(N+NP+2)=-ZI
      CALL COOR1A(PANOF,XS1,H,YIA,ZIA)
      X1A(N+NP+1)=YIA
      Y1A(N+NP+2)=-ZIA
      IF(N.NE.NP).GO TO 102
      PRINT 1003, Y,Z,X3,Y3,Z3,R,AGE,XS1D,YI,ZI
      PRINT 1004, R,ZIA
102  CONTINUE
C
C      ITERATE ACROSS BOTTOM OF RUNWAY
C
      Y=W/2P
      DO 103 N=1, P
      Y=Y-UY
C
C      TRANSFORM TO A/C COORDINATES
C
      X3=TXX3*X+TXX3*Y+TXZ3*Z
      Y3=TXY3*X+TTY3*Y+TZY3*Z
      Z3=TXZ3*X+TYZ3*Y+TZZ3*Z
      IF(X3.LT.0.)X3=1.0
C
C      TRANSFORM TO RADAR COORDINATES
C
      R=SQRT(X3**2+Y3**2+Z3**2)
      AS1=ACOS(Y3/R/GE)
      XS1D=XS1/R
C
C      CALCULATE IMAGE COORDINATES AND PLOT COORDINATES
C
      CALL COOR1(M,N,XS1,H,YI,ZI)

```

```

      XXI(N+2*NP+2)=YI
      YYI(N+2*NP+2)=-ZI
      CALL COOR1A(PANGF,XSI,H,YIA,ZIA)
      XXI(N+2*NP+2)=YIA
      YYI(N+2*NP+2)=-ZIA
      IF(NX3L.NP)GO TO 103
      POINT 1001,Z=Y-Z,X3=Y3,Z3=RANGF,XSI0,YI,ZI
      POINT 1001,XIA,ZIA
103  CONTINUE
      C
      C      ELIMINATE POINTS BEHIND A/C (X3 LESS THAN 0.0)
      C
      IF(NX3L-E)+C)GO TO 300
      DO 301 N=1,NX3L
      XXI(N)=XXI(NX3L+1)
      YYI(N)=YYI(NX3L+1)
      XXI(N)=XXI(NX3L+1)
      YYI(N)=YYI(NX3L+1)
301  CONTINUE
300  CONTINUE
      IF(NX3R.GE.0)GO TO 302
      NN=NX3R+1
      DO 302 N=NN, P
      XXI(NP+2+N)=XXI(NP+2+NX3R)
      YYI(NP+2+N)=YYI(NP+2+NX3R)
      XXI(NP+2+N)=XXI(NP+2+NX3R)
      YYI(NP+2+N)=YYI(NP+2+NX3R)
302  CONTINUE
      C
      C      DRAW RUNWAY AND MOVE TO NEW FRAME
      C
      CALL DRAW(XXI,YI,3*NP+2)
      CALL DRAA(XXIA,YYIA,3*NP+2)
      CALL MEKA(Z(15),Z(16))
100  CONTINUE
      C
      C      READ FROM A
      C
      GO TO 500
1  END
2  SUBROUTINE COOR1(PANGF,XSI,H,YI,ZI)
      C
      C      THIS SUBROUTINE COMPUTES EXACT IMAGE COORDINATES FROM RADAR COORD
      C
      COMMON YP,XP,CP,ZP,YAWER,PEN,PER,HFR,HMU,RANGFR,RANGMU,XSTER,
1 XSIMUL,YO-MUL,PUL,-MUL
      C
      C      COMPUTE A/C COORDINATES FROM RADAR COORDINATES OF P(X,Y,Z)
      C
      YI=RAYGE*COX(XSI)
      A=H**2*(SIN(P)**2+COS(R)**2*COS(P)**2)

```

```

H=2.0*H**2*COS(R)*COS(P)*(RANGE*COS(XSI)*SIN(R)*COS(P)-H)
C=-RANGE**2*H**2*SIN(XSI)**2*SIN(P)**2+H**2*(RANGE*SIN(R)*COS(P)*
1(COS(XSI)-1)**2
Z3=(-H+SQRT(ABS(R**2-4.0*H*(C))))/(2.0*H)
C
C      CALCULATE IMAGE COORDINATES
C
C
C      CALCULATE IMAGE COORDINATES
C
YI=XCRT*PI*F/COS(XSI)/SQRT(ABS(RANGE**2*SIN(XSI)**2-Z3**2))
ZI=Z3*YI/(RANGE*COS(XSI))
RETURN
END
SUBROUTINE COORDIA(RANGE,XSI,H,YI,ZI)
C
C      THIS SUBROUTINE COMPUTES APPROXIMATE IMAGE COORDINATES
C      FOR RADAR COORDINATES
C      WITH THE FOLLOWING ERRORS
C      THE APPROXIMATIONS ARE
C      / 1 =
C      SIN(XSI)=1.0   COS(XSI)=PI/2.0-XSI
C
COMMON YI,XI,P,R,ACHT,YAVER,PER,PER,HFR,HMUL,RANGEER,RANGMUL,XSIFR
IXSIMUL=YI*HMUL*PI*HIL*HMUL
PI=3.1415926
YA=P*YA**2*(1.0+YA*HIL)+YA*FR
PD=P*(1.0+P*HIL)+P*P
HD=H*(1.0+H*HIL)+H*P
RANGEV=RANGE**2*(1.0+RANGMUL)+RANGEER
XSIP=XSI+(PI/2.0-XSI)*XSIMUL+XSIFR
C
C      COMPUTE /C COORDINATES FROM RADAR COORDINATES OF P(X,Y,Z)
C
Y3=RANGE*P*(PI/2.0-XSIP)
Z3=HP
C
C      CALCULATE IMAGE COORDINATES
C
12 C
11 YI=XCRT*PI*F*P*(PI/2.0-XSIP)/SQRT(ABS(RANGE**2-Z3**2))
10 ZI=Z3*YI/(RANGE*P*(PI/2.0-XSIP))
9 RETURN
8 END
7
6
5
4
3
2
1

```

ORIGINAL PAGE IS
OF POOR QUALITY

REFERENCES

1. Anon.: A New Guidance System for Approach and Landing. Vol. II, Document No. 148, RTCA SC-117, December 18, 1970.
2. Sorensen, J. A.: Analysis of Instrumentation Error Effects on the Identification Accuracy of Aircraft Parameters. Systems Control, Inc., May 31, 1972.